Asymmetric Flow Field Flow Fractionation (AF4) of Polymers with Focus on Polybutadienes and Polyrotaxanes

by

Ashwell Craig Makan

Thesis presented in partial fulfillment of the requirements for the degree of **Master of Science (Polymer Science)**

at

University of Stellenbosch

Supervisor: Prof H. Pasch

March 2012

Stellenbosch

Declaration

By submitting this thesis electronically, I declare that the entirety of the work contained therein is my own, original work, that I am the sole author thereof (save to the extent explicitly otherwise stated), that reproduction and publication thereof by Stellenbosch University will not infringe any third party rights and that I have not previously in its entirety or in part submitted it for obtaining any qualification.

_____   March 2012

Ashwell Craig Makan   Stellenbosch

Abstract

Over the past two decades, field flow fractionation (FFF), as a polymer characterization technique, has become cutting edge technology. The demand for molar mass and size characterisation of complex polymer systems has increased, especially in cases where classical calibration techniques such as size exclusion chromatography (SEC) has shown several shortcomings. FFF is a technique resembling chromatography. It has several significant advantages over SEC, especially for the characterisation of ultrahigh molar mass (UHMM), branched and gel-containing polymers. In this study, polybutadienes, which often contain the abovementioned species, were analysed by SEC and asymmetric flow field flow fractionation (AF4). Both separation techniques were coupled to refractive index and multi-angle laser light scattering detection. Similarly, polyrotaxanes, which are polymers with complex and unique molecular architectures, were also investigated. Results showed that AF4 can explicitly be used as a superior tool over SEC. In the case of UHMM polybutadienes, much higher molar masses could be detected by AF4, due to the absence of shear degradation which is often encountered in SEC. Gel-containing species could be detected by AF4 as no filtering is required prior to injection. Abnormal retention behaviour, a phenomenon often encountered in UHMM branched polymers, was observed in SEC analysis of the polyrotaxanes materials. AF4 provided sufficient separation from low to high molar masses, without out any irregularities.

.

Opsomming

Gedurende die afgelope twee dekades het veldvloeifraksionering (FFF) as 'n polimeerkarakteriseringstegniek groot veld gewen. Die aanvraag na molekulêre massa en grootte-karakterisering van komplekse polimeersisteme het toegeneem, veral in die gevalle waar klassieke kalibrasietegnieke soos grootte-uitsluitingschromatografie (SEC) etlike tekortkominge getoon het. FFF is 'n tegniek soortgelyk aan chromatografie, en het voorheen bewys dat dit oor 'n redelike aantal voordele bo SEC beskik, veral in die geval van ultrahoë molekulêre massa- (UHMM-), vertakte- en jel-bevattende spesies. In die huidige studie is polibutadieenpolimere, wat dikwels bogenoemde spesies bevat, geanaliseer met behulp van SEC en onsimmetriese vloei-veldvloeifraksionering (AF4). Beide skeidingstegnieke is gekoppel aan 'n brekingsindeks en multihoek-laserligverstrooiingsdetektors. Op dieselfde wyse is polirotaksane (polyrotaxanes) met komplekse molekulêre argitektuur bestudeer. Daar is bewys dat AF4 uitsluitlik gebruik kan word as 'n meer geskikte tegniek bo SEC. Baie hoër molekulêre massas kon deur middel van AF4 vir UHMM polibutadieenpolimere raakgesien word as gevolg van die verminderde afbrekende degradasie wat dikwels voorkom met SEC. Jel-bevattende spesies is suksesvol geïdentifiseer met behulp van AF4 waartydens geen filtrering vir analise nodig was nie. Abnormale retensie was sigbaar tydens SEC analise van monsters van polirotaksane, wat dikwels voorkom in vertakte polimere. In teenstelling het AF4 bewys dat 'n bevredigende skeiding van klein na groot molekulêre massas, sonder enige tekortkominge, moontlik is.

.

Table of contents

Table of contents

Table of contents

List of figures

List of figures

List of figures

List of tables

List of abbreviations

ABS	acrylonitrile butadiene styrene
AF4	asymmetric flow field flow fractionation (room temperature)
BHT	butylated hydroxy toluene
BuLi	n-butyllithium
CD	cyclodextrin
CH_2Cl_2	dichloro methane
Co	cobalt
CuBr	copper bromide
$CuBr_2$	copper dibromide
DALLS	dual angle laser light scattering
DLS	dynamic light scattering
DMAC	N,N-dimethylacetamide
DMAP	dimethyl amino pyridine
DMF	N,N-Dimethylformamide
DMSO	dimethyl sulfoxide
dn/dc	specific refractive index increment
DRI	differential refractive index
DV	differential viscometer
EDTA	ethylene diamine tetra acetic acid
ElFFF	electrical field flow fractionation
ELSD	evaporative light scattering detector
Et_2O	diethyl ether
FFF	field flow fractionation
FlFFF	flow field flow fractionation
GELC	gradient elution liquid chromatography

List of abbreviations

HDC	hydrodynamic chromatography
HEMA	poly (hydroxyethyl methacrylate)
HFFFF	hollow fibre field flow fractionation
HMTETA	hexamethyltriethylenetetramine
HPLC	high performance liquid chromatography
HT-AF4	high temperature asymmetric flow field flow fractionation
IR	infrared
LAC	liquid adsorption chromatography
LALLS	low angle laser light scattering
LC	liquid chromatography
LC-CC	liquid chromatography at the critical point of adsorption
LiCl	lithium chloride
LS	light scattering
MALLS	multi-angle laser light scattering
MMD	molar mass distribution
M_n	number average molar mass
M_p	molar mass at peak maximum
M_w	weight average molar mass
NaH	sodium hydride
Nd	neodymium
Ni	nickel
PB	polybutadiene
PDI	polydispersity index
PEG,PEO	polyethylene glycol, polyethylene oxide
PI	polyisoprene
PMMA	poly (methylmethacrylate)
PR-MI	polyrotaxane macroinitiator
RALLS	right angle laser light scattering

List of abbreviations

R_g	radius of gyration
RI	refractive index
SBR	styrene-butadiene rubber
SdFFF	sedimentation field flow fractionation
SDV	styrene divinyl benzene
SEC	size exclusion chromatography
SLS	static light scattering
TCB	trichloro benzene
T_g	glass transition temperature
ThFFF	thermal field flow fractionation
Ti	titanium
UHMM	ultra high molar mass
UV	ultraviolet
ZN	ziegler natta

List of symbols

A_2	second virial coefficient
A_{aw}	area of the accumulation wall
c	concentration of analyte
c_o	concentration of analyte at the accumulation wall
d	diameter of molecule/particle
D	diffusion coefficient
dc/dx	change in concentration over the mean layer thickness
D_T	thermal diffusion coefficient
dT/dx	temperature drop between hot and cold walls
F	force field applied perpendicular to the inlet flow
G	gravitational force
J	net flux of energy
k	Boltzmann constant
K*	optical constant
K_d	distribution coefficient
l	mean thickness layer
m'	effective mass
N_A	avogadro's number
n_o	refractive index of the mobile phase
$P(\theta)$	particle scattering function
R	retention ratio
R_θ	raleigh ratio
T	temperature
t_o	retention time of an unretained component
t_r	retention time of analyte

List of symbols

U	flow induced field
$\overset{.}{V}_{out}$	detector flow rate
$\overset{.}{V}_{c}$	flow rate of the cross flow
V_e	elution volume
V_i	total volume of mobile phase in the intersitial space of the pores
V_o	volume of mobile phase outside the pores of the stationary phase (SEC)
V_o	volume of the channel (FFF)
V_p	volume of particle
V_t	total volume of mobile phase
w	width or thickness of the channel
ΔG	change in gibbs free energy
ΔH	change in enthalpy
ΔS	change in entropy
Δρ	difference in density between particle and mobile phase
η	viscosity of mobile phase
λ	retention parameter
π	pi

Chapter 1: Introduction and objectives

Chapter 1: Introduction and objectives

1.1 Introduction

Polymeric materials with complex molecular distributions require accurate analytical techniques in order to address molar mass, chemical composition, functionality and molecular topologies. The molar mass distributions of natural and synthetic polymers have been characterized for decades by classical methods such as size exclusion chromatography (SEC).[1,2] Calculations regarding molar mass are usually done by correlating the polymer in question with a set calibration curve which is constructed from measuring polymer standards of known molar mass.[1,2] The obtained result however only is true for the assumption that each fraction exiting the column is monodisperse in nature and separation takes place from high to low molar masses. For complex polymer systems, this is not always the case since high molar mass branched polymers will lead to an increase in local dispersity towards the late eluting species exiting the column.[3-9] The dispersity differences occur as a result of retardation of branched species by the pores of the stationary phase of the column.[10,11] Another reason for differences in dispersity could be due to adsorption of functional groups on the stationary phase, resulting in larger polymer structures eluting at a later stage together with the regular eluting species. Ultrahigh molar mass species are frequently shear degraded by the pores and frits of the columns, resulting in molar masses that are lower compared to the injected sample.[9,12-17] All of the abovementioned problems can lead to erroneous results and inaccurate interpretation of calculated results where the slightest of errors can lead to detrimental consequences in industries such as automobile companies.

Field flow fractionation (FFF) is a chromatography- like technique discovered in the 1960's by J. Calvin Giddings which has shown a lot of potential over the last few decades. Most of the problems observed in SEC for complex polymer systems can be overcome by FFF and additional information can be retrieved by the various sub-techniques of FFF. FFF has been applied in various industries and the most popular FFF technique is asymmetric flow field flow fractionation (AF4). Studies have been done using organic and aqueous mobile phases on natural and synthetic polymers in various fields. Examples are the investigations of virus-like particles, starches, hyaluronic acid for aqueous applications.[18-21] Organic applications include branched polymers, high temperature analysis of polyolefins, gel-containing polymers and SBR-rubber emulsions to name a few.[2,8,9,22-24] FFF in general is very powerful and with each unique sub-technique such as thermal FFF or centrifugal FFF, a lot of information can be acquired from complex polymer systems, which was previously not accessible by conventional characterization methods.[18]

1.2 Objectives

The rationale of the study was to do a comprehensive study on two different polymer systems utilizing AF4 using an organic mobile phase. SEC and AF4 analyses were done to compare the two separation techniques and to identify the limitations of SEC. Various parameters such as the column sets in SEC and various flow parameters in AF4 were investigated. The aim of the study was to investigate polybutadienes and polyrotaxanes.

2

Chapter 1: Introduction and objectives

Polybutadienes specifically are very complex systems in terms of branching, gel species and ultrahigh molar masses. The main focus was to explore properties such as branching and gel content of the polybutadienes. SEC was used as an initial starting point and AF4 was used to eliminate most of the problems which were observed in SEC.

The second polymer system is cyclodextrin-based polyrotaxanes, which is a polymer with an extremely unique molecular architecture. In this system SEC was initially used and AF4 was subsequently implemented to study the effect of various instrumental parameters on the elution profile and the resultant molar masses and hydrodynamic sizes.

1.3 Layout of thesis

Chapter 2

The background theory of the polymers used in this study is discussed while a brief overview of the basic principles of the separation methods and detectors is given.

Chapter 3

In this chapter the characterization of polybutadienes by SEC and AF4 is discussed in detail with the focus on dissolution time and temperature, branching, ultrahigh molar mass species as well as gel-containing species.

Chapter 4

This chapter entails the investigation of polyrotaxane polymers with complex molecular architectures. Both SEC and AF4 analysis were done in depth and are discussed accordingly.

Chapter 5

Overall conclusions of each of the result chapters are given followed by future recommendations.

Chapter 1: Introduction and objectives

1.4 References

(1)   Kuo C.-Y.; Provder T. *ACS Symp. Ser.* **1987**; 352, 2-28.

(2)   Podzimek S. *Light Scattering, Size Exclusion Chromatography and Asymmetric Flow Field Flow Fractionation: Powerful Tools for the Characterization of Polymers, Proteins and Nanoparticles.* New York: John Wiley & Sons; **2011**.

(3)   Johann C.; Kilz P. J. *J. Appl. Polym. Sci.*: Appl. Polym. Symp. **1991**; 48, 111-122.

(4)   Wintermantel M.; Antonietti M.; Schmidt M. *J. Appl. Polym. Sci.*: Appl. Polym. Symp. **1993**; 52, 91-103.

(5)   Podzimek S. *J. Appl. Polym. Sci.*. **1994**; 54(1), 91-103.

(6)   Percec V.; Ahn C. H.; Cho W. D.; Jamieson A. M.; Kim J.; Leman T.; Schmidt M.; Gerle M.; Möller M.; Prokhorova S. A.; Sheiko S. S.; Cheng S. Z. D.; Zhang A.; Ungar G.; Yeardley D. J. P. *J. Am. Chem. Soc.* **1998**; 120, 8619-8631.

(7)   Gerle M.; Fischer K.; Roos S.; Muller A. H. E.; Manfred S. *Macromolecules* **1999**; 32, 2629-2637.

(8)   Mes E. P. C.; de Jonge H.; Klein T.; Welz R. R.; Gillespie D. T. *J. Chromatogr. A* **2007**; 1154(1-2), 319-330.

(9)   Otte T.; Pasch H.; Macko T.; Brüll R.; Stadler F. J.; Kaschta J.; Becker F.; Buback M. *J. Chromatogr. A* **2011**; 1218(27), 4257-4267.

(10)   Hirabayashi J.; Ito N.; Noguchi K.; Kasai K. *Biochemistry* **1990**; 29(41), 9515-9521.

(11)   Liu Y.; Radke W.; Pasch H. *Macromolecules* **2006**; 39(5), 2004-2006.

(12)   Slagowski E. L.; Fetters L. J.; McIntyre D. *Macromolecules* **1974**; 7(3), 394-396.

(13)   Zammit M. D.; Davis T. P.; Suddaby K. G. *Polymer* **1998**; 39(23), 5789-5798.

(14)   Aust N. *J. Biochem. Bioph. Methods* **2003**; 56, 323-334.

(15)   Cave R. A.; Seabrook S. A.; Gidley M. J.; Gilbert R. G. *Biomacromolecules* **2009**; 10(8), 2245-2253.

(16)   Messaud F. A.; Sanderson R. D.; Runyon J. R.; Otte T.; Pasch H.; Williams S. K. R. *Prog. Polym. Sci.* **2009**; 34(4), 351-368.

(17)   Stadler F. J.; Kaschta J.; Münstedt H.; Becker F.; Buback M. Rheol. Acta **2009**; 48, 479-490.

(18)   Schimpf M. E.; Caldwell K.; Giddings J. C. *Field Flow Fractionation Handbook*. New York: John Wiley & Sons; **2000**.

(19)   van Bruijnsvoort M.; Wahlund K. G.; Nilsson G.; Kok W. T. *J. Chromatogr. A* **2001**; 925(1-2), 171-182.

(20)   Rojas C. C.; Wahlund K.-G.; Bergenståhl B.; Nilsson L. *Biomacromolecules* **2008**; 9(6), 1684-1690.

(21)   Rolland-Sabaté A.; Guilois S.; Jaillais B.; Colonna P. *Anal. Bioanal. Chem.* **2011**; 399(4), 1493-1505.

(22)   Bang D. Y.; Shin D. Y.; Lee S.; Moon M. H. *J. Chromatogr. A* **2007**; 1147(2), 200-205.

(23)   Otte T.; Brüll R.; Macko T.; Pasch H.; Klein T. *J. Chromatogr. A* **2010**; 1217(5), 722-730.

(24)   Otte T.; Klein T.; Brüll R.; Macko T.; Pasch H. *J. Chromatogr. A* **2011**; 1218(27), 4240-4248.

Chapter 2: Historical and theoretical background

Chapter 2: Theoretical background

2.1 General aspect of polymers

2.1.1 Polybutadienes

Polybutadiene rubber (PB rubber) is the second most produced synthetic rubber after styrene butadiene rubber (SBR), and is primarily used in automotive tires. Other applications for PBs are predominantly in footwear, golf balls, and technical goods. PB rubber is typically polymerized in solution to obtain high stereospecificity by making use of alkyl metals like n-butyllithium (BuLi), transition metals which are typically Nickel (Ni), Cobalt (Co) and Titanium (Ti) as well as lanthanides for example Neodymium (Nd). The polymerizations that take place with transition metal catalysts are called Ziegler-Natta (ZN) polymerizations since accurate control over stereochemistry is obtained (Fig. 2.1).[1]
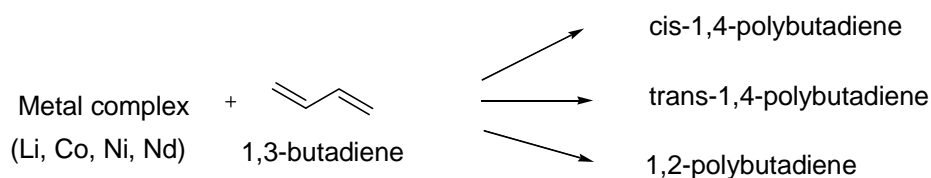
Fig. 2.1 Simplified reaction scheme of polybutadiene polymerization, typically carried out in 20% monomer and 80% solvent, respectively, to reduce viscosity and heat build-up

Nd has the same characteristics as ZN catalysts but in addition it is capable of producing higher cis-contents. PB rubber is a perfect candidate for the tire industry since it offers the ideal properties when cured or vulcanized. PB rubber can be obtained commercially in two distinct forms which are the most important in industry namely PB rubber with cis-contents between 90% and 98% (high-cis PB) and a cis-content of approximately 40% (low-cis PB or trans-PB), see Fig. 2.2.[1] The cis-conformation is where the polymer chain is situated on the same side of the carbon-carbon double bond of the repeating unit whereas the trans-conformation has the polymer chain on opposed sides of the double bond (Fig. 2.2).

cis-1,4-polybutadiene   trans-1,4-polybutadiene
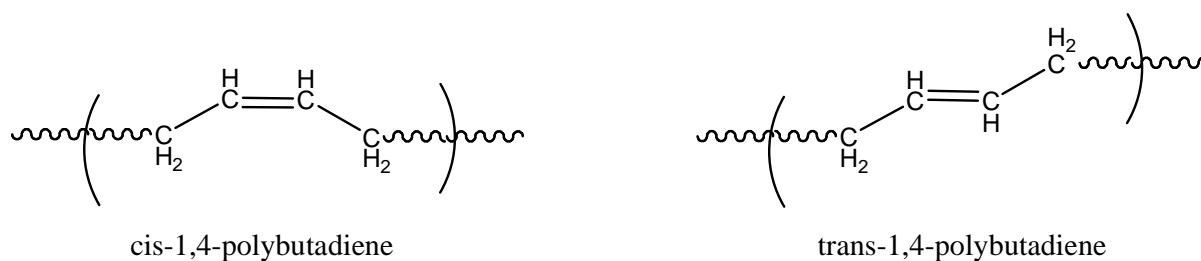
Fig. 2.2 Cis- and trans-isomers of polybutadiene

Vinyl-PB or 1,2-polybutadiene is formed as a result of a 1,2-addition of the butadiene monomer to the PB backbone chain resulting in side chains with vinyl character (Fig. 2.3). The vinyl content increases

6

the T_g of the polymer since it creates stiffer chains compared to chains with little to no vinyl content having a lower T_g.
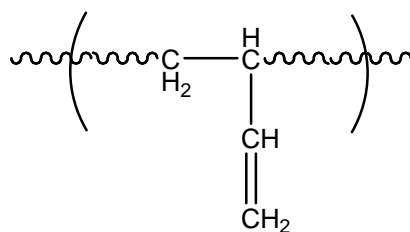
vinyl polybutadiene

Fig. 2.3 Repeat unit of 1,2- or vinyl-polybutadiene

PB rubber which has a high vinyl content makes it very susceptible to cross-linking and branching. Cross-linking will affect the solubility of the polymer, and can result in insoluble gel which usually gives problems when analysing rubbers by chromatographic methods such as size exclusion chromatography (SEC). Intermediate cis-containing PB is usually manufactured by making use of BuLi as catalyst resulting in a cis-content of about 40% and trans- and vinyl-contents of approximately 50% and 10%, respectively.[1] Li-based catalysts also have the potential of producing PB free of any gel species, making the material a good candidate for plastic modification and applications where the presence of gel can lead to detrimental effects for example in the tire industry.[1] Gel content within PB rubber can lead to unwanted species which are very high in molar mass and can influence the processing and final product properties immensely.

Branching in polymers can be of different kinds and can influence several structural properties. Examples of properties altered by branching in naturally occurring polymers as well as synthetic polymers are the T_g, mechanical properties like tack, peel strength, crystallizability, viscosity, rheological properties, solubility, and swellability to name a few.[2] Different types of branched polymers exist for example stars, dendrimers and comb polymers (Fig. 2.4).[2]   Each of the branching architectures can also consist of long and short chain branches (Fig. 2.4).

Branches which are oligomeric in chain length are known as short chain branches while branches containing polymer chains are called long chain branches.[3-5] Branching occur as a result of chain transfer between polymer chains, side reactions or polymerization of a double bond either in the repeating unit in the case of synthetic rubbers like PI or PB rubber,[6] or the double bond of a vinyl repeating unit. In polyolefin research branching plays an important role in producing different grades of polyethylene and polypropylene. Polyolefins with various degrees of branching will result in end products of different structure property relationships. This has paved the way for much research done in the plastic industry in both the synthesis as well as characterization divisions. The main effect branching has on the hydrodynamic size of a polymer molecule in solution is that branching reduces the size of the polymer coil in solution.[2,4] The solution behaviour plays a significant role in the characterization of branched polymer molecules and causes difficulties when analyzed by SEC, especially for randomly branched PB rubbers and ultrahigh molar mass fractions.
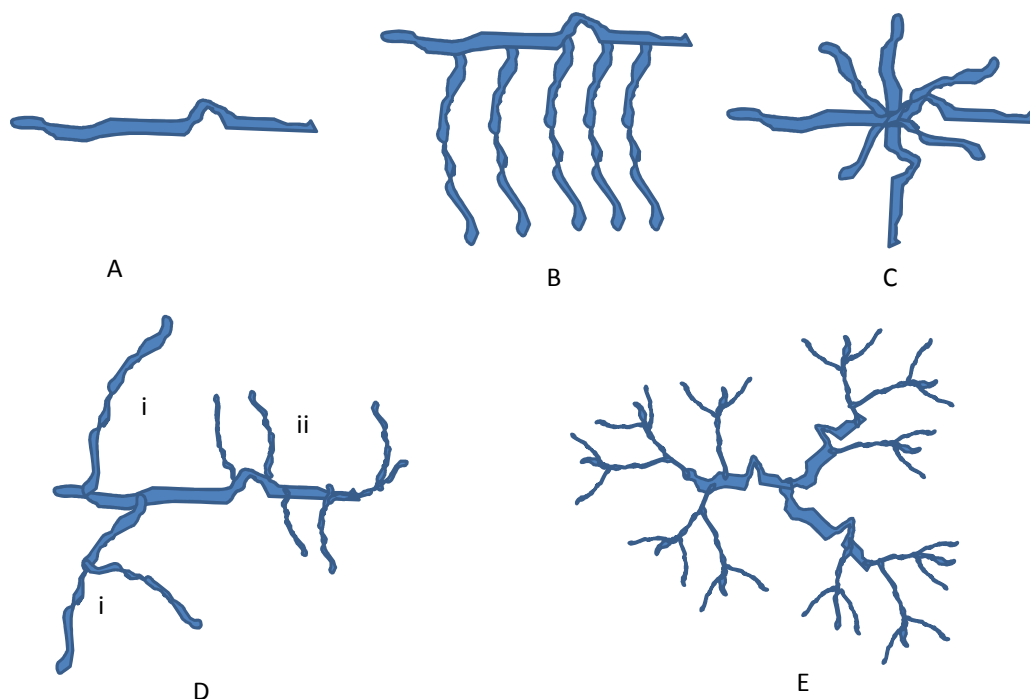
Fig. 2.4 Different architectures of branched polymers compared to a linear polymer chain (A): (B) combs, (C) stars, (D) polymers showing (i) long chain branching and (ii) short chain branching, (E) dendrimers

2.1.2 Polyrotaxanes

Polyrotaxanes are polymers with a unique molecular architecture that comprise of properties that are unique compared to other synthetic polymers. Polyrotaxanes are based on cyclic molecules like cyclodextrins (CDs) that are 'hooked' or threaded onto a polymer backbone chain such as polyethylene oxide (Fig. 2.5).[7] Rotaxane is derived from Latin and means wheel (rot) and axle (axane). The CDs are not covalently linked to the backbone chain and have distinct translational properties. CD molecules are able to move laterally as well as transversely. The cyclic molecules form non-covalent bonds when threaded onto the backbone chain.[7] Examples of the non-covalent bonds are van der Waals and hydrophobic interactions between the interior of the CD rings and polymer chains, as well as hydrogen bonding between adjacent rings resulting from hydroxyl groups.[8] The ease of threading is therefore determined by the forces between the cyclic rings and polymer chains, i.e. the stronger the forces the better threading can occur and dethreading will be minimised. Weaker forces imply that threading of the rings is difficult and dethreading will be more probable.[9]
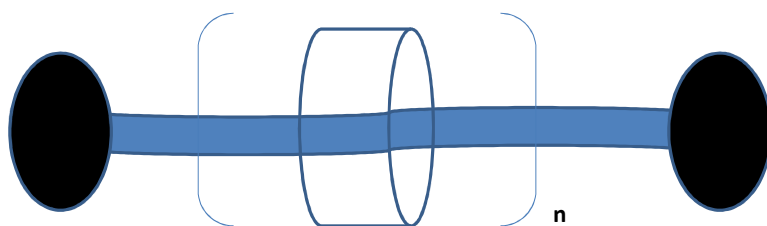
Fig. 2.5 Polyrotaxane illustration with cyclic rings and stopper molecules

Chapter 2: Theoretical background

The CD rings are prevented from being dethreaded by attachment of bulky pendant groups (stoppers) at the ends of the polymer chains. Examples of stoppers are aromatic compounds like anthracene and naphthalene. Polyrotaxanes can be synthesized via many pathways[10] and a simplified example is showed in Fig. 2.6.
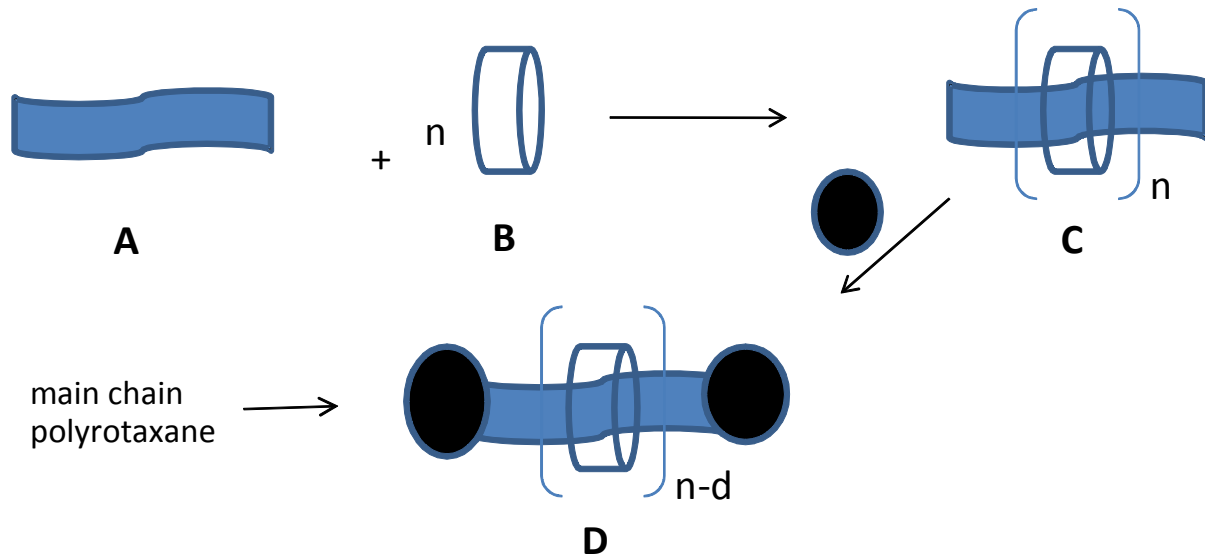
Fig. 2.6 Simplified reaction scheme of various steps in polyrotaxane synthesis: A) polymer chain, B) cyclic structures, C) pseudopolyrotaxane, D) polyrotaxane and d) number of cyclics which dethreaded before attachment of the stopper groups

Other architectures like side-chain pseudorotaxanes and side-chain polyrotaxanes are also possible where the side chains appear as branch-like structures.[10] CD-based polyrotaxanes are the most commonly investigated which include the α-, β- and γ-forms (Fig. 2.7).[11] Other cyclics include crown-ethers and calixarenes.[8,12]
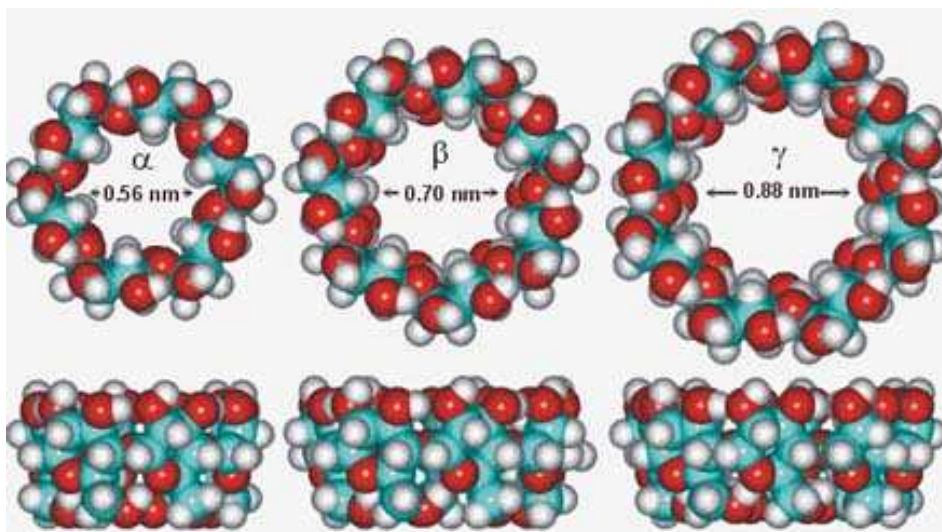
Fig. 2.7 Representation of the different cyclodextrin cavities, with α, β and γ containing 6, 7 and 8 glucose entities respectively.[11]

Chapter 2: Theoretical background

Typical applications of polytotaxanes are in light sensors, nanotechnology applications, drug delivery, tissue scaffolding, coatings and adhesives.[10] These complex polymers have been studied intensively since they were first synthesized by Harada in 1990.[7] Molar mass determinations of these compounds have been carried out typically with SEC based on polystyrene calibration. SEC can be used for the investigation of the presence of species A through to D in Fig. 2.6. It is, for example, possible to determine whether there are unreacted starting materials (A and B in Fig. 2.6) or pseudorotaxanes (C) present in solution in addition to the final obtained product D. Species A to C will therefore in effect elute at different volumes due to differences in hydrodynamic volume.

Polyrotaxanes have never been analysed by FFF until now and will be discussed in addition to SEC-MALLS characterization in Chapter 4. FFF offers several advantages for characterization of these complex molecules; one such advantage is the mild operating conditions in FFF which prevent shear degradation of polymer chains. The FFF technique is discussed in Section 2.2.2.

2.2 Characterization techniques

Polymeric materials with useful properties and well-defined molecular characteristics have become increasingly important for various applications in light-weight construction[13], alternative sources of energy[14-16], drug delivery[17,18] and automotive industry.[19] The characterization of complex polymeric materials requires accurate analytical techniques that address the various parameters of molecular heterogeneity (Fig. 2.8).
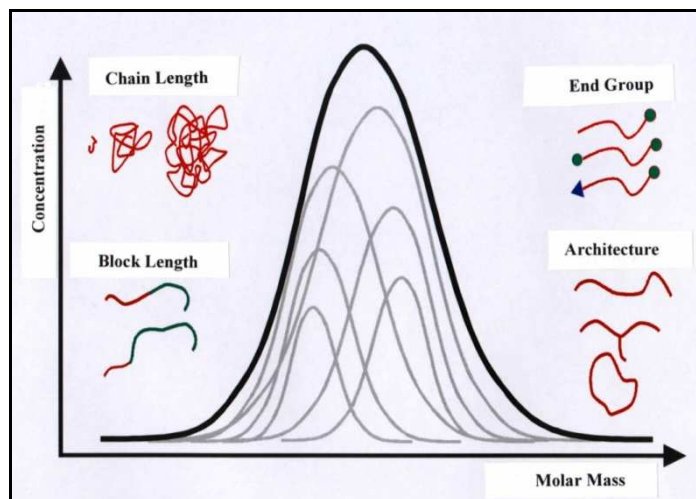
Fig. 2.8   Illustration of different heterogeneities in a complex polymer[20]

Chemical composition, molar mass, functionality type, and molecular topology[20-22] are amongst the different molecular heterogeneities and the exact knowledge about the different distributions is essential since they influence the processing and application properties to a large extent. For this reason the correct analysis of polymers which are heterogeneous in more than one distribution is a very important aspect to focus on. Liquid Chromatography (LC) or HPLC is commonly used in order to address the heterogeneities in complex polymer systems. Different modes of HPLC exist which include size exclusion chromatography (SEC), liquid adsorption chromatography (LAC), gradient

Chapter 2: Theoretical background

elution liquid chromatography (GELC) and liquid chromatography at the critical point of adsorption (LC-CC). Another technique used for fractionation is hydrodynamic chromatography (HDC) where flow effects determine separation. All of the above techniques make use of a column which is filled with either non-porous silica (glass) beads (HDC), porous silica beads or chemically modified porous particles (HPLC). The separation principle of each HPLC sub-technique differs in the interactions that take place between the sample of interest (solute molecules), the carrier liquid (mobile phase) and the stationary phase (packed column). In HDC molecules are separated according to size and flow effects (parabolic flow) govern the separation.[23-26] No form of specific interaction takes place between the solute and the silica beads. Elution is based on hydrodynamic volume and larger molecules or particles (for example colloids) elute earlier than smaller molecules. Adsorption chromatography can be divided into (i) normal phase LAC where the stationary phase is based on silica particles (polar) and a non-polar mobile phase is used, and (ii) reversed phase LAC where a non-polar stationary phase (e.g. C_8 or C_{18}) and a polar mobile phase is used.[22,27] Separation principles in HPLC are based on changes in the Gibbs free energy:

$$\Delta G = \Delta H - T\Delta S \qquad\qquad\qquad (1)$$

where ΔH, T and ΔS are the enthalpy, temperature and entropy terms, respectively. In the case of interaction chromatography (LAC) separation is based on enthalpic interactions between the solute and the stationary phase in the ideal scenario. ΔS is negligible in this case and the solute molecules can be separated according to their degree of adsorption with the stationary phase. In LAC mode molecules are separated mainly according to chemical composition. In the SEC mode of separation entropy effects are the dominant forces present and enthalpic effects are negligible in an ideal situation. In SEC molecules are separated according to their hydrodynamic volumes and the elution order is the same as in HDC. In LC-CC mode the entropy and enthalpic effects balance out and $\Delta G = 0$. LC-CC is typically used for characterization of copolymers which are difficult to classify by SEC or LAC alone. At critical conditions molecules are separated irrespective of their hydrodynamic volume and all the chains of the same chemical composition, different in molar mass elute in one peak. It is therefore possible to identify one block of a copolymer according to its chemical composition (LAC) or hydrodynamic volume (SEC) while making the other block chromatographically invisible (critical conditions). After the one block has been identified or quantified, similar conditions can be applied in order to identify the other block.[20,28,29] When these fractionation techniques are coupled to proper detectors valuable information regarding different structure-property relationships can be elucidated in order to identify the different heterogeneities and their distribution as shown in Fig. 2.8.

2.2.1 Size exclusion chromatography (SEC)

The most frequently used liquid chromatographic technique for the separation of polymers according to their hydrodynamic volume is SEC. Polymer molecules are injected into SEC columns after which they are fractionated into monodisperse (in the ideal case) fractions. Each fraction is consequently identified by coupling the column to an appropriate detector system. The packing material of the SEC column is an arrangement of small porous particles known as the stationary phase. The stationary

Chapter 2: Theoretical background

phase typically consists of cross-linked divinylbenzene particles (SDV) with a fixed particle size and mixed pore size distribution also known as mixed-bed columns. The separation range for SDV mixed-bed columns usually spans from oligomers (mixed E: 162–30000 g/mol) up to very high molar masses (mixed A: >10 million g/mol). SDV stationary phases are the most commonly used in practice for organic mobile phases while poly(hydroxyethyl methacrylate) (HEMA) columns are used for aqueous applications.[2] Other stationary phases also exist where pore sizes are fixed and have to be connected in series with other columns of different pore sizes to extend the separation range of the columns. The particles can also be made of other cross-linked materials such as cyclodextrins, polyacrylamide and poly(vinyl alcohol) gels.[2] Mixed-bed columns are more popular since the mixed pore sizes instantaneously provide a wider separation range compared to columns with fixed pore sizes, resulting in possible cost reduction in column set costs. The elution volume of a given polymer molecule is given by:

$$V_e = V_0 + K_d V_i \tag{2}$$

where V_o and V_i are the total volume of the solvent outside and inside of the pores, respectively (Fig. 2.9), and K_d the distribution coefficient which is equal to the ratio of the concentration of the solute in the stationary phase and mobile phase, respectively. The total volume of the mobile phase is given by

$$V_t = V_0 + V_i \tag{3}$$
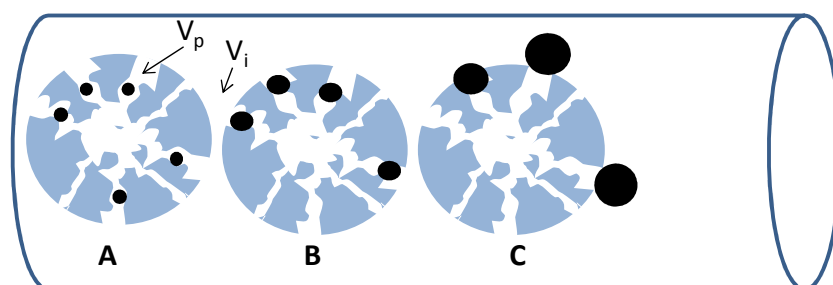
Fig. 2.9   Figurative illustration of SEC stationary phase pores with A) total permeation, B) retention, C) partial retention and total exclusion, with an indication of the pore (V_p) and interstitial (V_i) volumes, respectively

K_d ranges from 0 to 1 with $K_d = 0$ indicating that molecules elute with the void volume V_o which is the limit of total exclusion. This means that the molecules are too big to penetrate the pores of the stationary phase no matter how many conformational changes (entropy changes) the polymer chains undergo. This results in no retention and total exclusion of the molecules takes place.

When $K_d = 1$ molecules are too small compared to the pore size and can penetrate all the pores with equal probability since the polymer chains do not need to undergo any conformational changes in order access the pores. As a result total permeation occurs and the molecules elute with the solvent peak which is the total solvent volume V_t of the column. Therefore:

$$V_e = V_0 \ \ \text{for } K_d = 0 \ \text{ and} \tag{4}$$

Chapter 2: Theoretical background

$$V_e = V_t \quad \text{for } K_d = 1 \tag{5}$$

In order to get sufficient separation the desired K_d should typically be between 0 and 1 so that the elution volume V_e of the polymer peak is well resolved from the exclusion and permeation limits, V_o and V_t, respectively. It is therefore important to choose a column set in such a way that it covers the whole molar mass range for the sample in question. The elution volume of an unknown sample is usually converted back to molar mass from an existing calibration curve of well-known reference materials and is discussed in detail in literature (Fig. 2.10).[2,30]
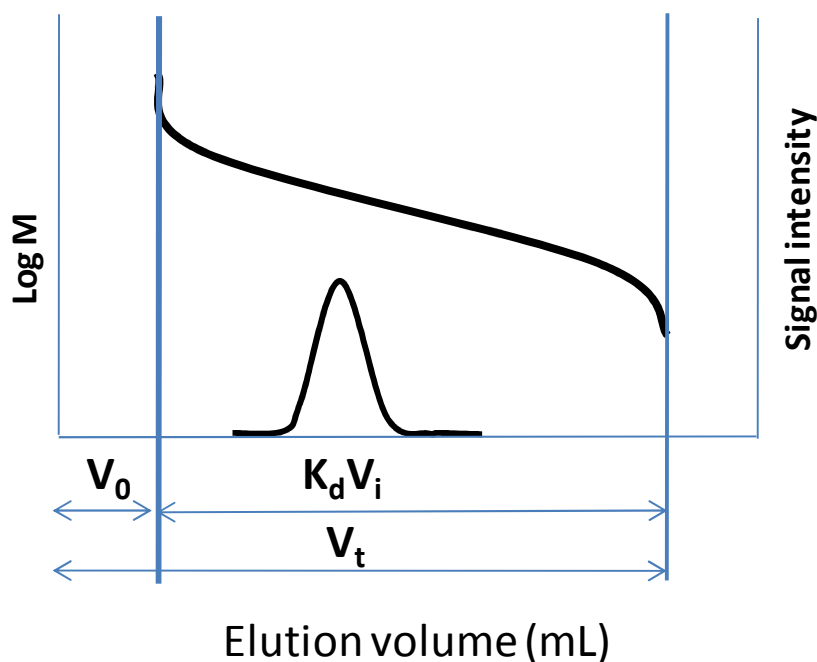
Fig. 2.10 Diagram of the exclusion and permeation limits in SEC as well as a typical calibration curve of a well known reference material

Each elution slice of the chromatogram in question is related back to molar mass from the obtained calibration curve and the subsequent signal intensity- and weight fraction (w_i) vs. molar mass plots can be deduced respectively. This is the most common procedure for determining molar masses from SEC when the calibration method is utilized.

In reality, adsorption effects (enthalpic interactions, $\Delta H \neq 0$) cannot be ignored in SEC mode since interactions between the solute and the stationary phase packing will definitely affect the separation. Adsorption effects in SEC cause complications in molar mass determinations since even a small degree of interaction can lead to wrong interpretation of results. Peak broadening due to column insufficiency, diffusion effects or inadequate separation can also lead to erroneous molar mass calculations. These form part of the secondary SEC mechanisms or non-size exclusion effects that influence the separation in some way.[2]

To summarize, the difference in hydrodynamic volume of polymer molecules in SEC leads to different residence times of macromolecules inside the pores. Macromolecules with a large hydrodynamic volume will be excluded from the pores of the stationary phase and as a result will have a shorter path

length through the stationary phase of the column. Macromolecules with a smaller hydrodynamic volume are able to access the pores more readily and will therefore have a longer residence time inside the column. As a result the molecules with the largest hydrodynamic volume will elute earlier than the molecules of smaller hydrodynamic volume.[22,31-33]

As mentioned before, SEC is the most prominent method for the analysis of MMDs.[20,22,31-34] SEC coupled to a concentration detector such as a refractive index (RI) or ultraviolet (UV) detector together with well-characterized calibration standards are commonly used for the determination of relative molar mass (M_w, M_n, M_p) values. When SEC is coupled to molar mass sensitive detectors such as viscometer or light scattering detectors, absolute molar masses and radii of gyration (R_g) can be determined.[35] Additional information regarding molecular conformation and branching can be elucidated,[36,37] making molar mass sensitive detectors more useful compared to the classical approach where a calibration curve is used.[2,35]

Unfortunately SEC has limitations when it comes to the analysis of very high molar mass and highly branched macromolecules. When analysing such materials by SEC poor separation, shear degradation and co-elution of linear and branched macromolecules of high and low molar mass can be observed.[32,33,38] Very strong shear forces in the stationary phase or at the column frits cause degradation of high molar mass macromolecules[6,33,36,39-43] resulting in incorrect molar mass calculations. Another problem is the late elution effect in SEC which is a common occurrence for excessively branched macromolecules. Co-elution takes place due to a portion of the highly branched species being retained unusually longer on the stationary phase as compared to linear macromolecules.[6,35,36,44-49] Based on some of these disadvantages, alternative separation methods are required that minimize shear degradation and co-elution effects. Field flow fractionation (FFF) is an alternative technique which will be discussed in the following section.

2.2.2 Field flow fractionation (FFF)

Field flow fractionation (FFF) has been widely investigated over the years and several publications have proven that FFF is a novel technique for the characterization of polymers. The FFF technique was developed by J.C. Giddings in 1966 and enables the existing molar mass range for size separation to be extended. FFF offers the possibility to analyze a wide variety of macromolecules and particles ranging from the nanometer to the micrometer range with high resolution.[33,50-52] FFF consists of a family of sub-techniques and in each case separation is achieved by applying an external field which is perpendicular to the longitudinal or inlet flow.[50-52] In flow FFF (FlFFF), separation takes place according to diffusion coefficient differences while in thermal FFF (ThFFF) separation is achieved due to differences in thermal diffusivity and diffusion coefficient.[50] Centrifugal or sedimentation FFF (CF3 or SdFFF) separates according to diffusion coefficient as well as density differences.[50] These three FFF techniques have been used extensively over the past twenty to thirty years and are the most popular amongst all FFF techniques. Other FFF techniques are electrical FFF (ElFFF), hollow fibre FFF (HFFFF) as well as SPLITT FFF.[50]

Chapter 2: Theoretical background

A few advantages of FFF over SEC are:

1) no stationary phase is present, so shear degradation is strongly minimized,[50,53]

2) the very low surface area of the accumulation wall in FFF avoids unwanted adsorption and secondary separation effects,[50,54]

3) filtration is not necessary, since an open channel is used,[40,55]

4) the exclusion limit is at least two orders higher than in the case of SEC,[50]

5) complex mixtures of suspended particles, gels and soluble polymers can be analysed in one measurement,[50] and

6) working conditions in FFF are conducive for the analysis of sensitive molecules that degrade easily.[53]

In FFF separation is achieved by applying a field force U on the molecules of interest.   A counteracting motion of diffusion occurs in the opposite direction of U resulting in a net flux J. D and U are both concentration dependent:

$$J = Uc - D\frac{dc}{dx} \tag{6}$$

A separation scheme is depicted in Fig. 2.11:
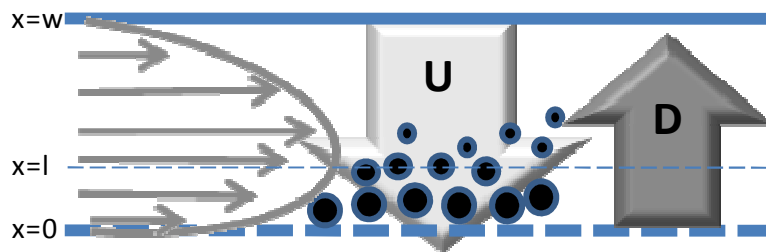
Fig. 2.11   Depiction of an induced field U and counteracting diffusion D in FFF. x = 0 represent the accumulation wall while x=w is the channel thickness and l the mean layer thickness

After a steady state condition where the two effects U and D cancel each other out, the net flux J = 0 and

$$Uc = D\frac{dc}{dx} \tag{7}$$

By means of integration and substituting the boundary values a concentration profile is obtained with

$$c(x) = c_0\, e^{\left(\frac{-|U|}{D}\right)x} \tag{8}$$

Chapter 2: Theoretical background

where c_o is the solute concentration at the membrane wall or accumulation wall, U is the applied force velocity and D the diffusion coefficient of the solute. As a result of the concentration gradient, the concentration decreases exponentially as the solute molecules reside further away from the accumulation wall. The mean layer thickness of a zone of solute molecules is given by l (Fig. 2.11)

$$l = \frac{D}{U} \tag{9}$$

and the retention parameter which is related to the interaction of the field with some physiochemical property of the solute and is given by

$$\lambda = \frac{l}{w} \tag{10}$$

where w is the thickness of the channel. λ is a representation of the zone density in relation to w as well as the zone fraction of the solute layer. Therefore equation (8) can also be written as

$$c(x) = c_o e^{\left(\frac{-x}{l}\right)} = c_0 e^{\left(\frac{-x}{\lambda w}\right)} \tag{11}$$

The diffusion coefficient D and the field induced by the force U can both be related to the frictional drag f and is given by

$$D = \frac{kT}{f} \quad \text{and} \tag{12}$$

$$U = \frac{F}{f} \quad \text{respectively,} \tag{13}$$

where k,T and F are the Boltzmann constant, temperature and applied force, respectively. By substituting these two relationships in λ term the retention parameter can be expressed as

$$\lambda = \frac{l}{w} = \frac{kT}{Fw} \tag{14}$$

This is the basic equation for the retention parameter and the force F will vary depending on which FFF technique is used. Retention in FFF is based on the flow velocity v(x), the concentration of solute molecules and the field induced force, and can be described solely on the dimensionless retention parameter λ.

$$R = 6\lambda \left(\coth \frac{1}{2\lambda} - 2\lambda \right) \tag{15}$$

R can also be described in terms of retention time in FFF and is related to the ratio of an unretained component t_o to the retention time of the solute t_r and is defined by

Chapter 2: Theoretical background

$$R \ = \frac{t_0}{t_r} = 6\lambda\left(\coth\frac{1}{2\lambda} - 2\lambda\right) \tag{16}$$

For λ close to zero R can be approximated to R ~ 6λ. Therefore t_r can be expressed as a function of t_o and the retention parameter λ:

$$t_r = \frac{t_0}{6\lambda} = \frac{|F|wt_0}{6kT} \quad \text{for } \lambda <<< 1 \tag{17}$$

This is the principle of separation for normal mode elution in FFF. The retention parameter and the field force F differ for each sub-technique of FFF and are briefly tabulated in Table 2.1 below for the commercialised techniques:[56]

Table 2.1   Commercial FFF techniques with corresponding external fields.[56]

FFF technique	Force (F)	Variables
Normal mode AF4	$= f\lvert U\rvert = \dfrac{kT\lvert U\rvert}{D} = 3\pi\eta\lvert U\rvert d$	η-viscosity of mobile phase d- diameter of molecule or particle D-diffusion coefficient U-field induced velocity
Thermal FFF (ThFFF)	$= kT\dfrac{D_T}{D}\dfrac{dT}{dx}$	D_T - thermal diffusion coefficient dT/dx - temperature drop between hot and cold walls
Centrifugal FFF(CF3)	$= m'G = V_p\lvert\Delta p\rvert G = \dfrac{\pi}{6d^3}\lvert\Delta p\rvert G$	m'- effective mass V_p- particle volume Δp- difference in density between particle and mobile phase G-gravitational force

Now that the different fields have been identified the basic retention equations can be deduced for each applied technique.[51] The perpendicular external field in AF4 is in the form of a cross-flow, and the force at which the cross-flow approaches the accumulation wall is related to a flow velocity U

which is equal to the ratio of the cross-flow $\dot{V_c}$ and area of accumulation wall A_{aw}. A_{aw} is equal to ratio of the volume of the channel V_o to the channel thickness w. By substituting the above parameters into the expression λ=D/Uw one obtains:

$$\lambda = \frac{DV_0}{\dot{V}_c \, w^2}$$

(18)

and since t_r is related to $t_o/6\lambda$

$$t_r = \frac{w^2 \dot{V}_c}{6D\dot{V}_{out}}$$

(19)

where $\dot{V}_c \big/ t_0$ is equal to the flow rate of the channel $\dot{V}_{out}$. This is however the case for symmetrical flow FFF. The cross-flow at the non-permeable wall is negligible for AF4 (asymmetrical FFF), therefore t_r is a logarithmic function of $\dot{V}_{out}$ and $\dot{V}_c$ and is given by:

$$t_r = \frac{w^2}{6D} \ln\left(1 + \frac{\dot{V}_c}{\dot{V}_{out}}\right)$$

(20)

The FFF technique used for this particular study is asymmetric flow field flow fractionation (AF4), where the external field is in the form of a cross-flow (Fig. 2.12, bottom). Separation takes place inside an empty channel which usually has a trapezoid geometry (Fig. 2.12, top).[57] The channel geometry is a cut-out from a spacer which is situated between two stainless steel plates that are bolted together. Asymmetry is realised due to the fact that the top plate is impermeable while the bottom plate is permeable by means of an imbedded porous frit (Fig. 2.12, top). The porous frit is covered by a semi-permeable membrane, also known as the accumulation wall. The membrane acts as a filter for the cross-flow so that only the solvent molecules can pass through and not the solute molecules. The average molar mass cut-off of the membrane is typically about 1kg/mol and 10kg/mol for aqueous and organic mobile phases, respectively. On top of the membrane is the spacer that can vary in its thickness (127 – 508 μm), depending on the required separation range.[50]

The high aspect ratio (length compared to breadth) inside the channel allows a laminar flow with a parabolic flow profile.[33] The flow velocity goes from a maximum in the centre of the channel approaching zero near the accumulation wall (Figs. 2.12 and 2.13). An external cross-flow field is applied perpendicular to the solvent flow inside the channel. The cross-flow forces the solute molecules towards the accumulation wall. Molecular diffusion, which is related to Brownian motion, generates a counteracting motion.[50]

Chapter 2: Theoretical background
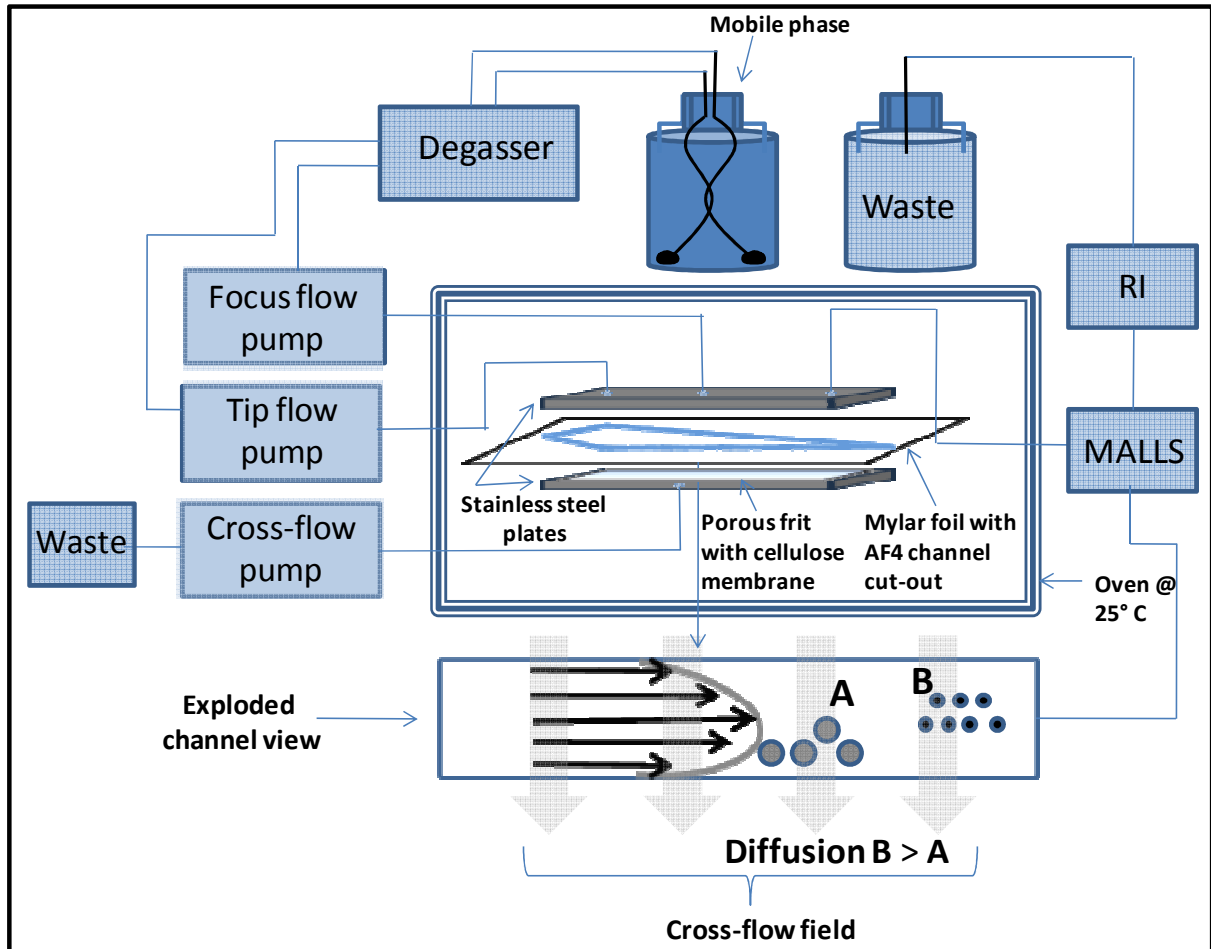
Fig. 2.12 AF4 instrumentation setup at Stellenbosch University with an a cross-section view of the channel at the bottom

While the cross-flow is active, a focus flow from the centre of the channel counteracts the longitudinal flow (Fig. 2.13). The focus flow prevents diffusion in the longitudinal direction minimizing axial band broadening. After a set time of focus or relaxation is applied the focus flow is switched off and the molecules in their respective flow velocity zones will elute towards the outlet of the channel to the detectors. The diffusion coefficient for smaller molecules is normally larger than for bigger molecules. As a result the smaller molecules will equilibrate (reach a position of steady state) further from the accumulation wall than the larger molecules (Fig. 2.13). Different flow velocities in the flow layers lead to a separation of molecules. The elution order for the normal mode of separation in AF4 is from small to larger molecules, which is reversed to the separation order known from SEC. It is therefore possible to selectively retain molecules of different sizes by adjusting the cross-flow profile accordingly.
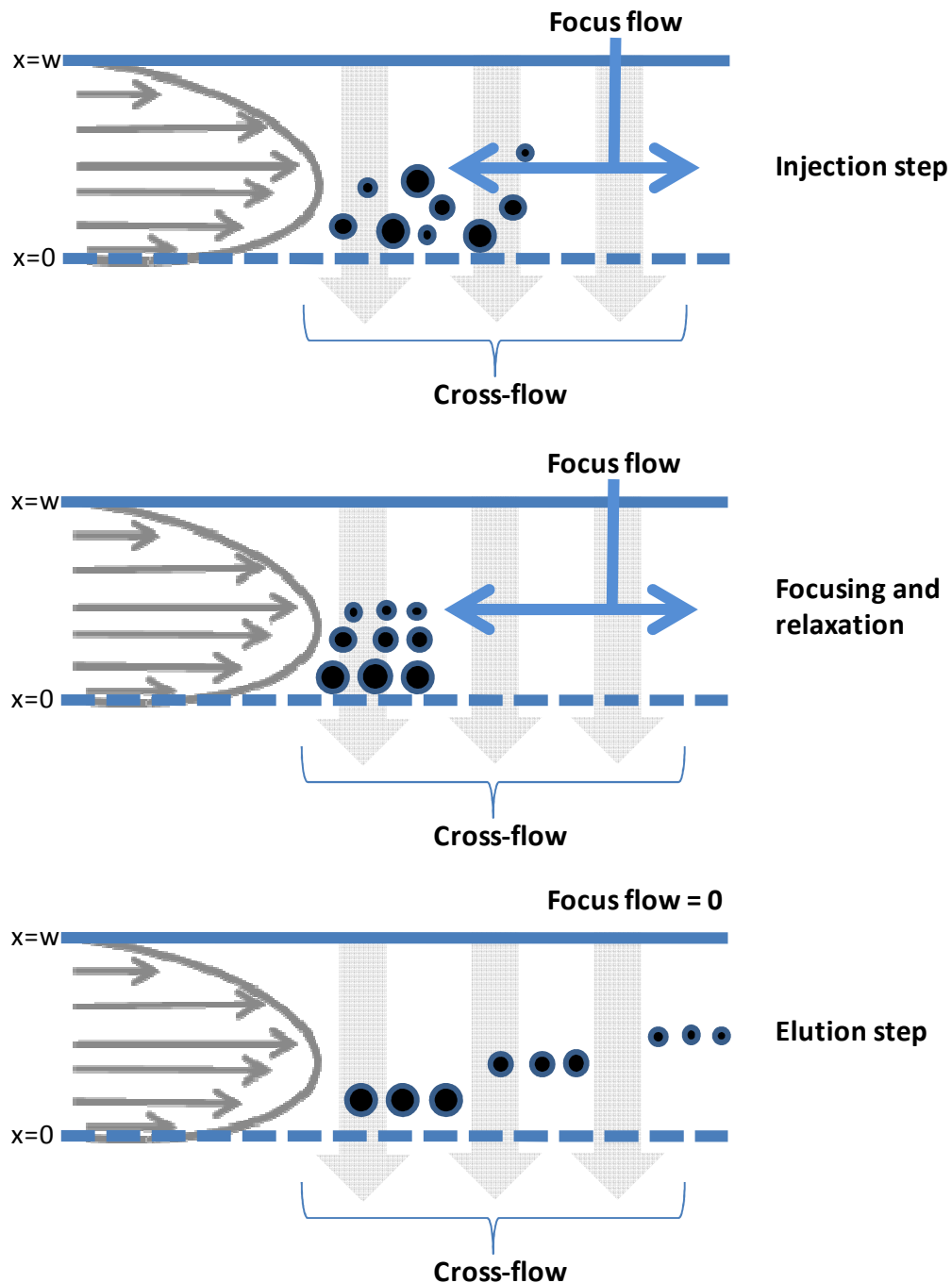
Fig. 2.13 Illustration of injection, focusing and elution steps in normal mode AF4

The two other modes of separation in AF4 are steric and hyper-layer modes[50,56] which are depicted in Fig. 2.14. In steric mode the elution mode is opposite to normal-mode elution, that is larger molecules elute first. In steric mode, molecules are usually in excess of 1 µm, diffusion effects are negligible and separation is based on the closest approach to the accumulation wall. The cross-flow forces molecules against the accumulation wall and diffusion away from the wall is highly unlikely due to the small diffusion coefficients of the large molecules. Portions of the larger micrometer molecules end up in faster flow velocity layer of the parabolic flow profile, and as a result will elute earlier than smaller molecules that are able to approach the accumulation wall more closely.

Chapter 2: Theoretical background

In hyper-layer mode a very high cross-flow field causes the larger molecules to bounce off the accumulation wall resulting in molecules ending up a short distance away from the wall. The elution behaviour is the same as in steric mode (larger molecules first) and it is therefore difficult to distinguish between steric and hyper-layer modes.[2,33,51]
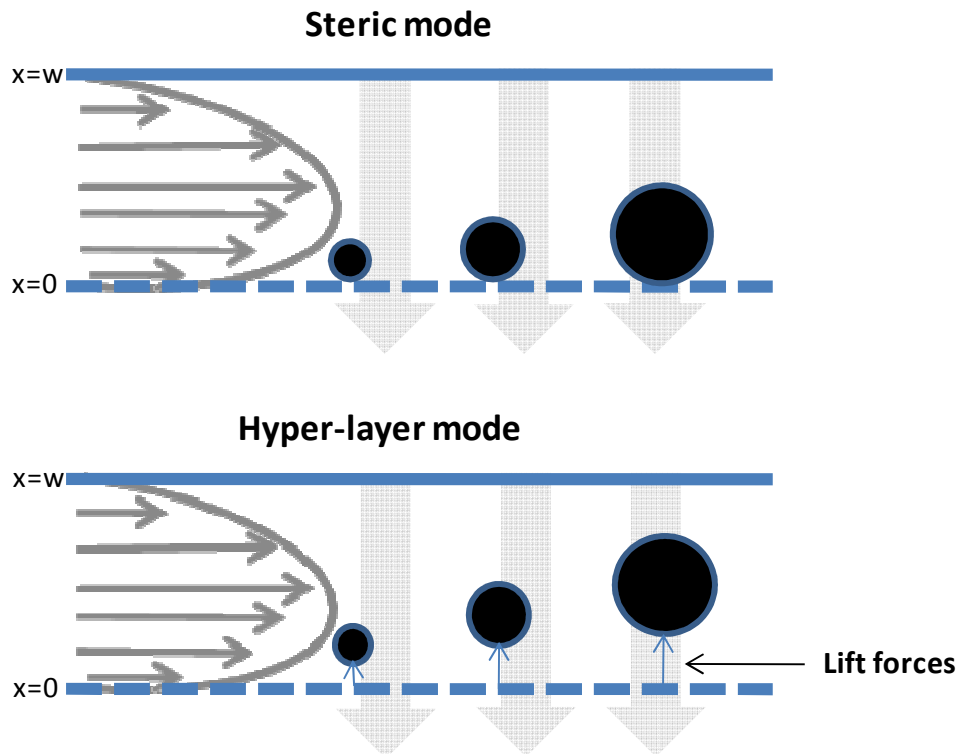
Fig. 2.14   Diagram of steric and hyper-layer modes in AF4

AF4 was initially implemented for aqueous based applications. Examples are in the biomedical, pharmaceutical, environmental and food science application fields. Water-soluble polymers such as polyacrylamides, polysaccharides (starches), and various proteins have been of primary focus for AF4.[58-60]

Organic mobile phase applications were a problem in the past due to the instability (dissolution or degradation) of the aqueous membranes and the application was only introduced by Kirkland[61] on PS and PEO standards using regenerated cellulose membranes. Various membranes for organic mobile phase applications have been developed since resulting in AF4 being the most versatile and robust compared to other FFF techniques. High temperature AF4 (HT-AF4) instruments for the analysis of crystalline polymers such as polyolefins have become available for high temperature solvents such as trichlorobenzene (TCB).[37,40,45,62]

Organo-soluble polymers have been investigated predominantly by ThFFF since no membranes are used and no significant interaction or adsorption takes place between sample molecules and the plates of the empty channel. Only a few aqueous applications on ThFFF have been reported.[63-65]

Chapter 2: Theoretical background

ThFFF is used for synthetic organo-soluble polymers especially in the elastomer field where ultrahigh molar mass (UHMM) polymer fractions might be present as well as insoluble gel fractions. The elastomer fractions may also be branched which will influence the structure-property relationship of these polymeric materials. ABS resins were separated by Shiundu et al. in THF in order to separate the soluble polymer fraction from the insoluble gel fraction.[66] Similarly van Asten was able to separate polybutadienes of different molar masses from each other in toluene.[67] In addition three polymers with similar hydrodynamic volumes but different chemistries were successfully separated proving that ThFFF can separate according to hydrodynamic volume as well as chemical composition. Several other elastomeric rubbers have been investigated by ThFFF.[38,53,68-71]

SBS and PB rubbers amongst others are some of the few elastomeric polymers already been analysed by AF4. SBR rubbers have been investigated and it was shown that it is possible to separate free and functionalised SBR from each other, i.e. the free SBR rubber was separated from coupled (high molar mass) SBR rubber.[72] The presence of branching and gel species in UHMM polybutadienes were successfully identified which in contrast was not possible in SEC due to shear degradation, filtration, and abnormal elution behaviour caused by co-elution of branched polymers together with their regular eluting linear counterparts.[40]

Based on the few applications mentioned above FFF, especially AF4 and ThFFF, is a superior tool in areas where SEC fails as discussed in Section 2.2.1.

2.3 Detectors

In order to track the progress of polymer molecules through any separation system, some form of detection system is required. The most important detectors for the characterization of macromolecules are differential refractive index (DRI), evaporative light scattering (ELSD), ultraviolet (UV), light scattering (LS), infrared (IR) and differential viscometer (DV) detectors. Each detector represents some form of physicochemical property of the solute molecules in question.[2] Concentration detectors like DRI and UV are dependent on the concentration of the solute molecules in the mobile phase while molar mass sensitive detectors like LS and DV are proportional to the product of concentration and molar mass. Detection limits play a very important role when quantifying chromatograms in the case of SEC or fractograms in FFF. The detection limit is related to the signal-to-noise ratio which is defined as the ratio of the eluted peak to the baseline noise.[2] This ratio should be high enough in order to avoid any discrepancies in quantification of the analysed molecules. The molecules of the polymer of interest can show different responses for different detectors for example a polydisperse polymer consisting of small quantities of very high molar masses as well as large fractions of smaller molar masses. When dual detection like RI and LS is applied for the polydisperse polymer the RI detector response will show a larger intensity for the molecules that are highest in concentration (small molar masses) compared to the high molar mass species which are less abundant. The LS detector response will show the exact opposite whereby the smaller molar mass molecules will show a weaker detector response compared to the high molar mass molecules. This phenomenon is due to the difference response factors of the two detectors.

2.3.1 Differential refractive index detection (DRI)

RI detectors are commonly used for the detection of the concentration of macromolecules when coupled to a separation system such as SEC, HPLC or FFF. The RI detector is a universal detector with a linear concentration dependence. Since the measurement is based on differences in refractive index, different polymers (with different refractive indexes) will have different detector responses. For example, when two polymers of distinct molecular properties such as PS and PMMA are dissolved in THF and the RI response is plotted as a function of concentration (Fig. 2.15) it is observed that the slopes differ from each other.

Based on these findings it is clear that the RI signal is not only a function of concentration but also dependent on some property of the sample,[73] which is the specific refractive index increment or dn/dc.[74] This value varies for different polymers in different mobile phases[2] and is also dependent on the incident wavelength and temperature at which it is measured. The dn/dc value is very important for molar mass determinations from light scattering measurements (Section 2.3.2) as an error in the dn/dc value will cause a large error equal to $(dn/dc)^2$ in molar mass calculations.
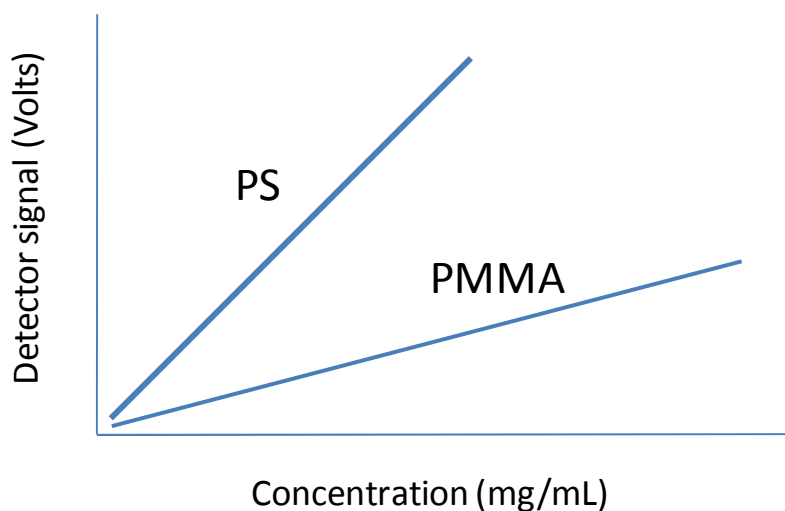
Fig. 2.15 Plot of RI detector response for PS and PMMA dissolved in THF as a function of concentration

2.3.2 Multi-angle laser light scattering detection (MALLS)

Molar mass sensitive detectors for polymers in solution are a promising attribute when coupled to SEC or FFF systems. The most commonly used detectors are DV and LS detectors. LS detectors yield absolute molar mass values while DV detectors need a universal calibration approach.[2] In addition to absolute molar masses and their distributions, LS also yields information regarding the size of a molecule in solution (R_g) and can also give conformational characteristics like the degree of branching and the branching frequency per set number of carbons.[35]

23

Chapter 2: Theoretical background

LS detectors can be classified as static and dynamic light scattering detectors (SLS and DLS). SLS detectors are different from each other due to difference in the number of angles per detector. Examples are right, dual-, low- and multi-angle laser light scattering detectors (RALLS, DALLS, LALLS and MALLS), respectively. Fig. 2.16 shows an illustration of an 18-angle MALLS detector.
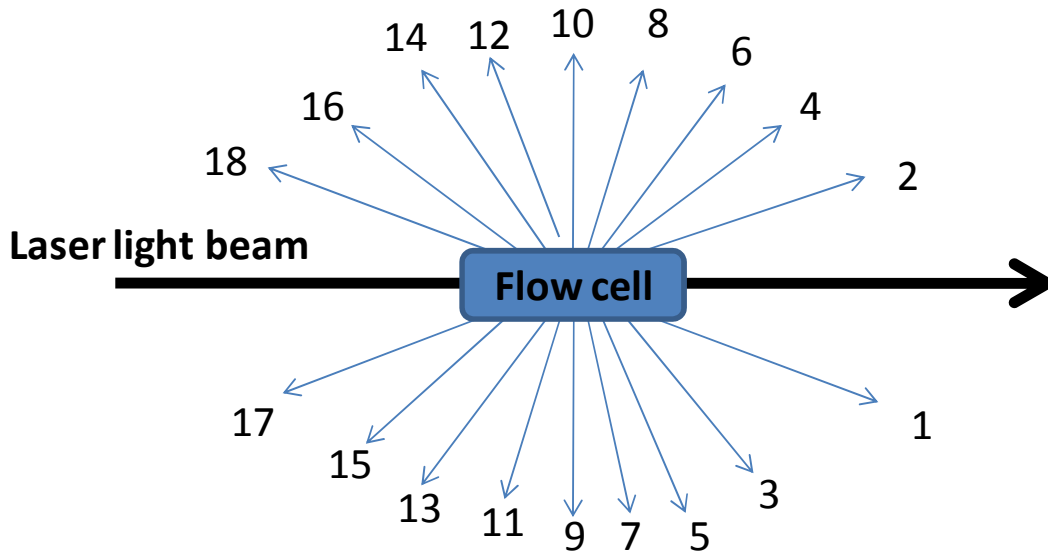
Fig. 2.16   Setup of an 18-angle MALLS detector with angles ranging from 22.5° to 147°

The most common equation used for light scattering is the Debye equation and is given by

$$\frac{R_\theta}{K^* c} = M_w P(\theta) - 2 A_2 c M_w^{\,2} P^2(\theta) \tag{21}$$

where R_θ is the Rayleigh ratio, K^* is an optical constant, c is the polymer concentration in solution, M is molar mass, $P(\theta)$ is the particle scattering factor (function of angular dependence) and A_2 is the second virial coefficient. The optical constant is:

$$K^* = \frac{4\pi^2 n_0^2}{\lambda_0^4 N_A} \times \left(\frac{dn}{dc}\right)^2 \tag{22}$$

where n_0 is the refractive index of the solvent, dn/dc the specific refractive index increment, λ_0 is the wavelength of the incident light and N_A Avogadro's number.[2,75,76] A_2 provides an indication of the thermodynamic quality of the solvent and is equal to zero for theta solvents, positive for good solvents and negative for poor solvents. By plotting R_θ/K^*c vs. $\sin^2(\theta/2)$, information regarding molar mass and R_g can be obtained. The intercept of each plot extrapolated to the zero angle ($\theta=0$) is proportional to M_w while the slope of the obtained plot is related to R_g. In addition, information regarding molar mass and radius averages as well as their distributions can be obtained by coupling LS and RI to a separation system such as SEC or FFF.

Conformational information such as the degree of branching can also be accessed by means of the conformational plot which is the log-log plot of R_g vs. molar mass. The slope of the conformation plot

varies between 0 and 1 and the value for a typical linear random coil is 0.588 in a good solvent.[47] The slope decreases if branching is present in a polymer dissolved in a good solvent.

The major advantages of a MALLS detector coupled to FFF and SEC systems are that no calibration curve needs to be constructed and due to absolute detection obtained; size and molar mass information from the fractionated species eluting from the column (SEC) or channel (FFF) are true representations. It is possible to differentiate between homopolymers and copolymers in solution given that the two are different in hydrodynamic volume, especially in the case where the quantity in solution is so small that not significant RI signal is visible.

Some of the disadvantages are that MALLS detectors generally can only produce accurate results down to polymer molecules that are about 1/20th of the incident wavelength which corresponds to approximately 30 000 g/mol.[76] Below this size all the molecules scatter light equally in all the directions and all the angles detect the same scattering intensity. Light scattering of molecules below this size is known as isotropic scattering.[2,35]

When polymer blends are analysed by SEC or FFF (AF4 in particular) and coupled to MALLS, it would be difficult to distinguish between two chemically different species which have the same hydrodynamic volume. Both SEC and AF4 separate molecules according to hydrodynamic volume, therefore one polymer peak would be observed for each fractionation technique if no significant size differences between the two homopolymers are present. The specific refractive index increment (dn/dc) is an important parameter to consider for molar mass determinations. In copolymers specifically, chemically different species will contribute differently towards the total dn/dc value. The weight percentage of the each comonomer and the dn/dc of each homopolymer play a significant role for the determination of the total dn/dc value.[2] The copolymer type (random, block or alternating) also plays a significant role for dn/dc determinations. In addition the wavelength, temperature and the solvent used will influence the dn/dc value.[2]

Chapter 2: Theoretical background

2.4 References

(1)   Pires N. M. T.; Ferreira A. A.; de Lira C. H.; Coutinho P. L. A.; Nicolini L. F.; Soares B. G.; Coutinho F. M. B. *J. Appl. Polym. Sci.* **2006**; 99, 88–99.

(2)   Podzimek S. *Light Scattering, Size Exclusion Chromatography and Asymmetric Flow Field Flow Fractionation: Powerful Tools for the Characterization of Polymers, Proteins and Nanoparticles.* New York: John Wiley & Sons; **2011**.

(3)   Gaborieau M.; Castignolles P. *Anal. Bioanal. Chem.* **2010**; 399(4), 1413-1423.

(4)   Hjertberg T.; Kulin L. I.; Sörvik E. *Polym. Test.* **1983**; 3(4), 267-289.

(5)   Mitra S.; Ghanbari-Siahkali A.; Kingshott P.; Hvilsted S.; Almdal K. *Appl. Surf. Sci.* **2006**; 252(18), 6280-6288.

(6)   Stadler F. J.; Kaschta J.; Münstedt H.; Becker F.; Buback M. *Rheol. Acta* **2009**; 48, 479-490.

(7)   Harada A.; Kamachi M. *Macromolecules* **1990**; 23(10), 2821-2823.

(8)   Wenz G.; Han B.-H.; Müller A. *Chem. Rev.* **2006**; 106(3), 782-817.

(9)   Zhao T.; Beckham H. W. *Macromolecules* **2003**; 36(26), 9859-9865.

(10)   Huang F.; Gibson H. W. *Prog. Polym. Sci.* **2005**; 30(10), 982-1018.

(11)   http://www.lsbu.ac.uk/water/cyclodextrin.html.

(12)   Li Y.; Ji L.; Wang G.; Song L.; He B.; Li L.; Nie Y.; Wu Y.; Gu Z. *Science China Chemistry* **2010**; 53(3), 495-501.

(13)   Halliwell S. *Polymers in building and construction.* Shawbury, Shrewsbury, United Kingdom: Rapra Technology Ltd.; **2002**.

(14)   Gurunathan K.; Murugan A. V.; Marimuthu R.; Mulik U. P.; Amalnerkar D. P. *Mater. Chem. Phys.* **1999**; 61(3), 173-191.

(15)   Heeger A. J. *Synth. Met.* **2001**; 125(1), 23-42.

(16)   Mark J. E. *Polymer data handbook.* New York: Oxford University Press; **1999**.

(17)   Grayson A. C. R.; Choi I. S.; Tyler B. M.; Wang P. P.; Brem H.; Cima M. J.; Langer R. *Nat Mater* **2003**; 2(11), 767-772.

(18)   Yoon H.-J.; Jang W.-D. *J. Mater. Chem.* **2010**; 20(2), 211-222.

(19)   Narula C. K.; Allison J. E.; Bauer D. R.; Gandhi H. S. *Chem. Mater.* **1996**; 8(5), 984-1003.

(20)   Pasch H. *Adv. Polym. Sci.* **2000**; 150, 1-66.

(21)   Mourey T. H. *Int. J. Polym. Anal. Charact.* **2004**; 9(1), 97 - 135.

(22)   Philipsen H. J. A. *J. Chromatogr. A* **2004**; 1037(1-2), 329-350.

(23)   Brewer A.; Striegel A. M. *Anal. Bioanal. Chem.* **2009**; 393(1), 295-302.

(24)   Small H. *J. Colloid Interface Sci.* **1974**; 48(1), 147-161.

(25)   Small H.; Langhorst M. A. *Anal. Chem.* **1982**; 54(8), 892A-898A.

(26)   Stegeman G.; Kraak J. C.; Poppe H.; Tijssen R. *J. Chromatogr. A* **1993**; 657(2), 283-303.

(27)   Pasch H.; Esser E.; Kloninger C.; Iatrou H.; Hadjichristidis N. *Macromol. Chem. Phys.* **2001**; 202(8), 1424-1429.

(28)   Esser K. E.; Braun D.; Pasch H. *Angew. Makromol. Chem.* **1999**; 271(1), 61-67.

(29)   Lee W.; Park S.; Chang T. *Anal. Chem.* **2001**; 73(16), 3884-3889.

(30)   Kuo C.-Y.; Provder T. *ACS Symp. Ser.* **1987**; 352, 2-28.

Chapter 2: Theoretical background

(31)   Barth H. G.; Boyes B. E.; Jackson C. *Anal. Chem.* **1998**; 70(12), 251-278.

(32)   Kostanski L. K.; Keller D. M.; Hamielec A. E. *J. Biochem. Bioph. Methods* **2004**; 58(2), 159-186.

(33)   Messaud F. A.; Sanderson R. D.; Runyon J. R.; Otte T.; Pasch H.; Williams S. K. R. *Prog. Polym. Sci.* **2009**; 34(4), 351-368.

(34)   Trathnigg B. In: Meyers R. A., (ed). *Encyclopedia of Analytical Chemistry*. Chichester, United Kingdom: John Wiley & Sons; **2000**; p. 8008-8034.

(35)   Wyatt P. J. *Anal. Chim. Acta* **1993**; 272(1), 1-40.

(36)   Angoy M.; Bartolomé M. I.; Vispe E.; Lebeda P.; Jiménez M. V.; Pérez-Torrente J. J.; Collins S.; Podzimek S. *Macromolecules* **2010**; 43(15), 6278-6283.

(37)   Otte T.; Klein T.; Brüll R.; Macko T.; Pasch H. *J. Chromatogr. A* **2011**; 1218(27), 4240-4248.

(38)   Lee S.; Molnar A. *Macromolecules* **1995**; 28(18), 6354-6356.

(39)   Aust N. *J. Biochem. Bioph. Methods* **2003**; 56, 323-334.

(40)   Otte T.; Pasch H.; Macko T.; Brüll R.; Stadler F. J.; Kaschta J.; Becker F.; Buback M. *J. Chromatogr. A* **2011**; 1218(27), 4257-4267.

(41)   Slagowski E. L.; Fetters L. J.; McIntyre D. *Macromolecules* **1974**; 7(3), 394-396.

(42)   Zammit M. D.; Davis T. P.; Suddaby K. G. *Polymer* **1998**; 39(23), 5789-5798.

(43)   Cave R. A.; Seabrook S. A.; Gidley M. J.; Gilbert R. G. *Biomacromolecules* **2009**; 10(8), 2245-2253.

(44)   Gerle M.; Fischer K.; Roos S.; Muller A. H. E.; Manfred S. *Macromolecules* **1999**; 32, 2629-2637.

(45)   Mes E. P. C.; de Jonge H.; Klein T.; Welz R. R.; Gillespie D. T. *J. Chromatogr. A* **2007**; 1154(1-2), 319-330.

(46)   Percec V.; Ahn C. H.; Cho W. D.; Jamieson A. M.; Kim J.; Leman T.; Schmidt M.; Gerle M.; Möller M.; Prokhorova S. A.; Sheiko S. S.; Cheng S. Z. D.; Zhang A.; Ungar G.; Yeardley D. J. P. *J. Am. Chem. Soc.* **1998**; 120, 8619-8631.

(47)   Podzimek S.; Vlcek T.; Johann C. *J. Appl. Polym. Sci.* **2001**; 81(7), 1588-1594.

(48)   Johann C.; Kilz P. J. *J. Appl. Polym. Sci.: Appl. Polym. Symp.* **1991**; 48, 111-122.

(49)   Wintermantel M.; Antonietti M.; Schmidt M. *J. Appl. Polym. Sci.: Appl. Polym. Symp.* **1993**; 52, 91-103.

(50)   Schimpf M. E.; Caldwell K.; Giddings J. C. *Field Flow Fractionation Handbook*. New York: John Wiley & Sons; **2000**.

(51)   Cölfen H.; Antonietti M. *Adv. Polym. Sci.* **2000**; 150, 67-187.

(52)   Janca J. Field-flow fractionation.In: Heftmann E., (ed). *J. Chromatogr. Libr.* Amsterdam: Elsevier; **1992** p. A449-A479.

(53)   White R. J. *Polym. Int.* **1997**; 43(4), 373-379.

(54)   Liu Y.; Radke W.; Pasch H. *Macromolecules* **2006**; 39(5), 2004-2006.

(55)   Moon M. H. *J. Sep. Sci.* **2010**; 33(22), 3519-3529.

(56)   Giddings J. C. *Science* **1993**; 260(5113), 1456-1465.

(57)   Ahn J. Y.; Kim K. H.; Lee J. Y.; Williams P. S.; Moon M. H. *J. Chromatogr. A* **2010**; 1217(24), 3876-3880.

(58)   van Bruijnsvoort M.; Wahlund K. G.; Nilsson G.; Kok W. T. *J. Chromatogr. A* **2001**; 925(1-2), 171-182.

(59)   Rojas C. C.; Wahlund K.-G.; Bergenståhl B.; Nilsson L. *Biomacromolecules* **2008**; 9(6), 1684-1690.

(60)   Rolland-Sabaté A.; Guilois S.; Jaillais B.; Colonna P. *Anal. Bioanal. Chem.* **2011**; 399(4), 1493-1505.

(61)   Kirkland J. J.; Dilks C. H. *Anal. Chem.* **1992**; 64(22), 2836-2840.

(62)   Otte T.; Brüll R.; Macko T.; Pasch H.; Klein T. *J. Chromatogr. A* **2010**; 1217(5), 722-730.

(63)   Mes E. P. C.; Tijssen R.; Kok W. T. *J. Chromatogr. A* **2001**; 907(1-2), 201-209.

(64)   Shiundu P. M.; Munguti S. M.; Williams S. K. R. *J. Chromatogr. A* **2003**; 983(1-2), 163-176.

(65)   Shiundu P. M.; Williams S. K. R. Thermal Field-Flow Fractionation for Particle Analysis: Opportunities and Challenges. *Particle Sizing and Characterization*. Washington, D.C.: American Chemical Society; **2004** p. 185-198.

(66)   Shiundu P. M.; Remsen E. E.; Giddings J. C. *J. Appl. Polym. Sci.* **1996**; 60(10), 1695-1707.

(67)   van Asten A. C.; Venema E.; Kok W. T.; Poppe H. *J. Chromatogr. A* **1993**; 644(1), 83-94.

(68)   Lee S.; Eum C. H.; Plepys A. R. *Bull. Korean Chem. Soc.* **2000**; 21(1), 69-74.

(69)   Sibbald M.; Lewandowski L.; Mallamaci M.; Johnson E. *Macromolecular Symposia* **2000**; 155(1), 213-228.

(70)   Lohmann C. A.; Haseltine W. G.; Engle J. R.; Williams S. K. R. *Anal. Chim. Acta* **2009**; 654(1), 92-96.

(71)   Lee D.; Williams S. K. R. *J. Chromatogr. A* **2010**; 1217(10), 1667-1673.

(72)   Bang D. Y.; Shin D. Y.; Lee S.; Moon M. H. *J. Chromatogr. A* **2007**; 1147(2), 200-205.

(73)   http://www.iisrp.com/WebPolymers/00Rubber_Intro.pdf.

(74)   Maezawa S.; Takagi T. *J. Chromatogr. A* **1983**; 280(0), 124-130.

(75)   Andersson M.; Wittgren B.; Wahlund K.-G. *Anal. Chem.* **2003**; 75(16), 4279-4291.

(76)   Wyatt P. J. *J. Chromatogr. A* **1993**; 648(1), 27-32.

Chapter 3: Analysis of polybutadienes by SEC- and AF4 coupled to MALLS-RI detection

Chapter 3: Polybutadienes

3.1 Introduction

AF4 has been applied in various fields, ranging from synthetic and biological macromolecules to particles of different natures.[1] Studies of AF4 coupled to light scattering detection have been used extensively in recent years for in-depth investigations of structural parameters in addition to absolute molar mass detection. Intensive studies have been done in both aqueous[2-6] and non-aqueous[7-9] mobile phases. Since FFF is based on an empty channel configuration, sample filtration is not required and, therefore, it is possible to fractionate and identify gel containing species. [10-13]

In the present work AF4- and SEC-MALLS-RI are used to fractionate and analyze polybutadienes regarding molar mass and branching. So far, the molar mass, molar mass distribution (MMD) and size distributions of synthetic and natural rubbers have been characterized by SEC,[14-18] thermal FFF (ThFFF)[12,19-24] and AF4.[9,25,26] Industrial polybutadiene samples synthesized using Ziegler-Natta catalysts[27-29] were analysed via AF4- and SEC-MALLS. Various measurements were done regarding different aspects of these materials, in particular the effect of branching and dissolution time upon the retention time. Polystyrene standards were used as reference materials for validation of the AF4-MALLS system. For optimization of the separation process a mixture of different narrowly distributed PS standards was fractionated with different cross-flow gradients. The obtained cross-flow conditions have been used as starting conditions for separation of the more complex polybutadiene samples. Results showed that as a specialized tool, AF4 can be used for the extended and more accurate analysis of synthetic rubber materials, especially in the case of very high molar masses. The comparison of SEC and FFF showed that due to the high molar masses and branched species, SEC is not suitable enough for the complete characterisation of these polybutadienes while FFF gives more reliable results and can be used for tailoring of the size separation due to the adjustable cross-flow force.

3.2 Experimental

3.2.1 Instrumentation setup

The experiments were performed on an ambient temperature AF4-Instrument (AF2000, Postnova Analytics, Landsberg/Germany) which was coupled to a MALLS- (Dawn DSP, Wyatt Technology, Santa Barbara, USA) and a RI-detector (PN 3140, Postnova Analytics, Landsberg/Germany). The channel was connected to three different pumps (tip, focus and cross-flow) while the injection port was equipped with a manual injection valve (Rheodyne, Rohnert Park, USA). A regenerated cellulose membrane was installed for the AF4 channel with an average molar mass cut-off of 10 kg/mol. The Mylar spacer used for definition of the channel height had a thickness of 350 µm. The SEC setup consisted of a set of two PL Gel columns (mixed B and mixed C) in series. The inlet of the mixed B column was connected to the tip-pump while the outlet of the mixed C column was connected to the detectors (MALLS and RI). A schematic setup of the instrument is shown in Fig. 2.12, but a simple

representation is shown in Fig. 3.1. A mixture of both column types was chosen to ensure proper separation of low (mixed C, 5 μm particles) and medium-high molar mass components (mixed B, 10 μm particles) of the samples. In addition a mixed A column (20 μm particles) was used for comparison purposes.

3.2.2 Materials and sample preparation

Polystyrene samples used for calibration purposes were obtained from Fluka (Sigma Aldrich, South Africa), with molar masses of 62, 250 and 1000 kg/mol, respectively, and were dissolved in HPLC grade THF (Sigma Aldrich, South Africa). The concentrations of the polystyrene samples were 3 mg/mL (62 and 250 kg/mol) and 1 mg/mL (1000 kg/mol), respectively. These concentrations were used for both SEC and AF4 measurements. Each polystyrene sample was dissolved at room temperature for 4 hours without adding a stabilizer.

The polybutadiene samples used in the study had high cis-content with different polydispersities and various degrees of branching (Table. 3.1). The polybutadiene samples were dissolved in HPLC grade THF with a concentration of approximately 3 mg/mL. Butylated hydroxy toluene (BHT) obtained from Sigma Aldrich (South Africa) was added as a stabilizer (1mg/mL) to prevent oxidative degradation of the polymers. The basic dissolution procedure was to dissolve the samples for 16 hours at room temperature followed by 4 hours of heating at 50℃. This was not the optimal dissolution procedure as will be discussed later. The specific refractive index increment (dn/dc) of polystyrene and polybutadiene in THF were 0.184-[30] and 0.132[31] mL/g, respectively.
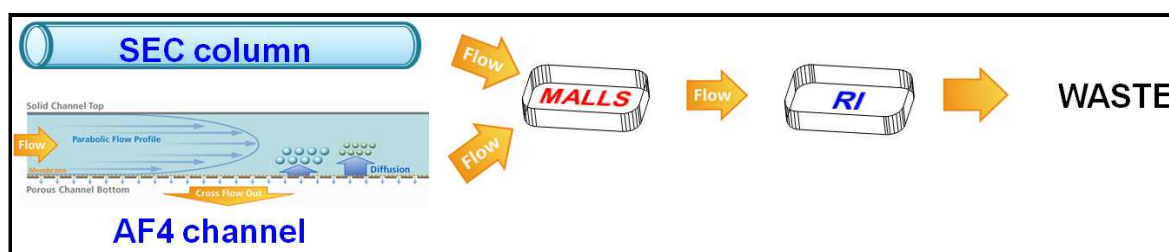
Fig. 3.1   Simplified depiction of the SEC/AF4 instrument setup, adapted from Fig. 2.12

Table 3.1   Characteristics of PB 1 – 6. Samples were polymerized with different ZN catalysts, varying in Mooney viscosity, branching, gel and polydispersities.

Sample name	Catalyst	Branching	Polydispersity	Gel
PB 1	Nd	lightly	broad	no
PB 2	Nd	lightly	broad	no
PB 3	Co	lightly	broad	no
PB 4	Nd	lightly	broad	no
PB 5	Co	heavily	broad	no
PB 6	Nd	lightly	broad	Yes

3.2.3 Analysis conditions

The samples were introduced into the channel by manual injection with a flow rate of 0.2 mL/min for a time of 4 minutes (Fig. 3.2). The low inlet flow rate was used to prevent shear degradation. While the samples were injected, the cross-flow was constant at 8.5 mL/min and the focus flow automatically adjusted to 8.8 mL/min to maintain a constant detector flow rate of 0.5 mL/min. The focus flow causes the injected sample to accumulate in a narrow concentration band minimizing band broadening and longitudinal diffusion. After injection the focus flow rapidly decreased to zero (transition), while the tip flow increased up to 9 mL/min. After 2.5 minutes the tip flow and the cross flow decreased by an exponential decay function to a value of 0.51 and 0.01 mL/min respectively (elution step).

In a further investigation polystyrenes and polybutadienes were analysed by making use of cross-flow B (Fig. 3.2). The exponential change in the cross-flow profile was the same as in the case of cross-flow A, but instead of 8.8 mL/min, a starting cross-flow of 5.5 mL/min was used.
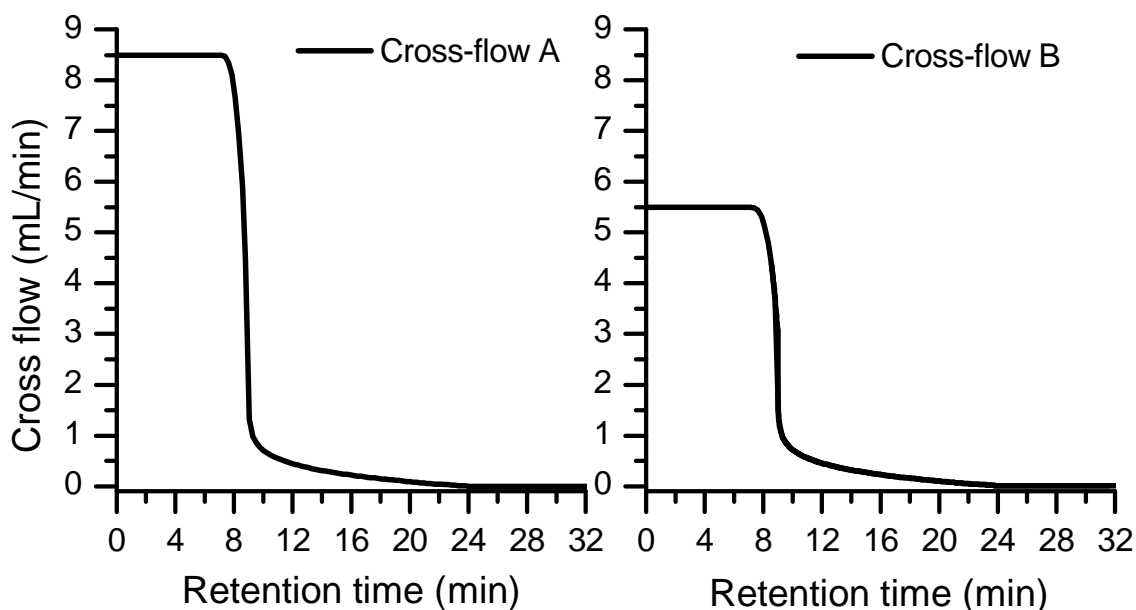
Fig. 3.2 Cross-flow profiles of cross-flows A and B

3.3 Results and discussion

3.3.1 Analysis of polystyrene standards as a method for the validation of the SEC and AF4 systems coupled to MALLS- and RI detection

Both SEC and AF4 separation systems were tested and compared by the separation of polystyrene standards with known molar masses (62, 250 and 1000 kg/mol, respectively). In SEC only one PL gel mixed C column was used for the separation of the polystyrene mixture to avoid shear effects. The

Chapter 3: Polybutadienes

calibration, normalization and determination of the correct inter-detector delay between MALLS and RI was determined by making use of an isotropic scatterer such as monodisperse polystyrene with a molar mass of 33 000 g/mol. The peak maxima of the RI and MALLS signals were overlaid to obtain a delay volume of 0.175 mL. In order to test whether the calibration between the MALLS and RI detector were correct, a mixture of the polystyrene standards was analyzed by AF4 by applying cross-flow A. The overlay of the SEC and AF4 measurements with RI and MALLS detection is shown in Fig. 3.3.

The model mixture was separated properly by both SEC and AF4. In AF4 the small molecules elute earlier than the larger molecules, which corresponds to a separation according to the normal mode elution in AF4.[32] In SEC the elution order is from high to low molar masses.
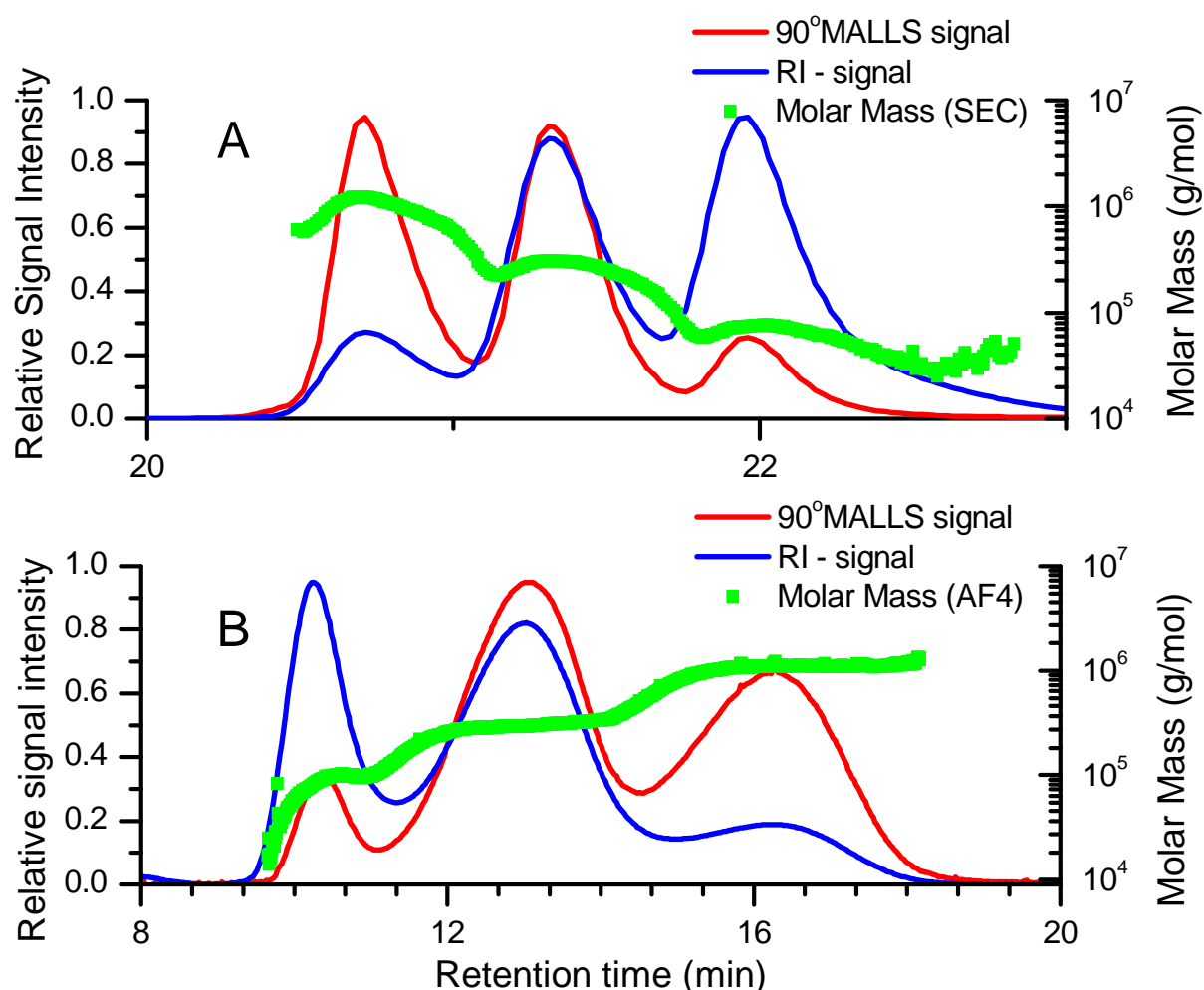
Fig. 3.3 SEC and AF4 separation for a mixture of polystyrene standards. A) SEC elugrams and molar mass reading; stationary phase (SEC): PL gel mixed C, B) AF4 fractograms and molar mass reading; flow rate (SEC and AF4): 0.5 mL/min

In the AF4 measurement the lowest molar mass standard does not correspond to the nominal molar mass. This is due to the fact that the 250- and 62 kg/mol standards slightly overlap, resulting in an

overestimation of the molar mass. The analysis of these polystyrene standards evidently shows that the system provides sufficient separation at still acceptable analysis time.

In addition, the nearly exact retrieval of the molar mass values with both techniques affirms an accurate calibration of the detectors creating an adequate platform for the analysis of the polybutadienes. The effect of changes in the cross-flow on the elution behaviour of the polystyrenes is shown for cross-flows B-D. Cross-flow gradient B (Fig. 3.4) was applied to the polystyrene mixture and linear cross-flow gradients (C and D) were introduced into the existing exponential cross-flow program to improve the separation efficiency.
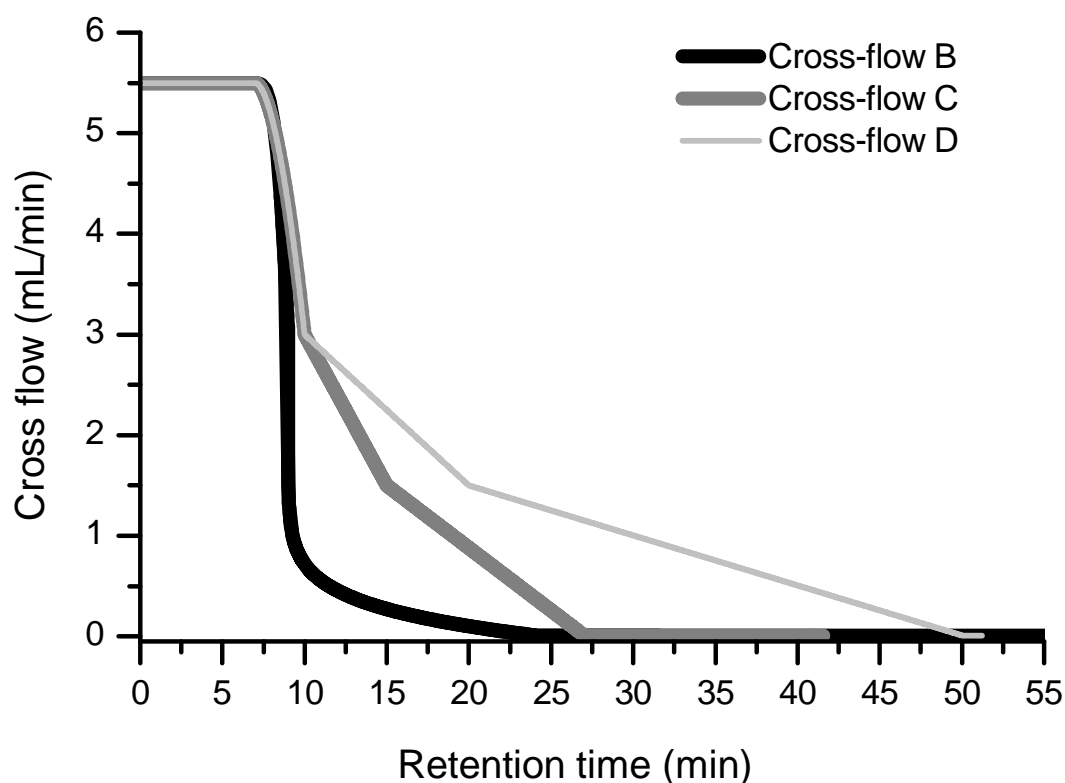
Fig. 3.4 Cross-flow profiles of cross flows B, C and D

The resultant fractograms (RI and MALLS) obtained from the AF4 measurements are shown in Fig. 3.5. It is apparent that as the linear gradient is elongated, the separation is improved significantly. For cross-flow D, the standards are almost baseline separated. A further linear step could be introduced to baseline separate all three standards completely.

This simple model of known standards clearly illustrates that the cross-flow in AF4 is a powerful tool in the separation of macromolecules other than the reference materials. The drawbacks of applying extended cross-flow steps are that the elution time and band broadening are significantly increased while the peak maximum intensity is slightly decreased.
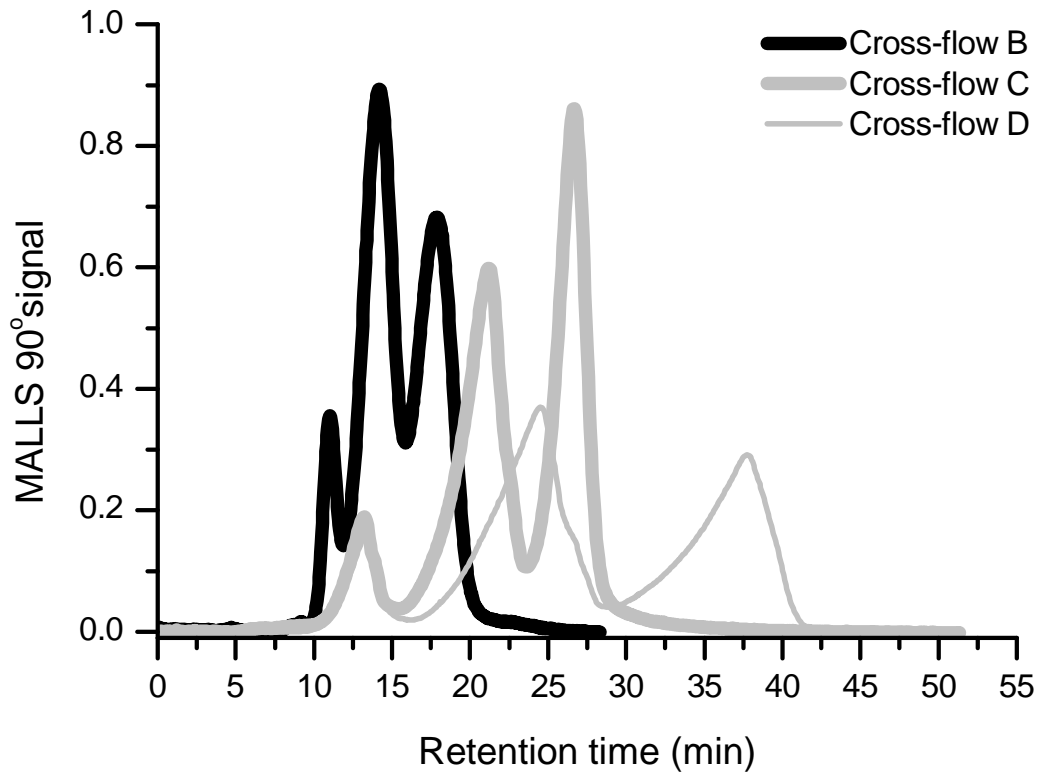
Fig. 3.5 AF4 fractograms for a mixture of polystyrene standards using cross flows B, C and D. MALLS (90°) detector readings are overlaid
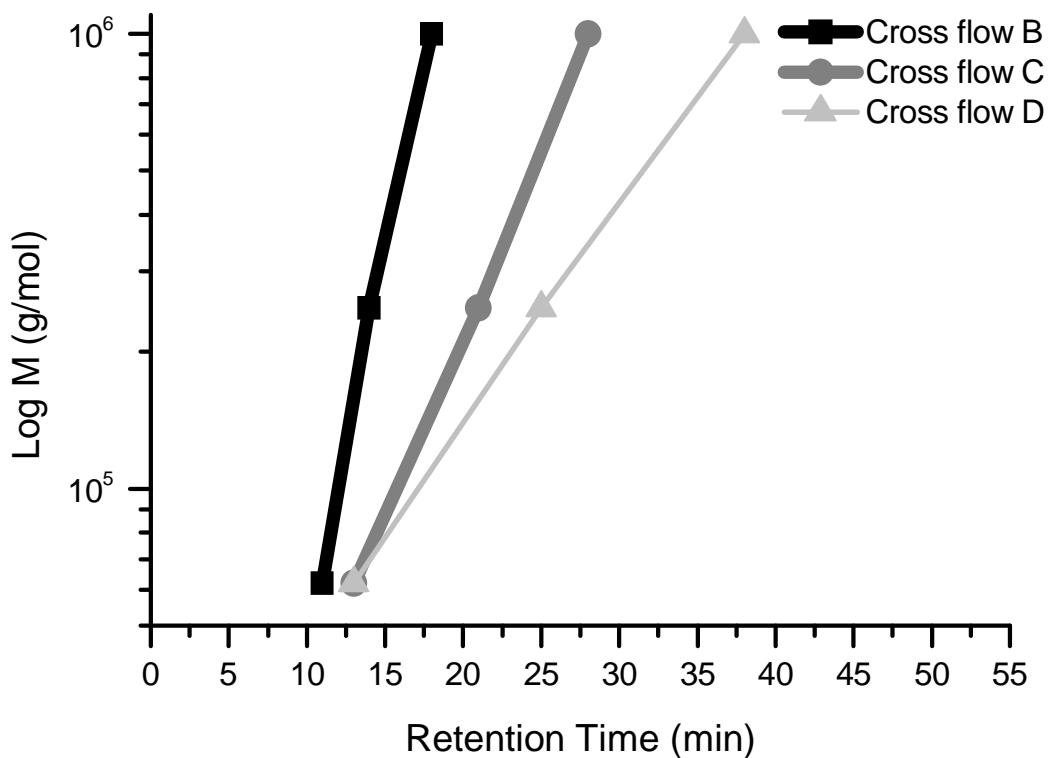
Fig. 3.6 Calibration curves for each cross flow gradient of the mixture of PS standards

Chapter 3: Polybutadienes

Polystyrene calibration curves can be constructed for each cross-flow gradient applied (Fig. 3.6) by constructing a log M vs. retention time plot. The resultant calibration curves could be used if an absolute molar mass detector like MALLS was not available or if only a concentration detector (UV or RI) was available. The peaks for each cross-flow gradient (A-D) as well as the SEC mixtures were processed and integrated by applying the random coil data fitting method (Table 3.2).

Table 3.2 Polystyrene molar masses obtained from different SEC column sets and different AF4 cross-flow gradients.

SEC					AF4				
Sample name	M_w (kg/mol)	M_n (kg/mol)	R_g (nm)	PDI	Sample name	M_w (kg/mol)	M_n (kg/mol)	R_g (nm)	PDI
PSmix 1[a]					Cross-flow A				
62kg/mol	65.7	60.2	16.5	1.09	62kg/mol	81.7	70.0	11.5	1.17
250kg/mol	273	265	22.0	1.03	250kg/mol	306	293	24.8	1.05
1000kg/mol	964	878	44.5	1.10	1000kg/mol	1070	1060	46	1.01
PSmix 2[b]					Cross-flow B				
62kg/mol	55.8	52.2	15.3	1.07	62kg/mol	71.5	70.3	15.9	1.02
250kg/mol	221	197	21.7	1.12	250kg/mol	246	239	26.9	1.03
1000kg/mol	842	753	44.3	1.12	1000kg/mol	764	749	46.3	1.02
PSmix 3[c]					Cross-flow C				
62kg/mol	98.9	90.1	29.2	1.10	62kg/mol	68.3	66.1	17.8	1.03
250kg/mol	308	289	41.1	1.07	250kg/mol	244	242	21.4	1.01
1000kg/mol	910	892	56.9	1.02	1000kg/mol	810	776	44.9	1.04
					Cross-flow D				
					62kg/mol	61.1	59.2	9.7	1.03
					250kg/mol	256	252	22.4	1.02
					1000kg/mol	1090	1030	45.4	1.06

[a]   one PL mixed C column used at flow rate of 0.5mL/min

[b]   one PL mixed B and one PL mixed C column in used at flow rate of 0.5 mL/min

[c]   one PL mixed A and one PL mixed B column used at flow rate of 0.5 mL/min

Chapter 3: Polybutadienes

For the SEC measurements presented in Table 3.2, it can be seen that the calculated molar masses are incorrect due to the overlapping of peaks in the various elugrams, even after varying the column sets in series (mixed A and B columns). The same applies for the AF4 measurements for cross-flows A to C. The molar mass values calculated from cross-flow D is the closest to the values given by the producer and corresponds well to the radius calculation given by $R = 0.014\ M^{0.585}$ for linear polystyrene in THF as solvent at 25℃.[33] In SEC the only option for an improvement in separation is by means of adapting the column set and injection flow amongst others. This could lead to additional problems since high flow velocities and more SEC columns will lead to pronounced shear degradation and filtration effects. In AF4 one of the options is to change the cross-flow gradient for an improvement in separation making it a superior tool over SEC regarding optimisation of the separation. Different from SEC the user is not bound to the separation characteristics of the system that is always determined by the column set.

3.3.2 Analysis of polybutadienes

3.3.2.1   The effect of dissolution time and temperature on elution behaviour in SEC and AF4

In this section the effect of dissolution on the elution behaviour of a few polybutadiene samples was investigated. After the initial dissolution step, polybutadienes PB 1-3 were measured by SEC to see whether the samples have been dissolved completely. Blockage of the SEC columns was prevented by filtering the samples with a 0.45 µm filter prior to injection. Only 10% of the injected mass was recovered as is shown in Table 3.3 indicating that after the initial dissolution step a large percentage of the samples were not fully dissolved. As a result of incomplete dissolution, a large part of the macromolecules was probably present in solution as swollen gel particles and was filtered off or trapped in the SEC column.

Table 3.3   Effect of different dissolution times on recovery, with the calculated molar masses, radii and polydispersity indices for PB 1-3.

Sample name	Recovery % (eluted mass/injected mass)	M_w (kg/mol)	M_n (kg/mol)	PDI	R_g (nm)
PB1 (short, 20 hrs)	11	343	168	2.05	49.5
PB1 (long, 68 hrs)	93	280	133	2.11	55.7
PB2 (short)	13	461	172	2.68	78.2
PB2 (long)	100	386	113	3.41	80.8
PB3 (short)	13	327	111	2.94	53.7
PB3 (long)	100	270	99	2.73	53.3

Chapter 3: Polybutadienes

For a further improvement of the sample preparation, the samples were dissolved for another 48 hours at room temperature. The sample flasks were rotated regularly to allow proper mixing and homogenisation of the solutions. The recovery was checked again by analyzing the samples with SEC, the total dissolution time now being 68 hours. The resultant recovery, even after filtration, was in the region of 100 % (Table 3.3) indicating a good dissolution state. After prolonged dissolution times the aggregates or large gel-resembling species have been dissolved into individual macromolecules which were able to pass the filter and frits of the columns.
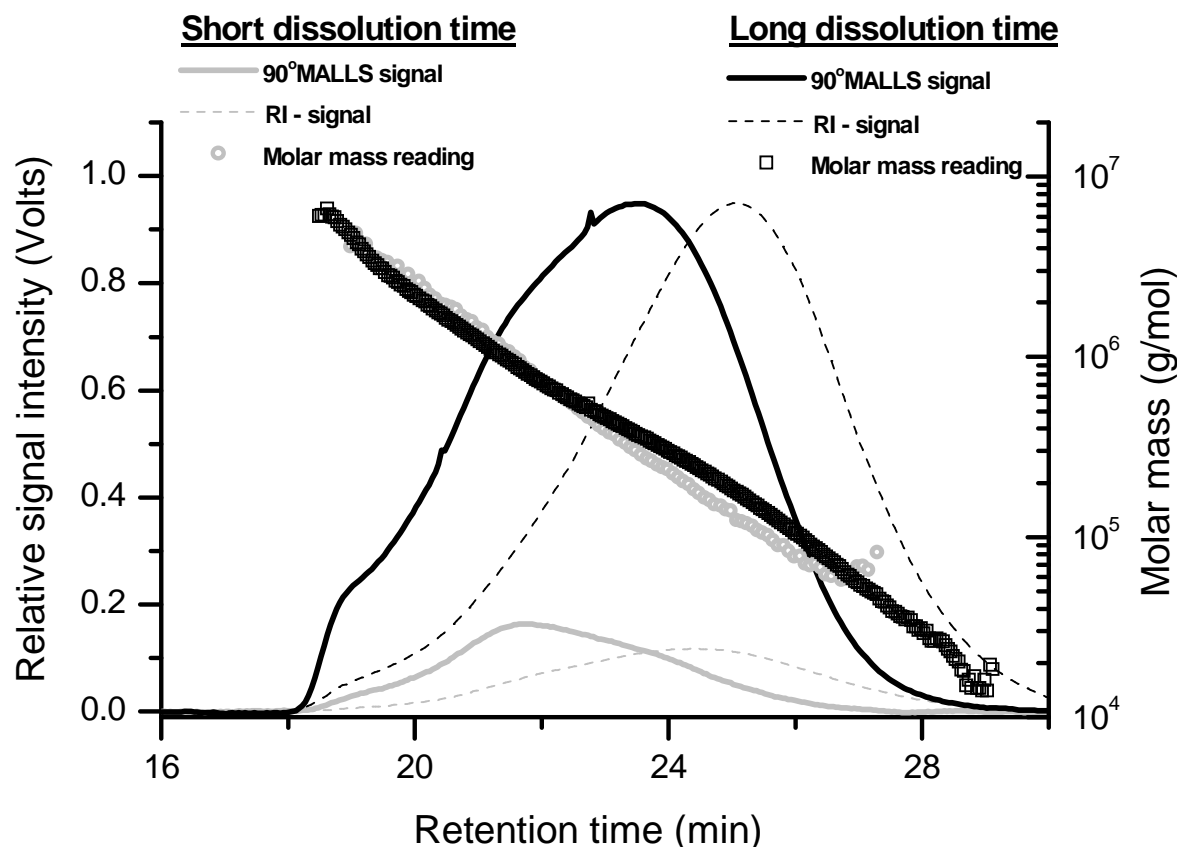
Fig. 3.7 SEC elugrams and molar mass readings for different dissolution times (sample PB 2)

The elugrams with the molar masses and R_g of the measurements for both the short and long dissolution times of PB 2 are shown in Figs. 3.7 and 3.8, respectively. It is clearly visible that the normalised signal intensities of the RI and MALLS signals are much more intense (± 5 fold) for the longer dissolution time compared to the shorter dissolution time measurement. The immense differences in intensities and recoveries of the two measurements are a clear indication that complete dissolution took place only after longer dissolution times. The fact that for the short dissolution time not all macromolecules are properly dissolved yet and some entanglements are still present is also visible in the R_g plot given in Fig. 3.8. While for the long dissolution period R_g decreases monotonally with increasing elution time, this is not the case for the short dissolution period. In this case an upswing of the R_g reading is observed. This effect (upswing) will be discussed in detail later in the thesis.
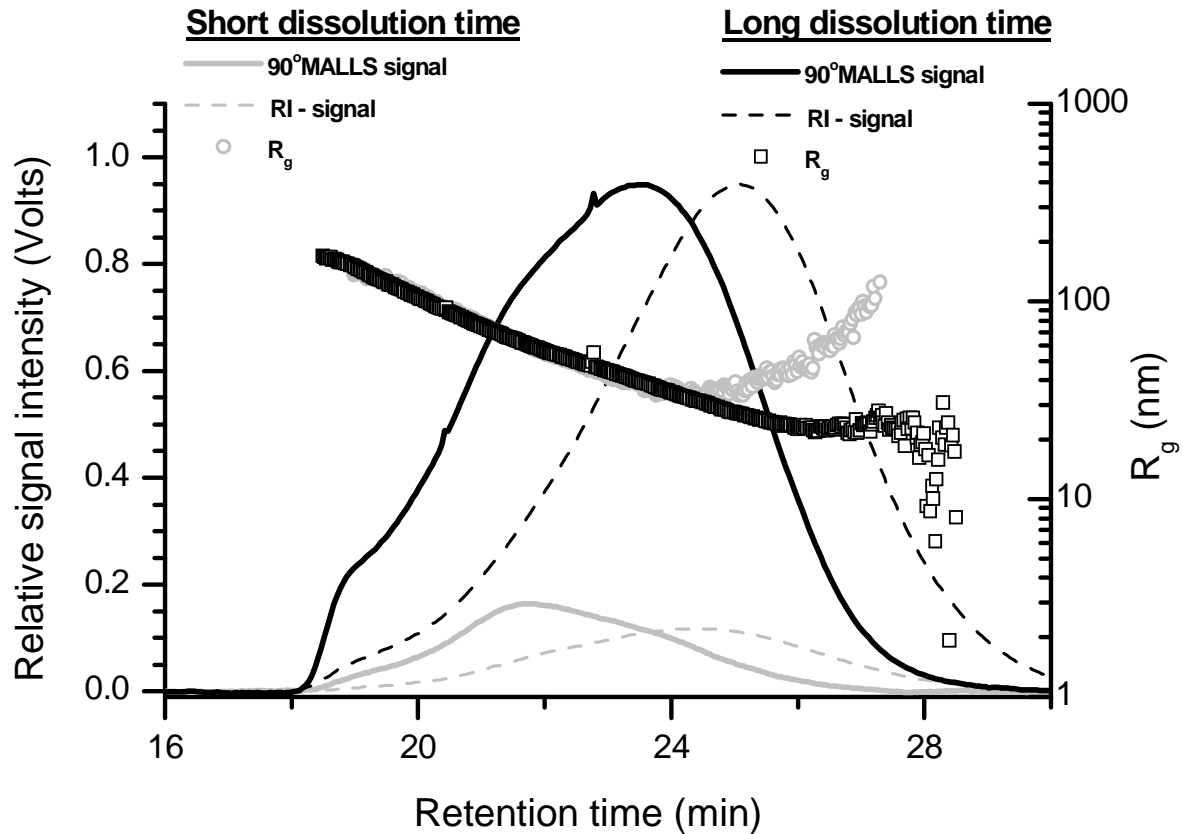
Fig. 3.8 SEC elugrams and R_g readings for short and long dissolution times (sample PB 2)

The molar mass distribution is obtained by extrapolation of the molar mass vs. retention time plot and is represented by a differential molar mass plot. The MMD for both short and long dissolution times closely overlaps as shown in Fig. 3.9. The cumulative weight fraction plots of both measurements are overlaid before and after extrapolation. It is visible that the different dissolution procedures have only a minor impact on the very low and high molar mass fractions which is one of the reasons why the improper dissolution is hard to identify just by comparison of the average molar mass values, radii and polydispersities as shown in Table 3.3.

However, longer dissolution times of minimum 68 hours were used as a basis for the analysis of all other polybutadiene samples since they provided more reliable results with regard to sample recovery and reproducibility.

Chapter 3: Polybutadienes
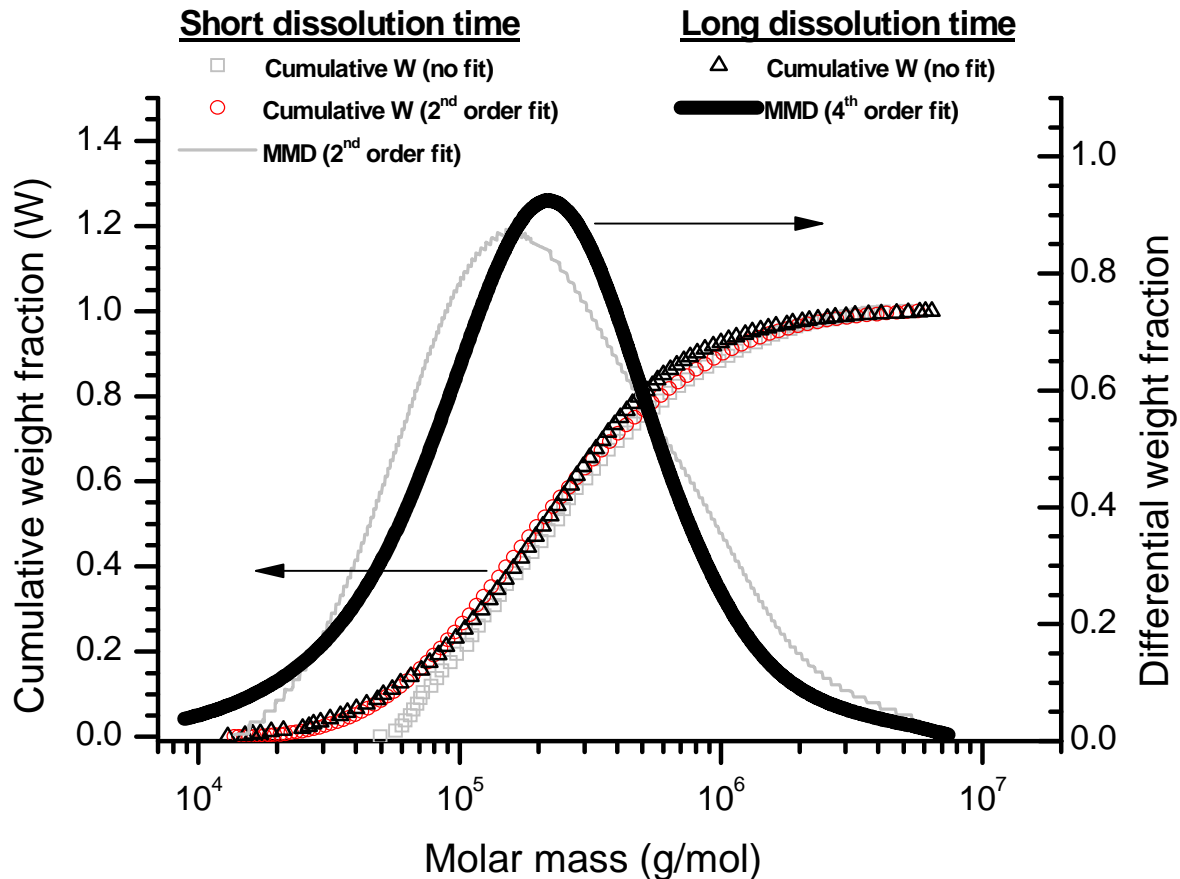
Fig. 3.9 Cumulative weight- and molar mass distribution of PB 2 at short and long dissolution times. Symbols □ and Δ are non-extrapolated while all the other plots are fitted with fit orders given in parenthesis

In another example (PB 4), the effect of dissolution was investigated by comparing SEC and AF4 results. The sample was treated similar to the previous one. In this example different heating steps and filtering were applied to investigate the effect of dissolution and heating upon elution behaviour. Fig. 3.10 shows the SEC elugram using the 90° MALLS signal and the molar mass reading. Measurements were taken after filtration with a 0.45 µm filter one and three days after the initial sample treatment and after a second heating step of five hours. An additional measurement after the second heating step was taken with a 0.20 µm filter.

One and three days after initial heat treatment (thick black and grey lines) a strong noise signal is observed at the high molar mass side in the MALLS signal which is possibly due to very small amounts of large gel-resembling species present in solution.

Chapter 3: Polybutadienes
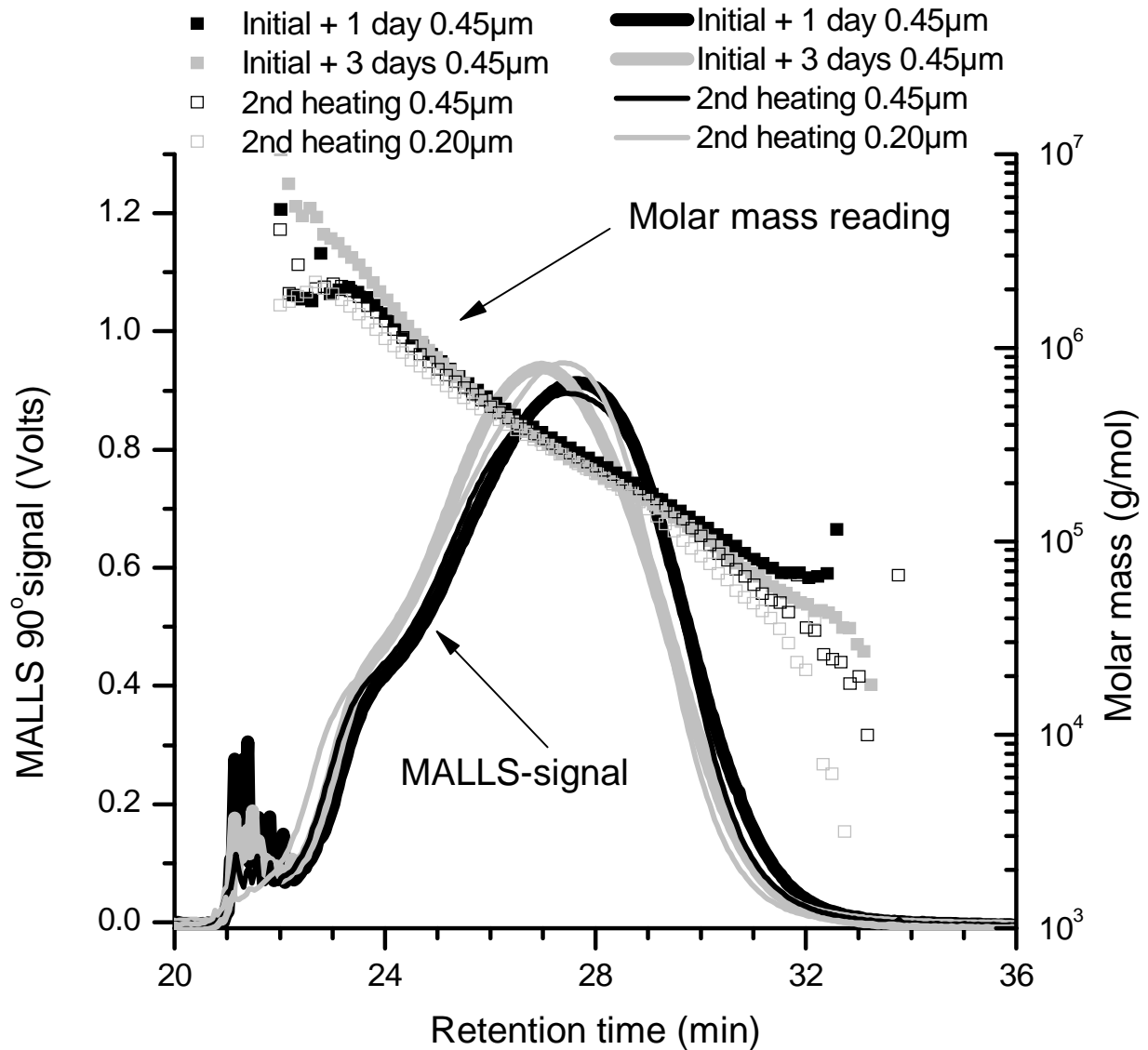
Fig. 3.10 SEC elugrams of PB 4 with MALLS signal and molar mass readings

Their concentration is too small to be detected by the RI detector (Fig. 3.11). The assumption is made that these gel-resembling species are not cross-linked macromolecules but entangled macromolecules that are only partially dissolved. The decrease of the noise with increasing heating or dissolution time is a clear indication that this assumption is valid.

After three days (thick grey line) the dissolution proceeded further and the noise decreased compared to the measurement after one day (thick black line). The measurement taken after the second heating step (thin black line) also suggests an increasing amount of properly dissolved macromolecules. The measurement after filtration with a 0.20 µm filter (thin grey line) shows almost no noise present in the light scattering signal. This is a possible indication that most of the gel-resembling species were filtered off or got stuck on the inlet frit of the column.[9] The corresponding RI-signals and R_g readings of the SEC measurement is shown in Fig. 3.11.

Chapter 3: Polybutadienes
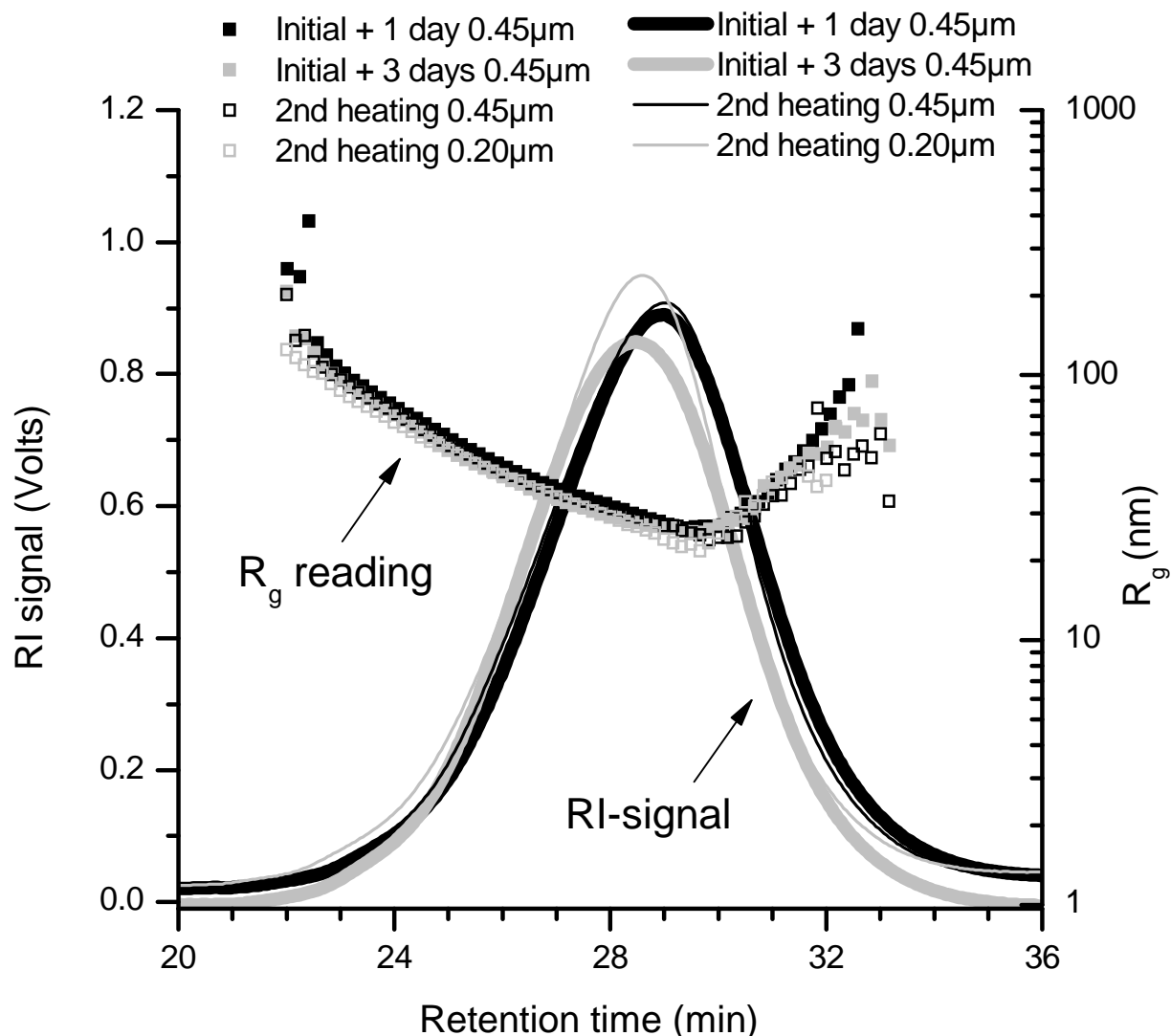
Fig. 3.11 SEC elugrams of PB 4 with RI signal and radius of gyration readings showing abnormal radius behavior at high elution times

The smooth RI curves do not show any noise or peaks at an elution time of about 21 min, emphasising the low sensitivity of the RI detector for elution slices containing large macromolecules that are very low in concentration.[10,22] At high elution times both the molar mass and R_g vs. elution volume plots (Figs. 3.10 and 3.11) show abnormal SEC behaviour.[9,34] In Fig. 3.10 the molar mass shows a minor increase at high elution time for the shorter dissolution procedures (filled squares). The corresponding radius values (filled squares in Fig. 3.11) show this behaviour much stronger as a clear curvature is visible towards the later eluting species.

Such behaviour is well known for highly branched molecules and was already discussed in various publications.[35-39] Explanations for the observed observation ranges from range from anchoring of branched species in the column packing up to molecular topology fractionation in small cavities.[34] In PB 4 however, the reason for the detected results is the unusually late elution of high molar mass species which are supposed to be highly branched together with regular eluting linear species of low

Chapter 3: Polybutadienes

molar mass.[40] The R_g reading is more sensitive to this phenomenon than the molar mass reading. The particular slice of the chromatogram which is affected by co-elution is an averaged value for the different radii and molar masses.[41,42] The molar mass represents a weighted average value while the radius represents a z-averaged value in the case of these polydisperse portions.[33] This causes the radius plots to be more responsive to tiny amounts of larger molecules compared to the molar mass plots, which results in a more pronounced upswing of the radii.[7,9,33] The effect of branching on the elution behaviour will be discussed later in the manuscript. However, until now it can be stated that for both samples PB 2 and PB 4 the abnormal elution behaviour in SEC is increased at short dissolution times or improper dissolution or sample preparation conditions.
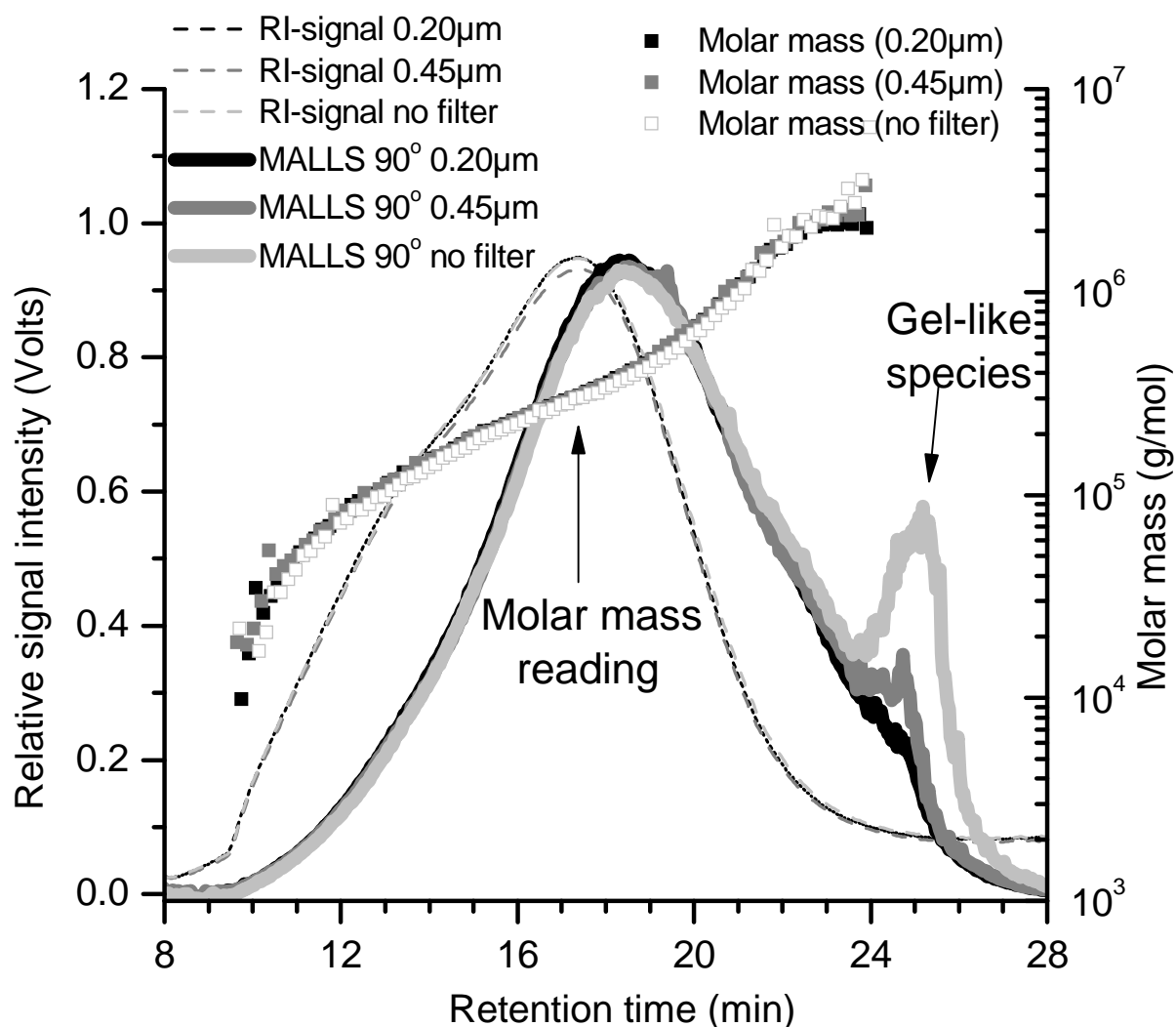
Fig. 3.12 AF4 fractograms of PB 4 with RI, MALLS and molar mass readings

The same sample (PB 4) was measured using AF4 after the second heating step by making use of cross-flow B. Three different measurements were done with a 0.2 µm filter (thick black line, filled black squares), a 0.45 µm filter (dark grey line, filled dark grey squares) and without filtration (light grey line, open squares). Fig. 3.12 shows the AF4 fractograms and molar mass readings of PB 4. The molar mass increases with increasing elution time which is indicative of normal mode AF4.[43]

Chapter 3: Polybutadienes

The MALLS signal shows that for the unfiltered sample, larger gel species are present in the sample in comparison with the two filtered samples. An unfiltered sample could not be measured in SEC, due to column sensitivity towards micro gel species. Even for the measurement after filtration with a 0.2 μm filter, a tiny amount of gel-resembling species can be observed. This possibly indicates that the small amount of this material which was able to pass the 0.2 μm filter in SEC got stuck on the column frit or in narrow inter-particle cavities of the packing material, since a smooth curvature was observed in the SEC measurement. In AF4 no frit is used and the MALLS signal is a true reflection of the total material in solution which was able to pass the 0.2 μm filter. The molar mass readings of the three measurements are in excellent agreement until the gel-resembling spikes are observed at higher elution times, showing that the measurements in AF4 are reproducible. The RI- and MALLS traces support this assumption. Beyond this point data fitting is not accurate since the scattering is very intense although concentration is very low making data fitting very difficult or even impossible. As has been pointed out, these peaks are a possible indication of incomplete dissolution, entanglements between polymer chains or the presence of insoluble gel in solution. A possible explanation for the noise could be that if some very large species pass the light scattering cell, the movement of the structure can cause spikes since the low concentrations of the diluted sample are caused by only a few very large molecules. Consequently a movement of such highly scattering species through the laser beam will have a huge impact on the scattered light intensity as the scatter volume is typically low and the number of molecules is not sufficient to average the effect. These findings underline the importance of a light scattering detector as a highly sensitive tool for the detection of very small quantities of high molar mass or gel-containing macromolecules in solution.

3.3.2.2 The effect of branching on molar mass in SEC and AF4

For a given molar mass, branched species have a smaller hydrodynamic volume than the linear species of similar molar mass.[33] Since separation in SEC takes place according to hydrodynamic volume, two species of equal molar mass but different hydrodynamic volume can elute at different elution times.[40,44] Since branched macromolecules may co-elute with linear macromolecules this results in a region of medium to high polydispersity regarding molar mass. Having the same hydrodynamic volume but different coil densities linear and branched macromolecules will show different molar mass-radius of gyration behaviour. For linear macromolecules R_g will increase with molar mass. This effect is lowered or might not be the case for branched macromolecules. If the branching density increases then for the same molar mass R_g decreases. This will result in a decreased slope of the R_g vs. M plot for samples which are branched over the whole mass range. Samples which show significant branching only for the high molar mass molecules often show a decrease of the R_g vs. M slope for the high molar mass fractions.[44]

A second effect which is often found for branched material is the abnormal upswing of the radius and (to a lesser extent) the molar mass at low elution times in SEC-MALLS. This effect is also visible for sample PB 5 (Figs. 3.13 and 3.14). The reason for the re-increase is the abnormal late co-elution of large and high molar mass molecules together with regular eluting small molecules of low molar mass.

Species which differ highly in molar mass and size are co-eluting which was proven for polyethylene samples by fractionation of the late eluting part from SEC and re-injection of the fraction in FFF.[34]
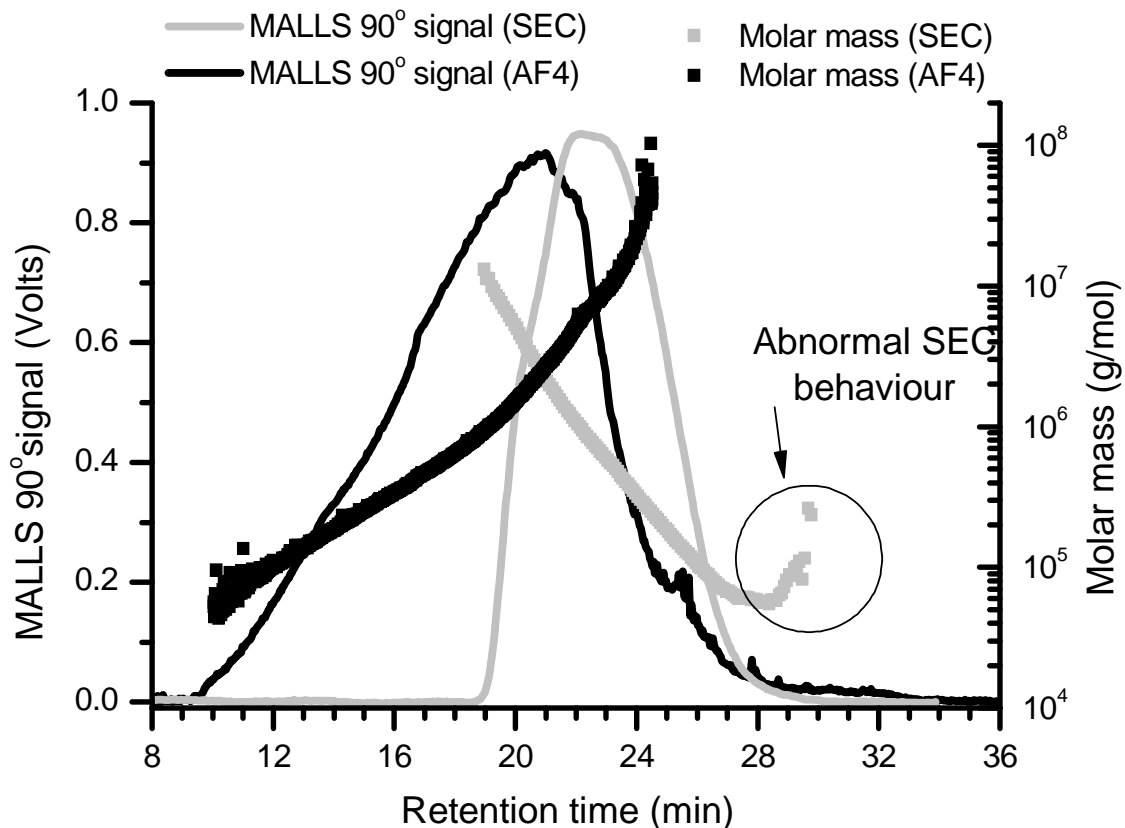
Fig. 3.13 MALLS signals of SEC and AF4 with molar mass readings overlaid, sample PB 5

Small and large molar mass molecules were isolated by proper FFF separation since no interactions are possible between polybutadiene molecules and the cellulosic membrane. Until now the reason for the upswing in SEC is not clear. Since the effect is preferably found for branched material[35-40,45] the branching seems to be one of the reasons for the abnormal late elution of large macromolecules. In addition the presence of small linear macromolecules and large excessively branched material might further increase the polydispersity effect, therefore, resulting in the differences between the detected molar mass and R_g values which are z- and weight (w) averages for polydisperse fractions, respectively. Consequently the bigger the polydispersity effects of the late-elution fraction the higher the impact of the different averaging of R_g and M.

Chapter 3: Polybutadienes
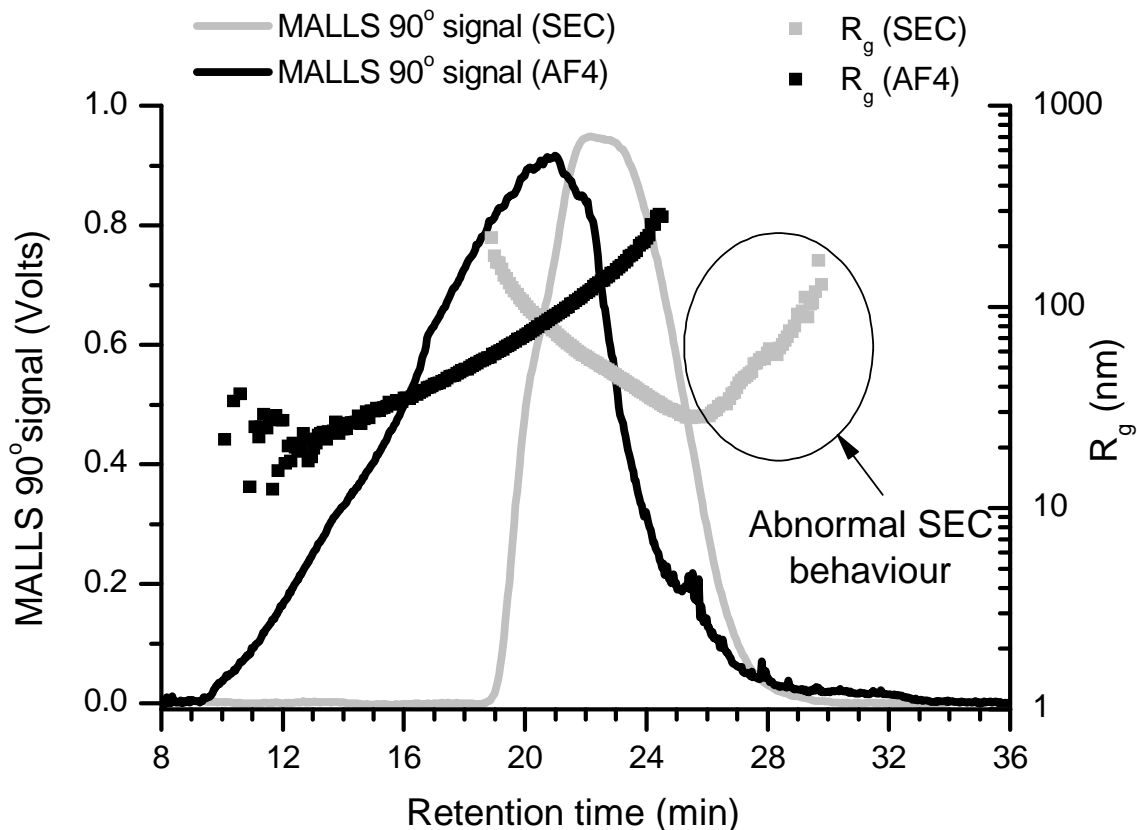
Fig. 3.14 MALLS signals of SEC and AF4 with radius of gyration readings overlaid, sample PB 5

The degree of branching from SEC-MALLS is typically calculated by the interpretation of the slope in the conformation plot which is the relationship between R_g and molar mass (Fig. 3.15).[40] Due to the upswing effect in the SEC plot, calculations related to branching will be falsified (slope of 0.36 in Fig. 3.15) since the co-elution effect leads to incorrect values of the slope. Two overlapping effects both related to branching are observed in this case. Firstly a decrease in the R_g-M slope is visible for: (1) partially branched molecules at high molar masses and (2) fully branched molecules throughout the molar mass range. Secondly, the up-swing of R_g at high elution times/low molar masses which is related to branching but cannot be correlated since it (the up-swing) influences the regular molecular contraction as described in the first effect. Thus, SEC may be very sensitive towards branching since upswing and molecular contraction get visible but a data evaluation is not possible due to the co-existence of a huge variety of effects caused by branching.

Chapter 3: Polybutadienes
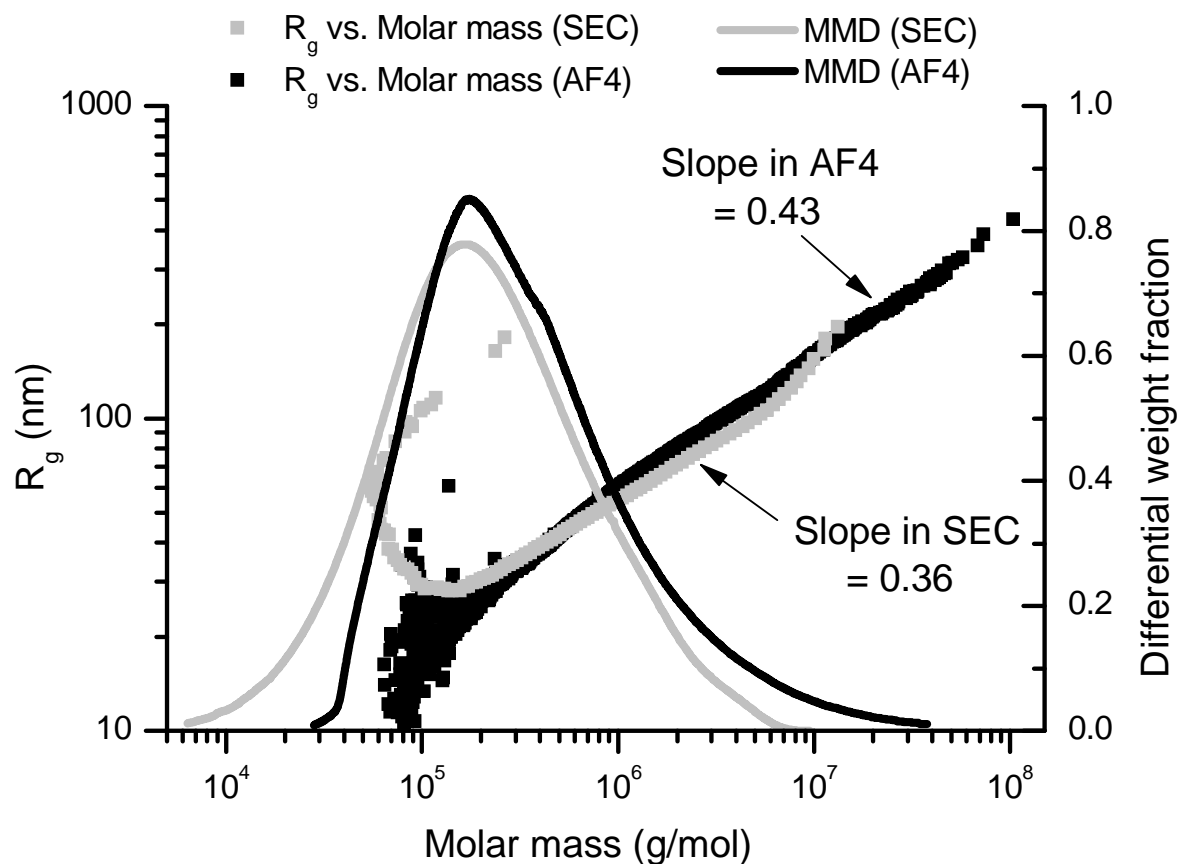
Fig. 3.15 Conformation plots (R_g vs. molar mass) for SEC (grey squares) and AF4 (black squares) of sample PB 5. MMD of SEC (grey line) and AF4 (black line) are overlaid

Table 3.4 Calculated molar masses, radii and polydispersity indices of PB 5 from SEC and AF4. Filtering was done with a 0.45 μm filter.

Sample name	Recovery % (eluted- /injected mass)	M_w (kg/mol)	M_n (kg/mol)	PDI	R_g (nm)
PB 5 (SEC,filter)	97	450	154	2.93	69.1
PB 5 (SEC,extrapolated)		420	103	4.09	60.9
PB 5 (AF4, filter)	87	920	187	4.92	141.4
PB 5 (no filter)	89	982	204	4.81	161.1

Table 3.4 shows the calculated molar masses and radii for the up-swing in Figs. 3.13 and 3.14. The extrapolated values are also calculated by applying a linear fit to the molar mass and R_g plots in SEC, giving the values that are estimated if no up-swing was present. As can be seen, the extrapolated molar mass and R_g values are smaller than in the case of the calculation without extrapolation. In AF4, no stationary phase is present, which avoids these unwanted irregularities (black lines, black

Chapter 3: Polybutadienes

filled squares in Figs. 3.13 and 3.14). The effects of shear degradation and co-elution are minimized, and the resultant branching calculations can be achieved accurately (Fig. 3.15, grey lines and squares). Cross-flow A was applied for this measurement and the slope observed in the conformation plot (Fig. 3.15) for AF4 was 0.43 which is below the reference value of 0.58 for linear molecules.[44] The reduced slope indicates that long chain branching was present in the sample. The conformation plot as well as the MMD in Fig. 3.15 shows that in AF4 much higher molar masses are detected compared to the measurement in SEC.

Higher molar masses are also confirmed in Table 3.4 for both the filtered and unfiltered measurements in AF4. This decrease in molar mass in SEC is possibly an indication that shear degradation and/or removal of ultrahigh molar mass components of the sample caused by the stationary phase occurred.

Additionally, it can be speculated that improper dissolution and, as a consequence, the presence of compact and only partially dissolved agglomerates of multiple polymer chains may lead to increased late elution behaviour in SEC. As a result they will elute late and thus they will be masked due to the local mass and radius average effects. Finally the species are invisible in the MMD and overall molar mass/radius average values. It is known that dissolution irregularity could cause polymer structures to behave like branched or even highly branched species since the contact points of the different polymer chains will act like physical branching points and thus they could also undergo the second separation mechanism which is often claimed to be a reason for late elution.[9] This observation is supported by the increased up-swing phenomenon of molar mass and radius for sample PB 2 and PB 4 if poor dissolution conditions were applied (Figs. 3.7, 3.8, 3.10 and 3.11).

3.3.2.3 The investigation of gel species in polybutadienes

The size heterogeneity of polymers is often correlated to the modality of the elugrams obtained by SEC.[33] In the present example (Fig. 3.16), the MALLS signal (thin grey line, open squares) illustrates that the sample PB 6 is monomodal over the entire elution profile. Since the MALLS detector is very sensitive towards the presence of small amounts impurities or different size regimes, it can be assumed that the SEC measurement is rather monomodal with respect to size and no additional size distribution is present in solution. When the AF4 results, where cross-flow B was used, are compared a bimodal distribution is observed in the MALLS signal. The measurements with and without filtration are seen in Fig. 3.16 (thick black- and grey lines and filled squares).

What is interesting is that even for the measurement after filtration, a bimodal peak is observed. This observed phenomenon is possibly a result of very small amounts of cross-linked or gel-resembling macromolecules, which were able to pass through the 0.45 µm filter. [19,22,46] It can be assumed that cross-linked structures have an increased mechanical stability retaining their high flexibility.[47] It is likely that such structures are able to pass the filter pores in a stretched conformation with very low effective hydrodynamic radius.

Chapter 3: Polybutadienes
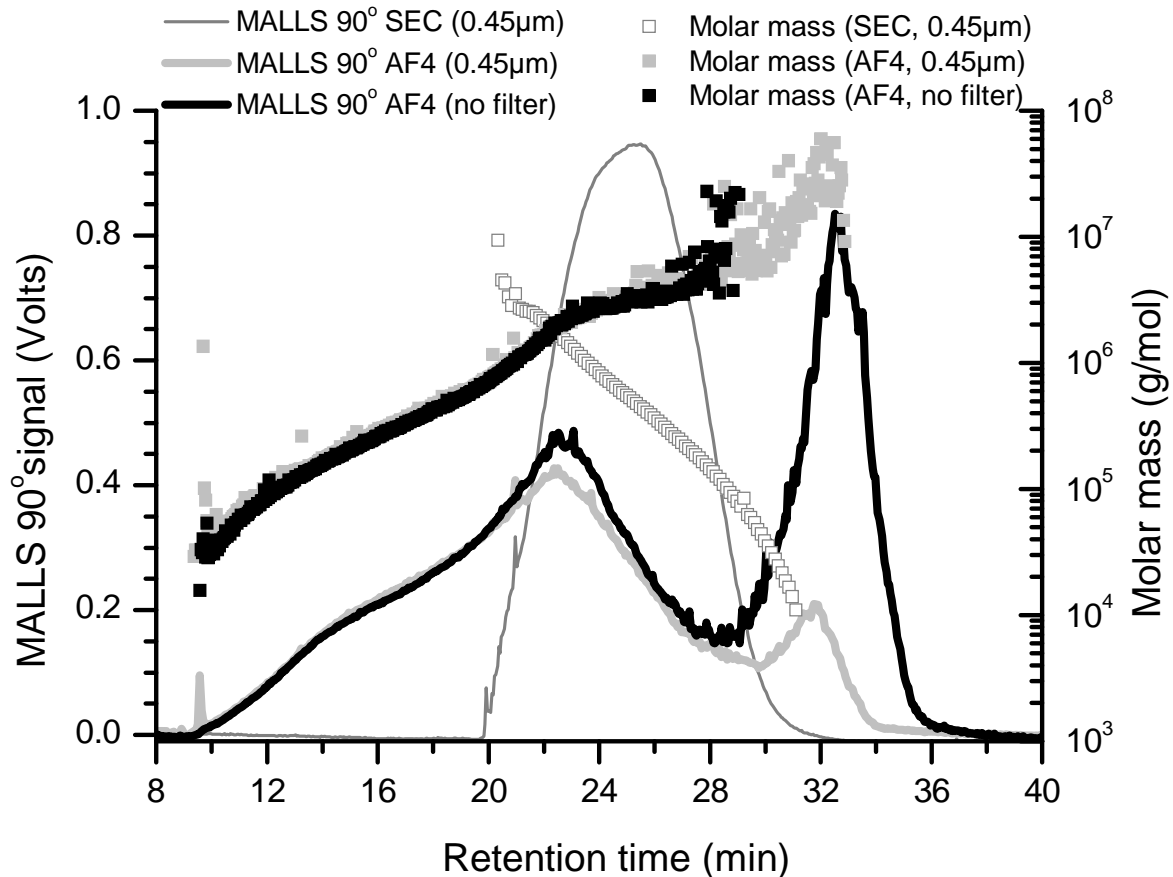
Fig. 3.16 MALLS signals of SEC and AF4 (filtered and unfiltered) for sample PB 6, molar mass readings are overlaid

Filtration will not degrade the chains due to the network-like structure which is more stable than a pure linear chain. After filtration the structure may go back to its original conformation with an increased diameter and thus it will elute later as a second peak due to the lower diffusion ability. In the SEC measurement these cross-linked network like molecules possibly got stuck or were degraded by the frits and pores of the columns.

The concentration profiles of the measurements together with the R_g readings are shown in Fig. 3.17. It is evident that the two AF4 measurements overlap each other very closely throughout the fractogram. At higher elution times, where the concentration signal intensity is close to zero, the later eluting species are observed in the fractogram of the MALLS 90° signal (Fig. 3.17). The unfiltered sample shows a very noisy peak (MALLS) which could be an indication of improper dissolution and/or extremely large species as already explained above. As a consequence of the noise, the software is not able to calculate average molar mass or R_g values in this region for the random coil fitting method.

Chapter 3: Polybutadienes
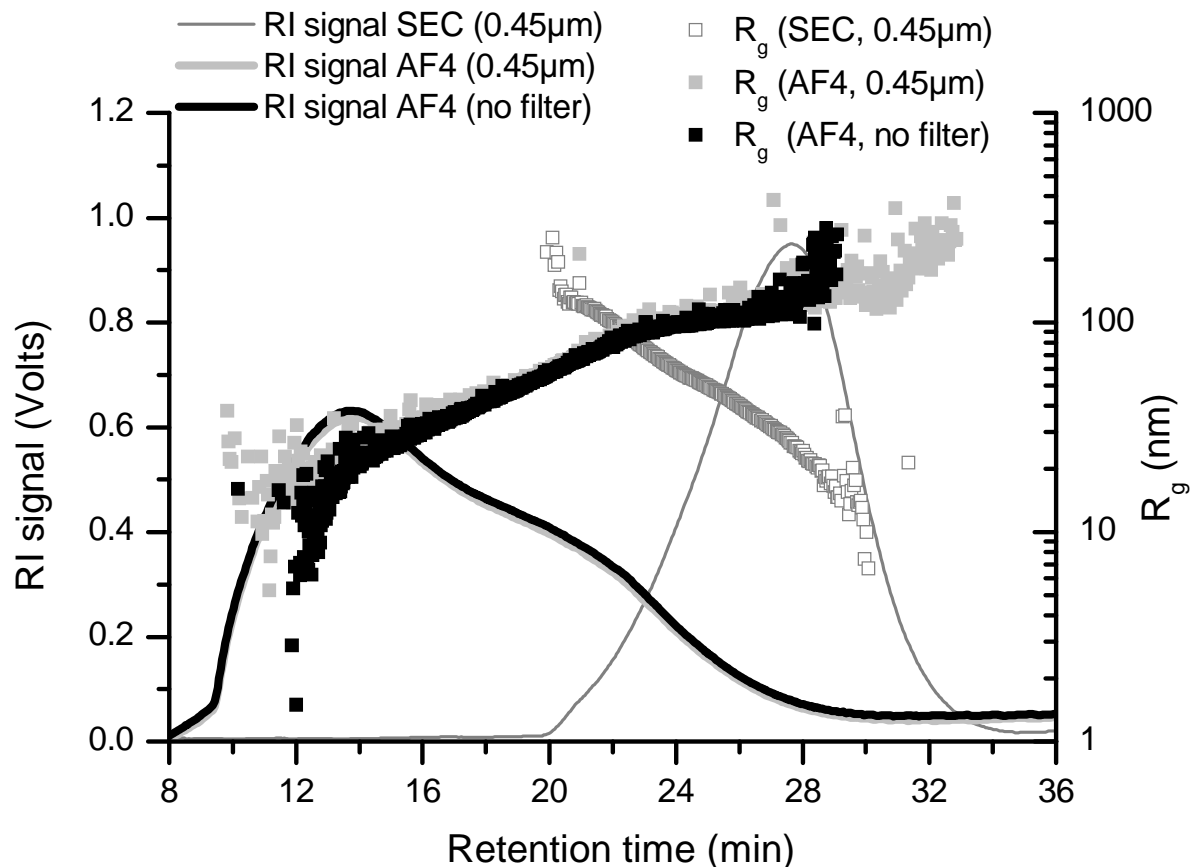
Fig. 3.17   RI signals of SEC and AF4 (filtered and unfiltered) for PB 6, radius of gyration readings are overlaid

The measurement after filtration gave molar mass and R_g readings in this region, since the intensity of the late eluting species is less pronounced and the signal is smoother than the measurement without filtration which made data fitting possible. The interesting question was to see whether it is possible to make use of the uniqueness of the AF4 cross-flow system and investigate the possibility of separating the bimodal peaks by adjusting the cross-flow gradients.

Numerous attempts were made by making use of the cross-flows observed in Fig. 3.18, and the resultant fractograms with MALLS 90° signals for th e unfiltered sample are given in Fig. 3.19. It was observed that there was no major improvement in separation upon cross-flow gradient, but merely a shift in elution time. The reason for this could be that the second observed peak could be due to cross-linking within the sample. This could result in similar diffusion coefficients for both species despite a difference in size in THF as solvent and as a consequence AF4 is not suitable for a complete separation.

Chapter 3: Polybutadienes
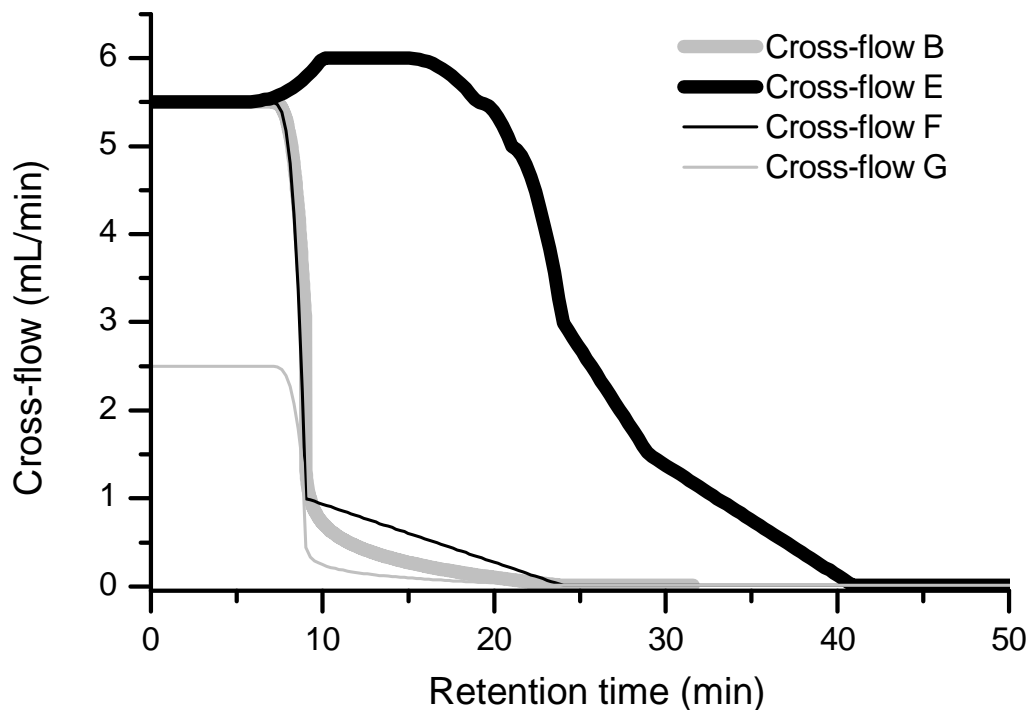
Fig. 3.18 Cross-flow profiles used in an attempt to separate the bimodal peaks of PB 6 observed in Fig. 3.16
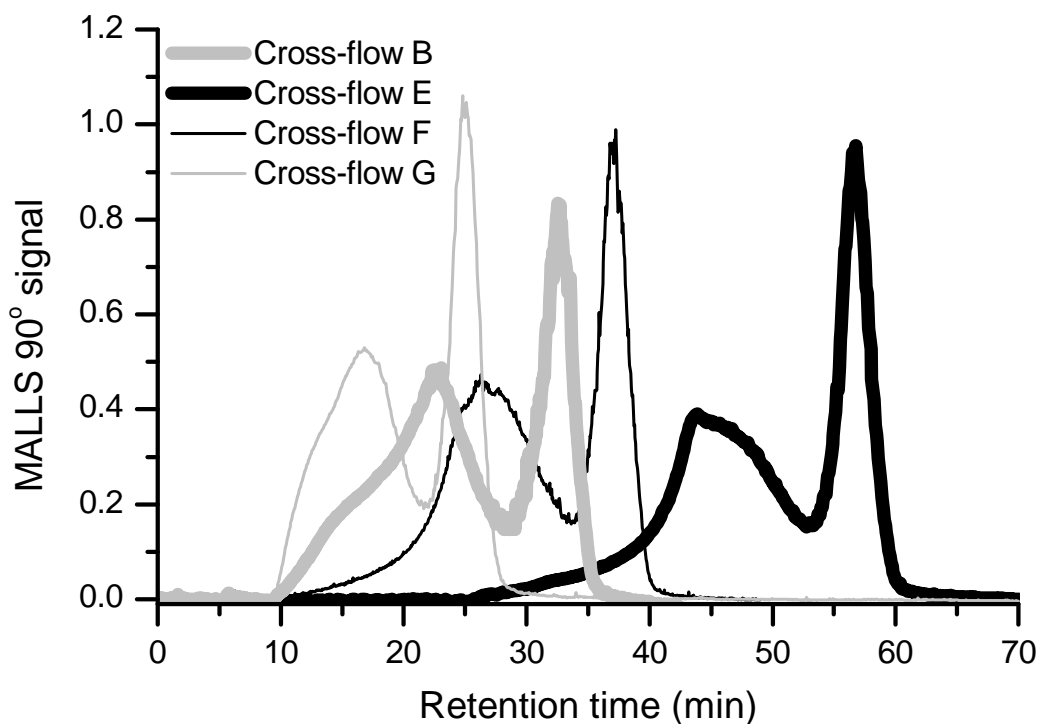
Fig. 3.19 PB 6 MALLS signals of the fractograms obtained using cross-flow profiles as given in Fig. 3.18

The similar diffusion coefficients may also be caused by differences in shape of both species since a rod-like structure would have a lower hydrodynamic radius/diffusion coefficient than a coil of the same

molar mass.[48-50] Further adjusting the cross-flow or making use of mixed mobile phases could be a solution for optimal separation in AF4. Thermal FFF (ThFFF) separates according to chemical composition and hydrodynamic volume and could also be a possible solution for this problem since the diffusion can be adjusted by temperature programming and thus the fractionation efficiency may be increased.

3.4 Conclusions

The AF4-MALLS-RI separation technique was successfully implemented for ultrahigh molar mass polymers. Comparisons of SEC with AF4 using polystyrene standards as reference materials were in good agreement with the expected values. The versatility of the cross-flow field in AF4 is an invaluable tool for the optimisation of separation as was shown for the mixture of polystyrene standards. As a result the correct molar mass and radius information can be obtained in the case of perfect separation. SEC analysis of polybutadienes showed overlapping effects of chain scission and entanglements of large molecules, while the co-elution of large macromolecules together with regular eluting species of smaller molar mass causes problems with regard to calculating the correct molar mass and radius distributions.

In contrast, AF4 analysis of the rubber materials showed a number of advantages over SEC, especially in the case of ultrahigh molar mass, branched and gel-containing samples. Due to the higher exclusion limit and absence of a stationary phase in AF4, accurate molar mass and radius distributions can be calculated for the branched or ultrahigh molar mass species since co-elution due to branching or shear degradation is minimised. AF4 is also a valuable tool for investigating dissolution compared to SEC where filtration is necessary. The MALLS detector is very sensitive to high molar mass species, therefore, as a result of the empty channel in AF4 it was possible to analyse very small amounts of gel species without filtering the samples. The experiments indicate that it is possible to use AF4 as a special tool for the extended analysis of synthetic rubber materials especially in case of very high molar mass or excessive branching. In future the new information from AF4 could offer the possibility to explain some differences in the processing behaviour of such samples.

3.5 References

(1)   Schimpf M. E.; Caldwell K.; Giddings J. C. *Field Flow Fractionation Handbook*. New York: John Wiley & Sons; **2000**.

(2)   Adolphi U.; Kulicke W.-M. *Polymer* **1997**; 38(7), 1513-1519.

(3)   Arfvidsson C.; Wahlund K.-G. *J. Chromatogr. A* **2003**; 1011(1-2), 99-109.

(4)   Dubascoux S.; Von Der Kammer F.; Le Hécho I.; Gautier M. P.; Lespes G. *J. Chromatogr. A* **2008**; 1206(2), 160-165.

(5)   Lee H.; Cho I.-H.; Moon M. H. *J. Chromatogr. A* **2006**; 1131(1-2), 185-191.

(6)   Ratanathanawongs Williams S. K.; Lee D. *J. Sep. Sci.* **2006**; 29(12), 1720-1732.

(7)   Mes E. P. C.; de Jonge H.; Klein T.; Welz R. R.; Gillespie D. T. *J. Chromatogr. A* **2007**; 1154(1-2), 319-330.

(8)   Otte T.; Brüll R.; Macko T.; Pasch H.; Klein T. *J. Chromatogr. A* **2010**; 1217(5), 722-730.

(9)   Otte T.; Pasch H.; Macko T.; Brüll R.; Stadler F. J.; Kaschta J.; Becker F.; Buback M. *J. Chromatogr. A* **2011**; 1218(27), 4257-4267.

(10)   Lee D.; Williams S. K. R. *J. Chromatogr. A* **2010**; 1217(10), 1667-1673.

(11)   Lohmann C. A.; Haseltine W. G.; Engle J. R.; Williams S. K. R. *Anal. Chim. Acta* **2009**; 654(1), 92-96.

(12)   Shiundu P. M.; Remsen E. E.; Giddings J. C. *J. Appl. Polym. Sci.* **1996**; 60(10), 1695-1707.

(13)   Williams S. K. R.; Runyon J. R.; Ashames A. A. *Anal. Chem.* **2010**; 83(3), 634-642.

(14)   Stojanov C.; Shirazi Z.; Audu T. *Chromatographia* **1978**; 11(5), 274-281.

(15)   Parth M.; Aust N.; Lederer K. *Macromolecular Symposia* **2002**; 181(1), 447-456.

(16)   Aust N. *J. Biochem. Bioph. Methods* **2003**; 56, 323-334.

(17)   Kim C.; Morel M.-H.; Beuve J. S.; Guilbert S.; Collet A.; Bonfils F. *J. Chromatogr. A* **2008**; 1213(2), 181-188.

(18)   Kim C.; Beuve J. S.; Guilbert S.; Bonfils F. *Eur. Polym. J.* **2009**; 45, 2249–2259.

(19)   Lee S.; Molnar A. *Macromolecules* **1995**; 28(18), 6354-6356.

(20)   Lee S.; Eum C. H.; Plepys A. R. *Bull. Korean Chem. Soc.* **2000**; 21(1), 69-74.

(21)   Lewandowski L.; Sibbald M. S.; Johnson E.; Mallamaci M. P. *Rubber Chem. Technol.* **2000**; 73(4), 731-742.

(22)   Sibbald M.; Lewandowski L.; Mallamaci M.; Johnson E. *Macromolecular Symposia* **2000**; 155(1), 213-228.

(23)   Kim W.-S.; Eum C. H.; Molnar A.; Yu J.-S.; Lee S. *Analyst* **2006**; 131(3), 429-433.

(24)   Ratanathanawongs Williams S. K.; Benincasa M.-A.; Ashames A. A. *Field Flow Fractionation in Analysis of Polymers and Rubbers*. John Wiley & Sons, Ltd; **2009**.

(25)   Bang D. Y.; Shin D. Y.; Lee S.; Moon M. H. *J. Chromatogr. A* **2007**; 1147(2), 200-205.

(26)   Awan M. A.; Dimonie V. L.; Ou-Yang D.; El-Aasser M. S. *Langmuir* **1997**; 13(2), 140-146.

(27)   Kwag G.; Kim P.; Han S.; Choi H. *Polymer* **2005**; 46, 3782–3788.

(28)   Nasirov F. A. *Iranian Polymer Journal* **2003**; 12(4), 281-289.

(29)   Pires N. M. T.; Ferreira A. A.; de Lira C. H.; Coutinho P. L. A.; Nicolini L. F.; Soares B. G.; Coutinho F. M. B. *J. Appl. Polym. Sci.* **2006**; 99, 88–99.

Chapter 3: Polybutadienes

(30)   Mori S.; Ishikawa M. *Journal of Liquid Chromatography & Related Technologies* **1998**; 21(8), 1107-1117.

(31)   Angelo R. J.; Ikeda R. M.; Wallach M. L. *Polymer* **1965**; 6(3), 141-156.

(32)   Giddings J. C. *Science* **1993**; 260(5113), 1456-1465.

(33)   Podzimek S. *Light Scattering, Size Exclusion Chromatography and Asymmetric Flow Field Flow Fractionation: Powerful Tools for the Characterization of Polymers, Proteins and Nanoparticles*. New York: John Wiley & Sons; **2011**.

(34)   Otte T.; Klein T.; Brüll R.; Macko T.; Pasch H. *J. Chromatogr. A* **2011**; 1218(27), 4240-4248.

(35)   Johann C.; Kilz P. J. *J. Appl. Polym. Sci.: Appl. Polym. Symp.* **1991**; 48, 111-122.

(36)   Wintermantel M.; Antonietti M.; Schmidt M. *J. Appl. Polym. Sci.: Appl. Polym. Symp.* **1993**; 52, 91-103.

(37)   Frater D. J.; Mays J. W.; Jackson C. *Journal of Polymer Science: Part B: Polymer Physics* **1997**; 35, 141-151.

(38)   Percec V.; Ahn C. H.; Cho W. D.; Jamieson A. M.; Kim J.; Leman T.; Schmidt M.; Gerle M.; Möller M.; Prokhorova S. A.; Sheiko S. S.; Cheng S. Z. D.; Zhang A.; Ungar G.; Yeardley D. J. P. *J. Am. Chem. Soc.* **1998**; 120, 8619-8631.

(39)   Gerle M.; Fischer K.; Roos S.; Muller A. H. E.; Schmidt M. *Macromolecules* **1999**; 32, 2629-2637.

(40)   Podzimek S.; Vlcek T.; Johann C. *J. Appl. Polym. Sci.* **2001**; 81(7), 1588-1594.

(41)   Wyatt P. J. *Anal. Chim. Acta* **1993**; 272(1), 1-40.

(42)   Podzimek S. *J. Appl. Polym. Sci.* **1994**; 54(1), 91-103.

(43)   van Bruijnsvoort M.; Wahlund K. G.; Nilsson G.; Kok W. T. *J. Chromatogr. A* **2001**; 925(1-2), 171-182.

(44)   Podzimek S.; Vlcek T. *J. Appl. Polym. Sci.* **2001** 2001; 82(2), 454-460.

(45)   Stadler F. J.; Kaschta J.; Münstedt H.; Becker F.; Buback M. *Rheol. Acta* **2009**; 48, 479-490.

(46)   Ratanathanawongs Williams S. K.; Benincasa M.-A.; Ashames A. A. *Field Flow Fractionation in Analysis of Polymers and Rubbers*. John Wiley & Sons, Ltd; **2006**.

(47)   Bell W.; Pethrick R. A. *Polymer* **1982**; 23(3), 369-373.

(48)   Chung S. E.; Chung I. J. *Polym. Bull.* **1989**; 21(1), 105-112.

(49)   Farzaneh S.; Hossein F. *The Journal of Chemical Physics* **2011**; 133(23), 234904.

(50)   Zero K. M.; Pecora R. *Macromolecules* **1982**; 15(1), 87-93.

55

Chapter 4: Analysis of polyrotaxanes: Polymers with complex molecular architectures

4.1 Introduction

Polyrotaxane based polymer brushes are polymers with a distinct molecular architecture. These novel polymer materials are realized by the threading of a backbone polymer chain by cyclic molecules. In this study, the backbone polymer chain was polyethylene glycol (PEG) with a target molar mass of approximately 10000 g/mol, while the cyclic molecules were α-cyclodextrins (α-CDs). After threading, bulky pendant groups were attached at the ends of the backbone chain to prevent the α-CDs from de-threading. The polymer brushes were formed by ATRP polymerization of poly (methyl methacrylate) (PMMA) onto the α-CD units (Fig. 4.1). The degree of substitution on the CD rings was targeted at approximately eight PMMA chains of 5000 g/mol each. These polyrotaxane-based polymer materials were analysed by size exclusion chromatography (SEC) and asymmetric flow field flow fractionation (AF4). Both fractionation techniques were coupled to MALLS and RI detection. The elution behaviour of the polyrotaxane-based samples was investigated and the initial SEC results showed a bimodal molar mass distribution. High- and low molar mass fractions were observed and a study was conducted based on SEC and AF4 to compare the two techniques and to identify the limitations of SEC. The main focus was to utilize AF4 in addition to SEC characterization to add more in-depth information on the elution behaviour of these specific polyrotaxane materials in a stationary phase-free environment. Results showed that as a specialized tool, AF4 can be used for the extended analysis of polymer molecules with sophisticated molecular architectures.

4.2 Experimental
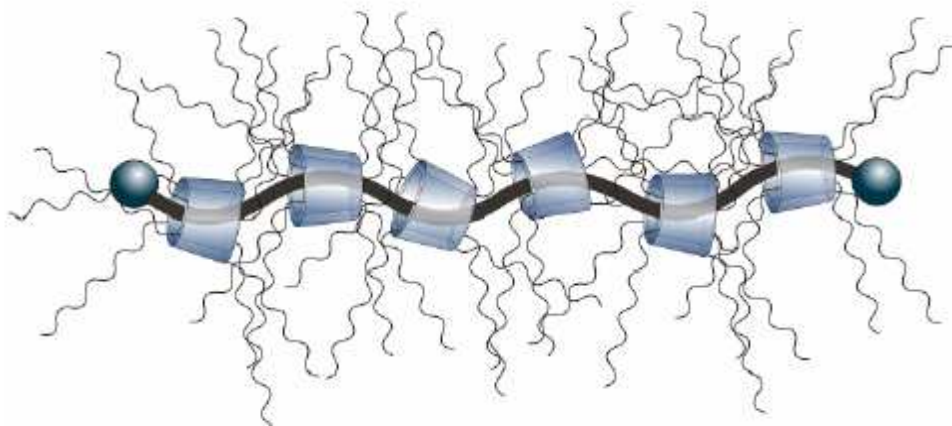
Fig. 4.1 Representation of a polyrotaxane polymer brush. Figure courtesy of Christian Teuchert, Saarland, Saarbrucken, Germany

The polyrotaxanes were prepared according to the published Beckham method.[1] The α-CD-PEG inclusion compound was obtained by adding an aqueous solution of PEG of 10 kg/mol to an aqueous solution that is saturated with α-CD at room temperature. The complexes forms and precipitates out of solution. A solution of 4-methoxynaphthol in absolute dimethylformamide (DMF) was added to NaH under nitrogen atmosphere. The mixture was stirred for 10 min. and then the pseudopolyrotaxane

(PEG chains threaded with CD) was added and rinsed down with DMF. The mixture was stirred overnight and the polyrotaxane was precipitated in methanol, and collected by centrifugation. The procedure was repeated by dissolution in dimethylsulfoxide (DMSO) and precipitated into water. The white solid product was dried overnight under vacuum.

Polyrotaxane-macroinitator (PR-MI)

To a solution of polyrotaxane in dry dimethyl acetamide (DMAC) containing lithium chloride (LiCl), pyridine and dimethyl amino pyridine (DMAP) were added at 0℃ under nitrogen atmosphere . After cooling bromoisobutyryl bromide was added drop-wise and stirred overnight. The crude product was precipitated from Et_2O, dissolved in acetone and precipitated from methanol several times. The PR-MI was filtered and dried in vacuum to get a brown powder.

Polyrotaxane polymer brush

To a solution of 40 mg PR-MI in 10 mL DMSO, 11.5 mg CuBr, 17.87 mg copper bromide ($CuBr_2$) and 66 mg hexamethyl triethylene tetramine (HMTETA) were added under argon atmosphere. The solution was degassed by freezing and thawing the flask three times. By addition of 1.4 g MMA the polymerization was started. After 3 hours the polymerization was stopped by addition of O_2. The excess monomer was removed under reduced pressure and then the residue was freeze dried to remove the DMSO. The green residue was dissolved in 10 mL chloroform (CH_2Cl_2) and washed with 10 mL aqueous ethylendiamine tetraacetic acid (EDTA) solution three times. The solvent was removed under reduced pressure to obtain the product as in Fig. 4.1.

The precursor polymer (CD84) was prepared by grafting PMMA onto the CD rings without any backbone or stopper groups.

Instrumental conditions

The polyrotaxane polymer brush and the precursor polymer which was synthesized in Germany (CD88) was analysed via SEC and AF4, respectively. Provisional SEC data were obtained from the University of Saarland, Saarbrucken in Germany. At Stellenbosch University, the experiments were performed on an AF4-Instrument (Postnova Analytics, Landsberg/Germany) which was coupled to MALLS- and RI-detection. Two column sets consisting of PL gel columns (1: mixed B and C, 2: mixed A and B) with dimensions of 30cm x 7.5mm i.d. each were used for the SEC measurements. The detector flow was kept constant at 0.5 mL/min and a 100µL sample loop was for both separation techniques. The dn/dc value for the polyrotaxane sample was measured at 0.047 mL/g in THF at 25 ℃. The cross-flow profile is given in Fig. 4.2 an d the progression of the flow profile after sample injection was already explained in Chapter 3:

The samples were dissolved in HPLC grade THF for 14 hours at room temperature without adding stabilizer. Sample CD88 was analyzed by both SEC (column set 1) and AF4 at various concentrations to see whether concentration plays a major role on the separation and consequently the average molar mass, molar mass distribution (MMD) as well as R_g. The obtained molar masses and radii were

calculated and compared with the results from University of Saarland. The fitting of results were done according to the random coil method.
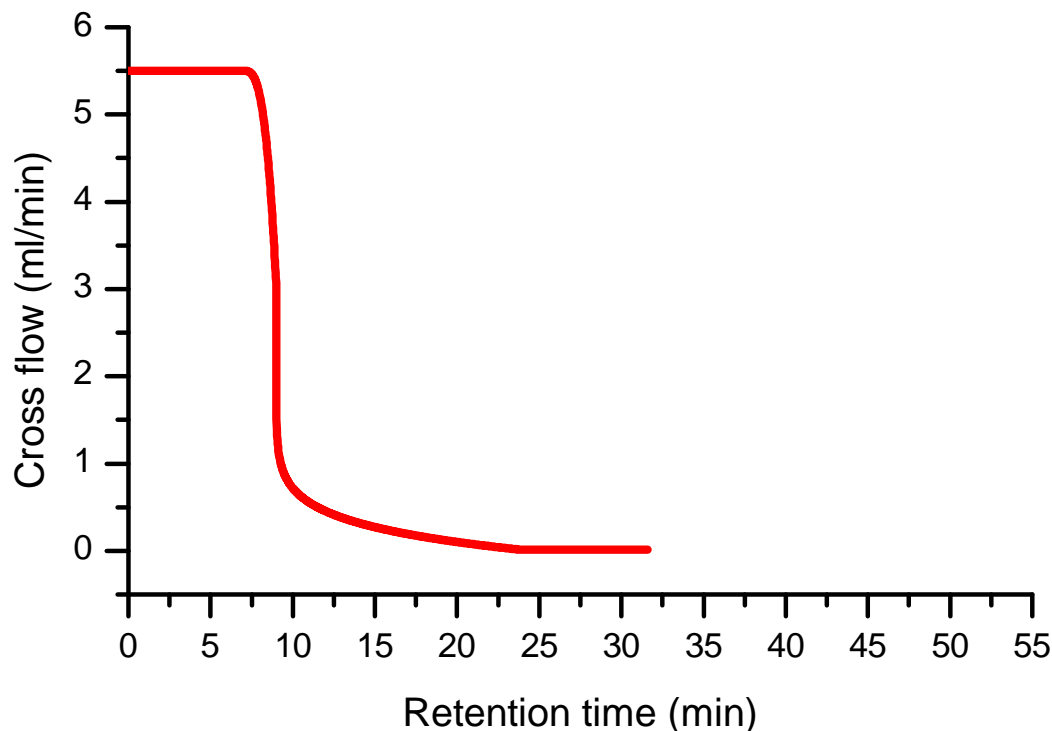
Fig. 4.2 Cross-flow profile used for AF4 measurements of polyrotaxanes based on cross-flow B in Chapter 3

4.3 Results and discussion

4.3.1 Comparative study of polyrotaxane and its precursor polymer brush using different concentrations and column sets in SEC.

For a comparison with the SEC results that were provided by Saarland University in Germany, we conducted our own measurements in THF using MALLS for molar mass and R_g detection. Since the expected molar masses for the polyrotaxane sample (CD73) were quite high, the effect of concentration on the SEC elution behaviour was investigated for both the precursor polymer (CD84) and the polyrotaxane brush (CD73).

Chapter 4: Polyrotaxanes

The precursor polymer which consists of PMMA grafted CD rings without a PEO backbone chain and stopper groups (sample CD84), was investigated and compared to the main-chain polyrotaxane polymer brush (CD73). The effects of concentration (SEC and AF4), cross-flow strength and focus-flow (AF4) on the elution behaviour were investigated. In addition different column sets were tested for the SEC measurements where different concentrations of sample CD84 were analysed starting with column set 1 (PL-gel mixed B and C columns).

The elution behaviour did not show change in the concentration range between 0.752 and 7.25 mg/mL at an injection volume of 100 µL. The RI and MALLS signal intensities did not show any band broadening upon an increase in concentration, an indication that the columns were not overloaded (Figs. 4.3 and 4.4).
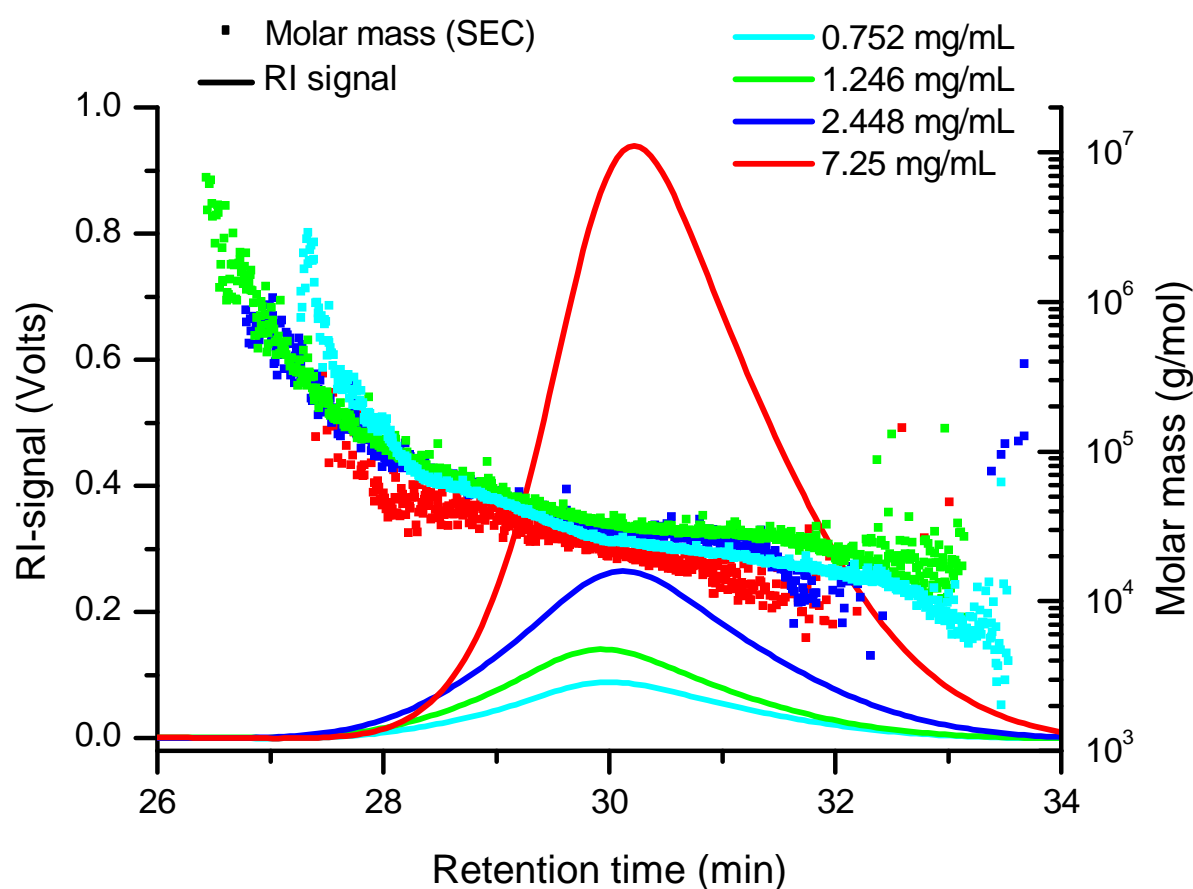
Fig. 4.3 SEC-elugram with molar mass overlaid for CD84 for column set 1. The lines and filled squares represent the RI-signal and molar masses, respectively.

Normal SEC behaviour is observed irrespective of concentration and monomodality is obtained for the precursor polymer. This is indicated by the molar mass reading in Fig. 4.3 showing a decrease towards smaller values without any irregularities.

Unexpectedly, the size distribution plot in Fig. 4.4 A does not show a regular decrease with increasing retention time as was expected from Fig. 4.3. Fig. 4.4 A shows that the size distribution of the early eluting species (26-29 min) corresponds very well with the later eluting species (31-33 min). This

holds true only for the measurement that had the highest concentration. At higher elution times size decreases but then suddenly increases again.

This could indicate the overlapping of two different effects: (1) the expected decrease in size with increasing elution time and (2) an unexpected late elution of larger molecules with increasing elution time. The second assumption cannot hold however since a monotonal decrease in molar mass is observed (Fig. 4.3). Another possibility might be a bimodal size distribution that appears as a monomodal peak in the RI and MALLS signals (Fig. 4 B). Fig. 4 B indicates that the deconvolution of the observed monomodal peak could result in the elution of different species with different interaction with the stationary phase. In this example the fully PMMA grafted-CDs (R_{g1}) is shown to be more dense compared to the proposed CD aggregates with only a few grafted PMMA chains (R_{g2}). As a result a higher molar mass reading is observed compared to the less dense proposed structure. Due to the lack of grafting, the cavities of the CDs might also play a role in the elution behaviour. The hydroxyl groups on the surface of the CD rings might interact with the stationary phase leading to an increase in the size distribution as observed in Fig. 4 A.

The highest concentration sample was measured four times and the R_g plot showed similar behaviour (not shown). The reason for the intense R_g scattering of the low concentration samples might have been due to the very low obtained average molar masses detected. The low average molar masses cause isotropic scattering if molecules well below the size of $1/20^{th}$ of the incident light wavelength from the MALLS laser are detected.[2] As a result no accurate radii could be calculated for the low concentrations, yet a molar mass determination was possible. The percentage recovery, molar mass and radii values for the highest concentration of CD84 are shown in Table 4.1.
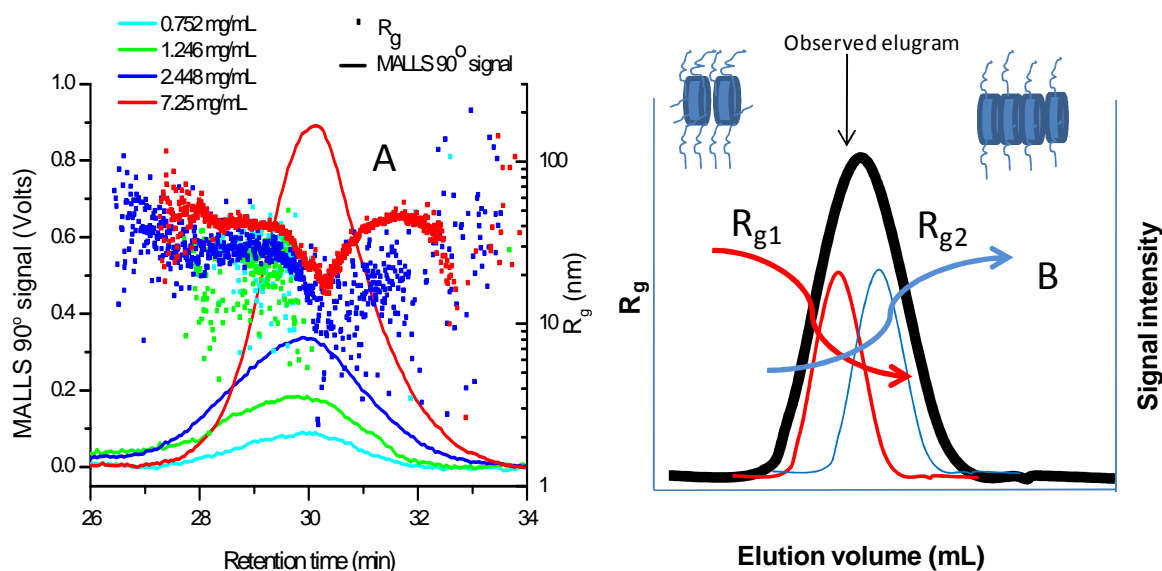
Fig. 4.4 A) SEC elugram of column set 1. MALLS 90° signal (solid line) with R_g overlays (filled squares) of CD84. B) Possible size overlapping effects for different species of CD84, with R_{g1} resembling fully PMMA-grafted CDs while R_{g2} represents unbound CD rings forming channel structures, with moderate PMMA grafting

Chapter 4: Polyrotaxanes

Table 4.1 Recovery percentages, molar masses and radii calculations for CD84 using column set 1. Results are compared from different laboratories. Saar-Saarbrucken, Stel-Stellenbosch

CD84	Recovery (%)	M_w (kg/mol)	M_n (kg/mol)	PDI	R_g (nm)
SEC Saar		33.8	17.9	1.89	
SEC Stel (7.25 mg/mL)	81.6	26	23.1	1.13	33.8
Run 2	81.5	25.4	21.9	1.16	34.4
Run 3	57.5	26.6	23.5	1.13	33.4
Run 4	82.2	28.3	25.2	1.12	32.9

The obtained values in Table 4.1 clearly show the reproducibility achieved when injecting the sample with the highest concentration multiple times. The recovery was in the region of 80 percent which indicates that there is a small possibility of sample adsorption onto the stationary phases of the columns. Another possibility could be the presence of small amounts of insoluble material which were excluded by filtering before being injected into the column. When comparing the results from the two laboratories the molar masses obtained were in fairly good agreement with each other except for the PDI values. It is possible that some of the high molar mass species were adsorbed onto the columns resulting in an underestimation of the molar masses and subsequent PDIs.

For the investigation of the polyrotaxane sample (CD73), dissolution problems were encountered. The sample did not dissolve in the initial 14 hours at room temperature, therefore additional time was allowed as well as moderate heating for an improvement in dissolution. A clear solution was obtained, but yet it was difficult to filter the solution through a 0.45 µm filter. This was probably caused by a fraction of the polymer molecules not fully dissolved, and as a result not being able to pass the 0.45 µm filter and being excluded from the measurement. This assumption was evident in the low recoveries obtained for the entire concentration range (Table 4.2) for the SEC measurements.

Despite the low recoveries bimodal MALLS and RI peaks were observed which are in good agreement with the initial results in terms of modality (Fig. 4.5 A and B). By comparing the calculated recoveries over the concentration range, it can be seen that the values differ from the lowest to highest concentration (Table. 4.2). This was probably due to improper solvation of the polymer chains as mentioned earlier. By comparing the calculated molar masses and radii, the values are relatively constant within the range of one order of magnitude, except for the third measurement where the recovery was seemingly low and the corresponding molar mass and R_g gave erroneous values. The calculated molar masses of both fractions were higher for column set 1 over the measurement done in Germany.

Chapter 4: Polyrotaxanes

Table 4.2   Comparison of recovery, molar mass and radii data from column set 1 for CD73. Results are for the whole concentration range. Concentrations based on Figs. 4.5 A and B.

CD73	Recovery (%)	High Molar mass fraction			Low Molar Mass fraction		
		M_w (kg/mol)	PDI	R_g (nm)	M_w (kg/mol)	PDI	R_g (nm)
SEC Saar	–	895	1.52	–	79.2	1.86	–
SEC Stel 0.6075 mg/mL	38.4	7890	1.06	38.3	1360	1.27	39.2
1.258 mg/mL	76.6	5370	1.05	33.2	1900	1.35	39.4
2.935 mg/mL	15.6	5650	1.06	24.4	6110	1.06	23.2
4.100 mg/mL	33.7	5220	1.06	32.5	1270	1.41	37.5

The molar mass vs. retention time plot showed a U-shaped curve representing non-SEC effects (Fig. 4.5 A). The molar mass reading was obtained from the MALLS detector at a scattering angle of 90°. As was expected based on the data that were provided by Saarland University a bimodal molar mass distribution was obtained with high molar mass fractions eluting first. The later eluting fractions exhibit lower molar masses up to a certain elution time (28 minutes) corresponding to normal SEC behaviour, i.e. elution from high to low molar masses. Beyond 28 minutes an up-swing of the molar mass reading is observed indicating that the latest eluting fractions have higher molar masses.

The molar masses of the early and late eluting fractions are unusually high compared to the obtained R_g values. As can be seen in Fig. 4.5 A, the molar mass readings of the polymeric species are as high as the exclusion limit of the mixed B column (10000 kg/mol), while the corresponding sizes are between 20 nm and 30 nm (Fig. 5 B). The theoretical size for a polydisperse polystyrene polymer with molar mass of 3600 kg/mol which was the average molar mass for the high molar mass fraction is approximately 100nm for a random coil in a good solvent.[3] The obtained average size for the present sample is much lower than 100nm and this is characteristic of a spherical structure.[3] Therefore it can be assumed that the shape of the polyrotaxanes is in the form of an extremely highly dense compact sphere which is densely populated with very high molar mass species.

Such SEC behaviour is known from high molar mass branched polymers where high molar mass branched fractions co-elute with low molar mass linear fractions whereby the branched chains can anchor themselves in the pores of the stationary phase.[4-11] For the present sample this is an unexpected observation. However, similar behaviour might be caused by high molar mass fractions

Chapter 4: Polyrotaxanes

that are degraded by strong shear forces in the SEC column or the rearrangement of macromolecules during the SEC separation process also known as slalom chromatography.[12,13]
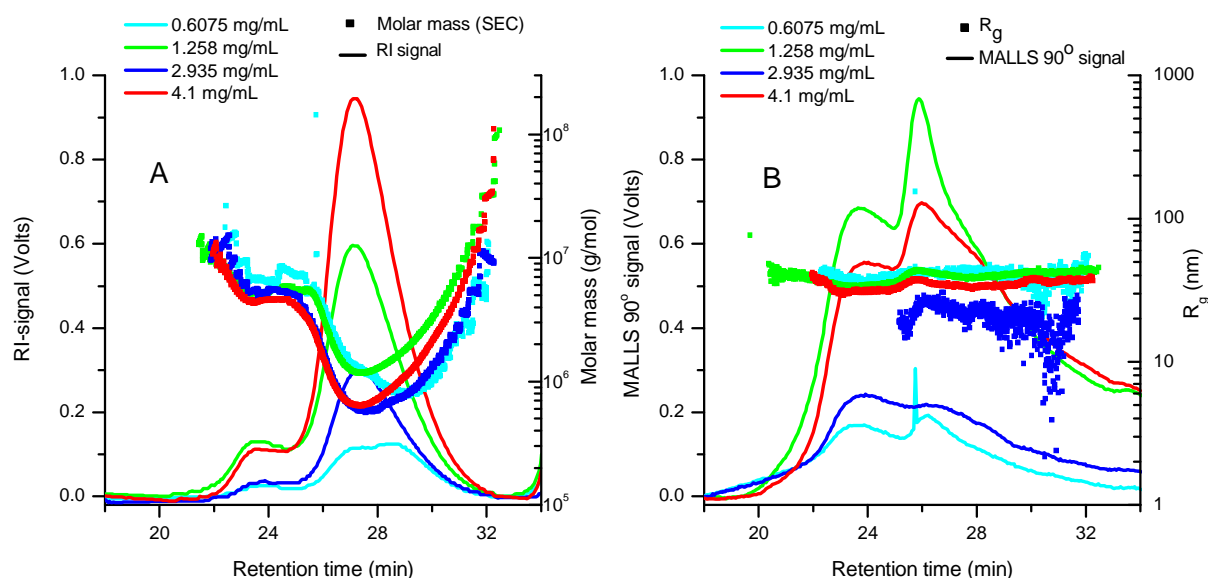
Fig. 4.5 SEC elugrams for column set 1. A) RI-signal with molar mass overlaid and B) MALLS 90° signal with R_g overlaid for CD73 with increasing concentration

Another explanation for the re-increase could be due to adsorption of polymer molecules onto the stationary phase of the SDV columns. Since the stopper groups are highly aromatic and the stationary phase consist of styrene functional groups, possible π-π interactions can take place causing adsorption onto the stationary phase resulting in interaction chromatography where enthalpic interactions dominate.[5,14-17]

The PMMA side chains that are grafted onto the CDs (Fig. 4.1) can act as branches and cause an anchoring effect in some of the pores of the stationary phase, resulting in high molar mass species being retained unusually long on the column. The anchoring effect can also cause the high molar mass molecules, where the degree of PMMA grafting might be high, to elute together with regular eluting linear species.

When the molar mass plots of CD73 and CD84 are compared for the highest concentration (Fig. 4.6 A) it can be observed that the later eluting fraction from CD73 is due to the presence of CD84 precursor polymers. The abnormal elution behaviour for the later eluting fraction of CD73 results in the absence of lower molar masses in the molar mass plot. Therefore the lower molar mass fraction and the subsequent calculations were masked by the upswing effect and much higher values were detected which were in the same order of magnitude as the earlier eluting fractions. Sample CD84 does not show abnormal SEC elution and proper elution of high to low molar mass species are observed according to normal SEC behaviour; therefore accurate molar mass determinations could be made for the precursor hairy PMMA-grafted cyclodextrins.. The R_g plots (Figs. 4.4 and 4.6 B) once more show a very interesting phenomenon.

Chapter 4: Polyrotaxanes
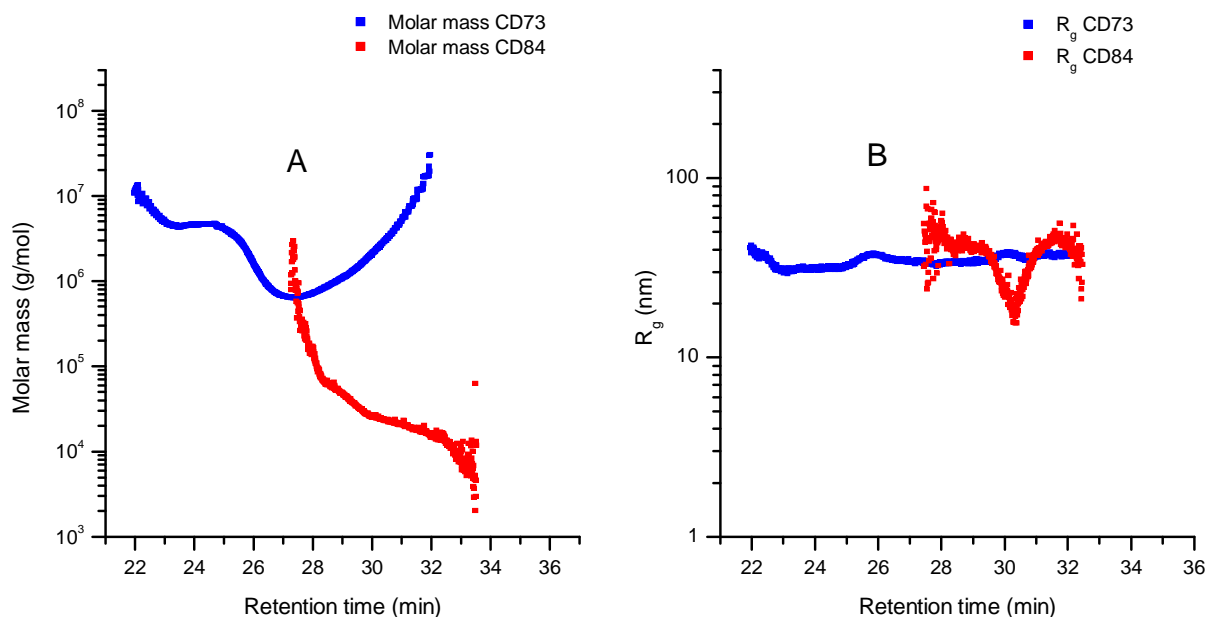
Fig. 4.6 A) Molar mass- and B) R_g overlays (SEC) of CD73 and CD84, respectively, indicating the uniform size irrespective of the molar mass behaviour for column set 1.

The size of the polymer molecules is homogeneous throughout the concentration range. CD73 shows a straight line throughout the elution range and the initial decrease and re-increase in the R_g plot observed in CD84 is not for this sample. This observation for CD84 is a possible indication that the decrease in size for CD84 could be an artefact and not a true size reflection. The R_g plot of the least recovered measurement (blue squares in Fig. 4.5 B) deviates from the rest of the measurements, possibly due to erroneous radius fitting from the software. Nevertheless for column set 1 the same outcome was observed for CD84 and CD73 in terms of the R_g plots, i.e. homogeneity irrespective of molar mass, concentration and light scattering fitting procedure (Fig. 4.6 B). The abovementioned discovery, even though in the presence of secondary separation effects, allows for an assumption that the size of the molecules stays relatively constant irrespective of the molar mass which corresponds to the extent of how densely populated each polyrotaxane molecule is in solution. For CD84, which did not have a backbone chain, the size is comparable with the polyrotaxane polymer sample, which is a possible indication that the cyclodextrins with the PMMA grafts somehow are able to orientate themselves in such a manner that the size are in good comparison as indicated by Topchieva *et. al.* illustrated.[18] They showed that unbound CD rings are able to stack against each other to form channel structures arranged in a head to head or tail to tail fashion.

The study was continued by changing the columns to column set 2 (PL gel mixed A and B), in effect increasing the exclusion limit of the molar mass separation range to 40 million g/mol compared to 10 million g/mol for column set 1. The permeation limit was increased as well from 200 to 2000 g/mol. The same study was done as for the mixed B and C column set.

At low concentrations a broad MALLS and a pronounced monomodal RI peaks are observed for CD84 (Fig. 4.7 A and B). If a closer look is taken for the lowest concentrations, a very small shoulder is observed in the RI signal for the earlier eluting species, which possibly indicates the presence of a

Chapter 4: Polyrotaxanes

very tiny amount of high molar mass species. This shoulder remains at a signal very close to zero, while the main peak increases in intensity upon an increase in concentration. The shoulder at 22 minutes is not an artefact since the signal becomes more intense upon concentration. The two highest concentration samples showed molar mass values larger than the rest of the concentrations. This could be attributed to the low RI-signal observed in the region of 20-26 minutes, resulting in questionable molar mass interpretations.

Fig. 4.7 A) Molar mass- and B) R_g vs. retention time plots with increasing concentration of CD84 for column set 2 (SEC). The RI- and MALLS 90° signals a re overlaid. Numbers 1 to 4 indicate the integration areas shown in Table 4.3

Four distinct high molar mass shoulders could be observed for the highest concentration (Fig. 4.7 B) which is possibly due to entanglement of polymer chains, but present in very small quantities. The R_g plots show homogeneity over the early eluting species but scatter a lot starting from an elution time of 28 minutes. The concentrations and fitting was difficult at such a low concentration, therefore the data points are more scattered over these elution slices and no concrete conclusions can be made regarding size for the later eluting species. The size interpretation from column set one might also be applicable in this case, and is rather excluded from the explanations. The evident multimodal peaks in Fig. 4.7 B were integrated over each peak in order to get an average R_g over each peak area and the calculations are shown in Table 4.3. As can be seen for the entire concentration range, the average size was more or less in the region of 30- to 40 nm, which corresponds very well with the R_g plots. Multimodality was not observed for the first column set (mixed B and C), possibly due to the presence of shear degradation and the absence thereof in the second column set. The calculated molar masses for each shoulder cannot be accurately explained at this point in time, since the concentration signal was near zero over the elution range from 20-28 minutes.

Chapter 4: Polyrotaxanes

Table 4.3 Recoveries, molar masses and radii for CD84 and CD73 using column set 2 with the individual molar masses for the multimodal peaks of the highest concentration. Concentrations are in the order as they appear in Figs. 4.7B and 4.8 respectively. The R_g values represent radii of the individual integrated peaks.

CD84	Recovery (%)	M_w (kg/mol)	M_n (kg/mol)	PDI	R_g (nm)
SEC (0.752 mg/mL)	91.5	82.3	36.9	2.24	37,32
1.246 mg/mL	80.1	83.2	37.7	2.21	36,37
2.448 mg/mL	83.5	93.7	42.6	2.20	37,41
3.259 mg/mL	79.3	91.2	35.7	2.50	34,37,28
5.488 mg/mL	79.6	145	36.8	3.94	–
Peak 1	–	9390	5670	1.66	37
Peak 2	–	1660	1550	1.07	32
Peak 3	–	5970	287	2.08	34
Peak 4	–	3480	32.7	1.07	26
CD73					
0.6075 mg/mL	25.8	551	231	2.39	–
1.258 mg/mL	30.4	290	194	1.49	–
2.935 mg/mL	21.1	250	152	1.64	–
4.100 mg/mL	29.0	179	134	1.34	–

The polyrotaxane sample CD73 had very low recoveries as observed in Table 4.3. Therefore the obtained molar masses and R_g are representative of a very small fraction of molecules (Fig. 4.8).
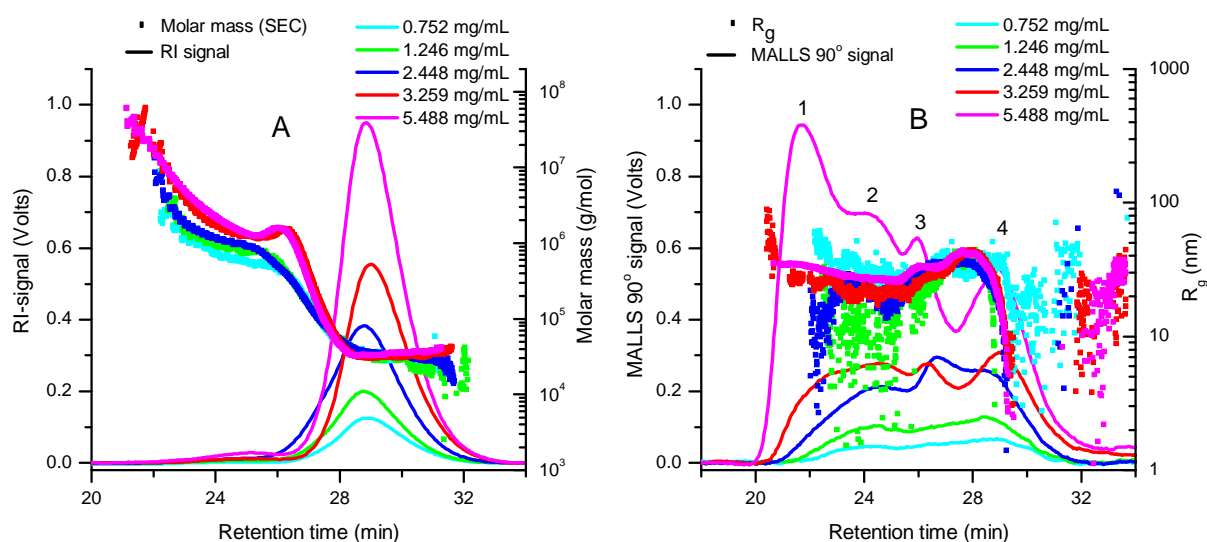
Chapter 4: Polyrotaxanes
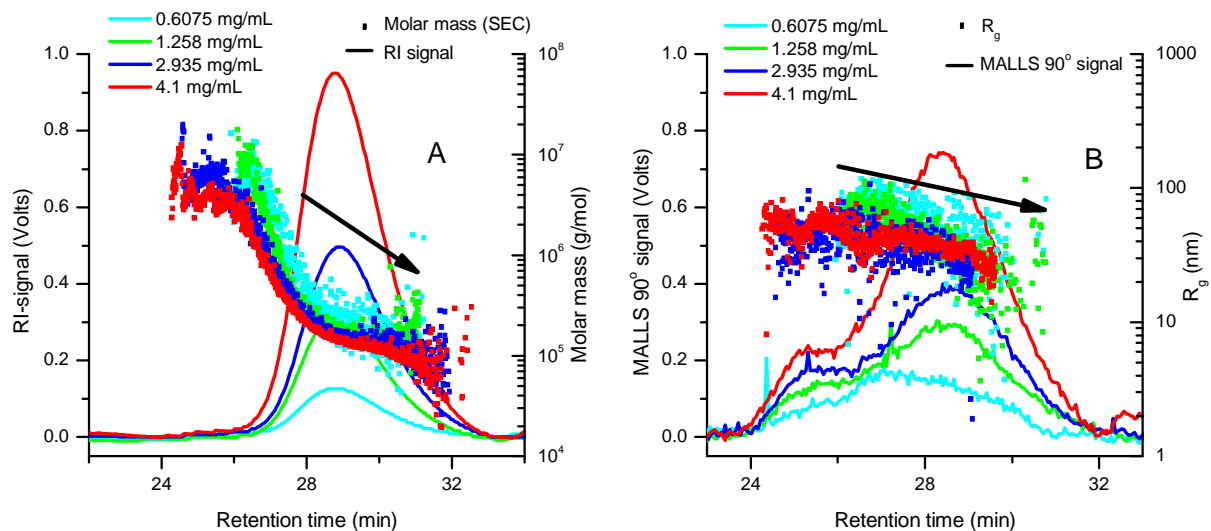
Fig. 4.8   A) Molar mass- and B) R_g vs. Retention time plots (SEC) with increasing concentration of CD73 for column set 2. The RI- and MALLS 90° signals are overlaid and normalized

Furthermore the observed MALLS signal is very spiky even after filtration through a 0.45 µm filter (Fig. 4.8 B). The difficulties with filtering the solution and the low recoveries are evidence of only partial solubility for CD73, hence the difficulties in analysing such samples with SEC. In contrast, enough polymer molecules were detectable in order to give a fairly reproducible molar mass reading for each concentration (Fig. 4.8 A). The obtained molar masses were in good comparison with the results from Saarbrucken University. The R_g plot however is scattered immensely, but a rather constant trend with respect to size can be observed despite the inaccurate data. Subsequent radii calculations were therefore not possible due to scattering. For this example, a trend towards lower molar masses and sizes are visible, despite the low recoveries observed, possibly indicating that a further optimization of the experimental conditions like flow rate or column selection, could aid in improving the separation and a better understanding of the molar mass and size behaviour.

4.3.2 AF4 study of CD84 and CD73: Investigation of the cross-flow strength and the presence or absence of a focus flow.

Both samples (CD84 and CD73) were analysed by AF4-MALLS-RI in order to identify the differences in elution behaviour compared to SEC. The cross-flow profile used has previously been used in Chapter 3 and is shown in Fig. 4.2. CD84 shows monomodal RI and MALLS signals upon concentration increase (Fig. 4.9 A and B), while CD73 shows bimodal RI- and MALLS signals with the earlier eluting low molar mass species showing a very weak light scattering response (Fig. 4.9 C and D). The argument for CD73 would be that the sample did not dissolve properly, but since in AF4 an empty channel is used as the separation platform, no filtering is necessary. After all, the sample in the solution flask was clear, and since no filtering is required, the measurement was a true reflection of the sample solution, which is at least true for the molecules that were recovered and not lost through the membrane. Therefore a perfect increase in signal intensity was observed as the concentration was increased, and proper analysis of the high molar mass macromolecules, which were filtered out for the SEC measurements, could be done.

CD84 shows more intense RI signals since the measured dn/dc value is almost double than for CD73 (0.094mL/g compared to 0.047 mL/g). The molar mass vs. elution time plots shows that the low molar mass fraction of CD73 corresponds fairly well with CD84, indicating that the CD73 sample also has unreacted PMMA grafted CDs (CD84) present. The outcome was a second distribution, which was also observed in the SEC measurements for the first column set. In SEC however no accurate interpretation could be made due to the non-SEC effects and abnormal elution observed.

The first difference in elution compared to SEC is that apparently in FFF there is a strong influence of the concentration on elution. The higher the concentration is the later do the macromolecules elute. Since a focusing step was applied of 4 minutes, this shift could be due to a larger percentage of high molar mass species accumulated in the slower parabolic flow layer near the accumulation wall. Due to the concentration build-up, the viscosity of that specific flow layer will increase, which results in a reduction in the diffusion coefficient. This causes the already slow moving molecules (at the accumulation wall) to move even more slowly towards the detectors, resulting in an increase in elution time and subsequent band broadening. In FFF the elution order is from small to large macromolecules. This assumption is supported by the RI and MALLS traces in Fig. 4.9 C and D for CD73. While the first eluting peak (corresponding to lower molar masses) is not affected by concentration, the later eluting peak (corresponding to higher molar masses) shows an increase in elution time with concentration.

For the highest concentration measurement in CD84 the sample were additionally filtered with 0.45µm and 0.20µm filters, respectively. Even though the solution was properly dissolved, distinct differences could be identified in the MALLS signals, namely a subtle reduction in the signal intensity upon filtering (Fig. 4.9 B) as well as a reduction in the elution time. In the RI-signal a perfect overlay was observed

Chapter 4: Polyrotaxanes

whether the sample was filtered or unfiltered supporting the fact that the quantities observed in the MALLS signal is almost zero (Fig. 4.9 A). These observations show the invaluable information which can be obtained by making use of a molar mass sensitive detector such as a MALLS detector. This observation was possibly due to very small amounts of either insoluble gel or entangled species of the precursor polymer. The R_g plot also shows a deviation from the rest of the measurements towards higher radii for the unfiltered sample shown in red. The measurements for the filtered samples showed that the high molar mass species were excluded from the measurements leading to a slight decrease of the molar mass readings as seen in Fig. 4.9 A.

Fig. 4.9 C shows an increase in molar mass until 14 minutes and a sudden decrease afterwards. This was probably due to co-elution of the high molar mass tail of unreacted precursor polymer overlapping with the lower molar mass end of the polyrotaxane sample. After the initial decrease the molar masses increases again to higher values according to normal mode AF4. The R_g reading corresponding to the overlapping region is rather constant, therefore it can be assumed that the species eluting from the channel had different coil densities, hence a change in molar mass reading.
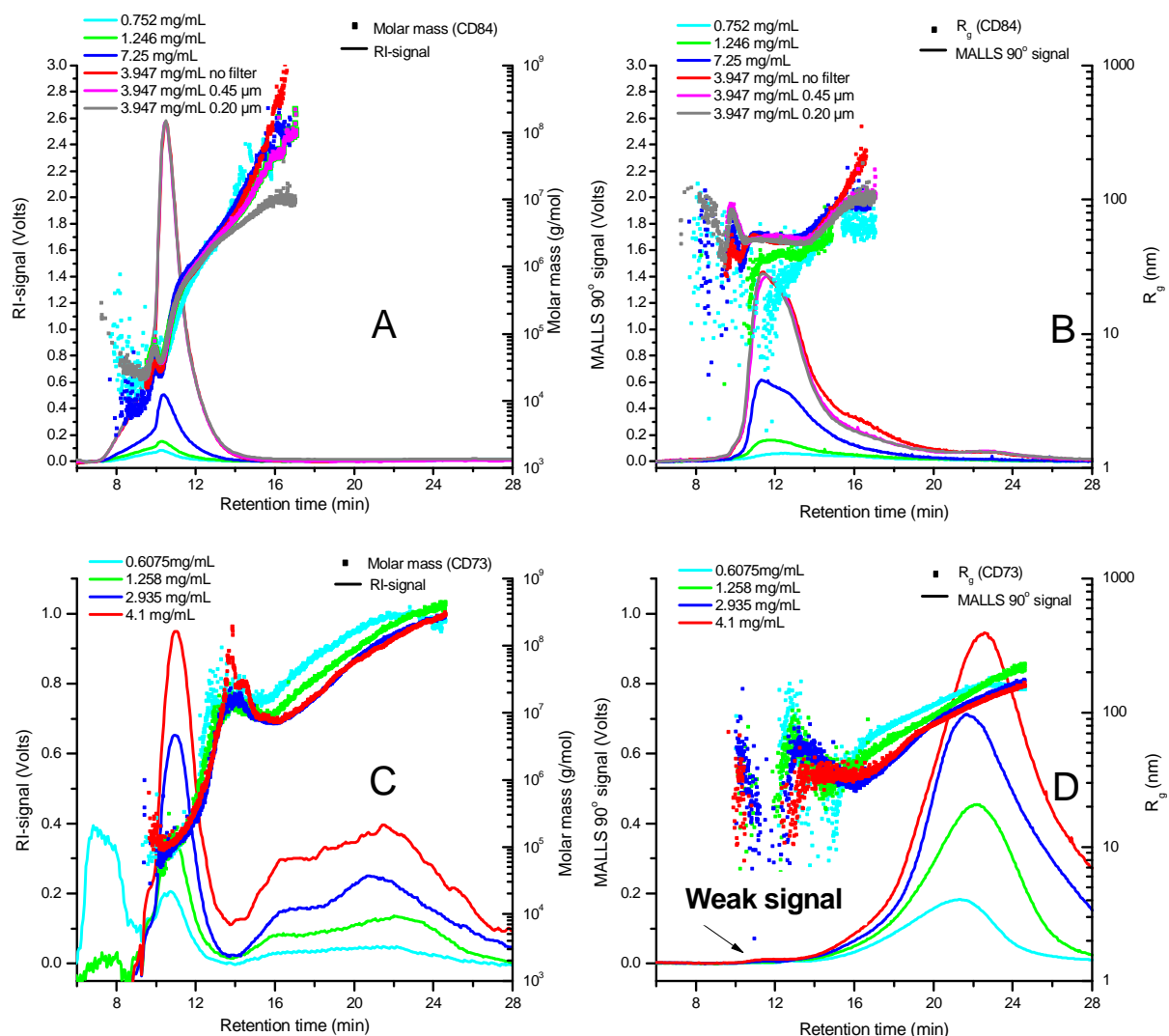

Fig. 4.9 Molar mass- (A, C) and R_g (B, D) plots (AF4) of CD84 (A, B) and CD73 (C, D), respectively, for the 5.5 mL/min cross-flow. The RI- and MALLS signals (solid lines) are overlaid

Chapter 4: Polyrotaxanes

When the AF4 (Fig. 4.9) and SEC (Figs. 4.3 to 4.8) results are compared it is evident that higher molar masses and radii are detected in AF4. When comparing the R_g plots of the two samples (CD84 and CD73), we see that the low molar mass fractions of CD73 are not well defined which could be due the low concentration detected as well as possible sample loss through the membrane resulting in even lower recoveries (Figs. 4.9 B and D) and even less accuracy in the radii determinations. However, when the average R_g values are compared (Table 4.4) the low molar mass species from CD73 and R_g values from CD84 are in excellent agreement for the higher concentration measurements. In Fig. 4.9 B and in Table 4.4 it is clearly visible that the lower concentration measurements deviate slightly in the R_g reading and calculated values, possibly due to the very low RI- and MALLS signals resulting in unreliable values.

Table 4.4 Comparison of recovery, molar mass and radii data from AF4 measurements using the cross-flow profile given in Fig. 4.2 for CD84 and CD73. Results are for the whole concentration range. Concentrations correspond to Fig. 4.9.

		High Molar mass fraction			Low Molar Mass fraction		
CD84	**Recovery (%)**	**M_w (kg/mol)**	**PDI**	**R_g (nm)**	**M_w (kg/mol)**	**PDI**	**R_g (nm)**
FFF 0.725 mg/mL	64.2	–	–	–	269	6.64	34.9
1.246 mg/mL	73.7	–	–	–	393	7.25	33.5
7.25 mg/mL	36.1	–	–	–	876	8.71	70.7
3.947 mg/mL	–	–	–	–	647	7.42	79.2
3.947 mg/mL 0.45 µm filter	–	–	–	–	605	6.40	64.8
3.947 mg/mL 0.20 µm filter	–	–	–	–	541	6.07	63.8
CD73							
FFF 0.6075 mg/mL	71.4	83800	1.56	113.5	–	–	–
1.258 mg/mL	77.7	90600	2.46	111.3	777	5.22	66.7
2.935 mg/mL	62.1	109000	3.842	146.4	528	3.82	71.9
4.100 mg/mL	78.1	96600	5.713	115	–	–	–

Chapter 4: Polyrotaxanes

The high molar mass later eluting fraction of CD73 also shows that much larger sizes are detected compared to SEC. These high molecular sizes could be due to the absence of shear degradation as well as the fact that no filtration was necessary prior to injection and the obtained results are a true representation of the sample solution. The recoveries observed are in the region of 70% for both samples, implying that some of the molecules were definitely able to pass the membrane irrespective of the concentration used.

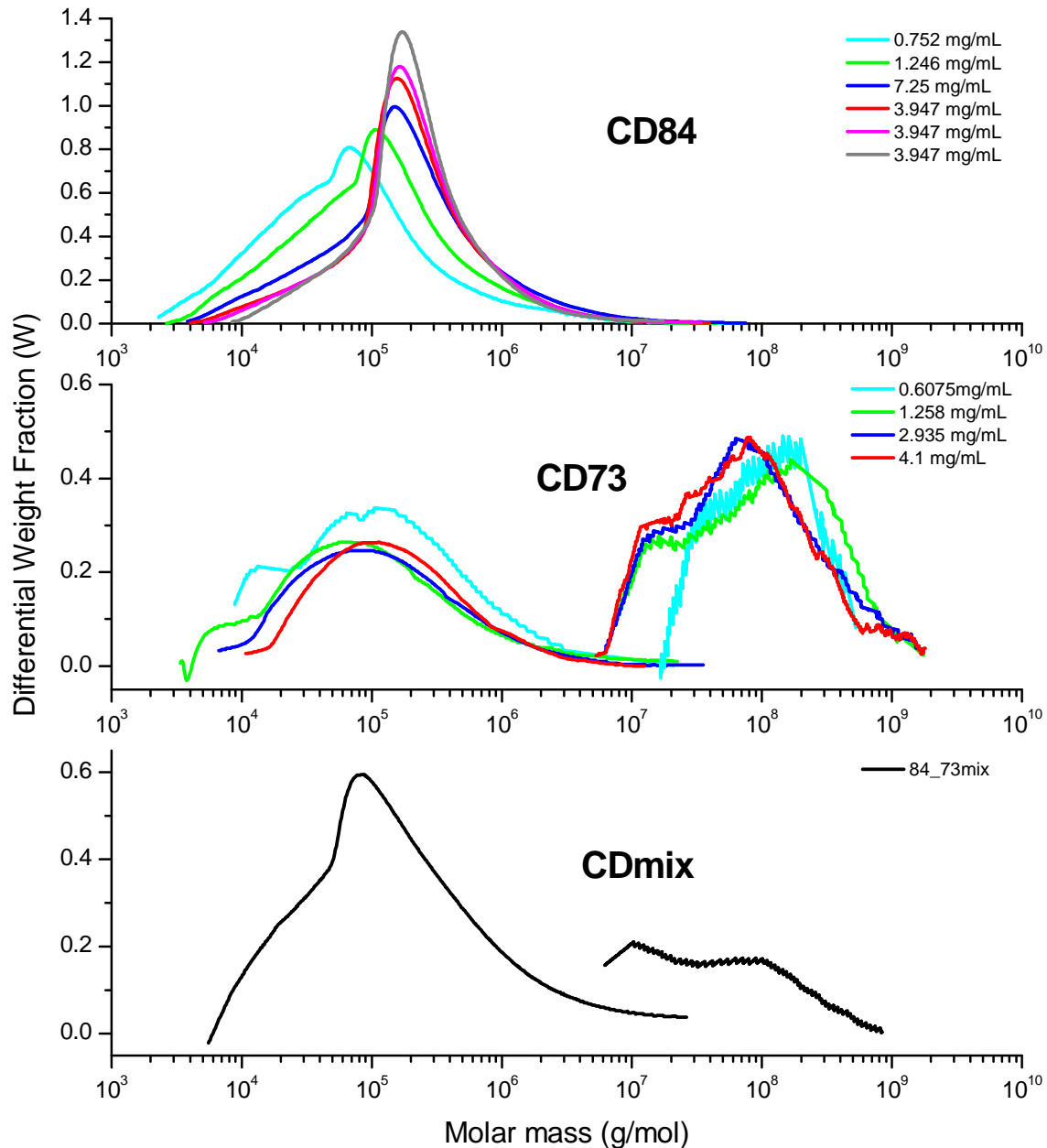**Fig. 4.10**   MMD plots of C84, CD73 and a blend of both samples in AF4, with clear evidence that the earlier eluting species corresponds extremely well with the precursor sample without a PEG backbone

The MMD plots of both species are overlaid in Fig. 4.10 and show that the low molar mass species of CD73 correlates very well with the MMD of CD84. Therefore the assumption of unreacted CD84

71

Chapter 4: Polyrotaxanes

present in CD73 is entirely valid, based on the bimodality and the MMD of these samples. A blend of CD84 and CD73 was measured in order to compare the elution behaviour against the individual measurements. The MMD plots were in exceptional agreement and very much congruent with the individual measurements in Fig. 10 C. The effect of the cross-flow field strength and activating and deactivating the focus flow was done with the aim of studying the elution pattern in AF4. Firstly the focus-flow was switched off at a starting cross-flow field of 5.5 mL/min, and secondly the cross-flow was reduced to a starting flow rate 2.5 mL/min and measured with and without a focus-flow. The rationale behind the switching off of the focus flow was to investigate whether focusing (when focusing is on) does not cause the polyrotaxane to aggregate in the narrow focused band at the inlet of the channel. Aggregation would in essence cause the polymer chains to overlap which will be detected as larger structures and as a result much higher molar masses and radii. For the 5.5 mL/min cross-flow measurement without focusing, three different MALLS peaks are observed for CD84 (Fig. 4.11 B) while broad bimodal RI peaks are observed.
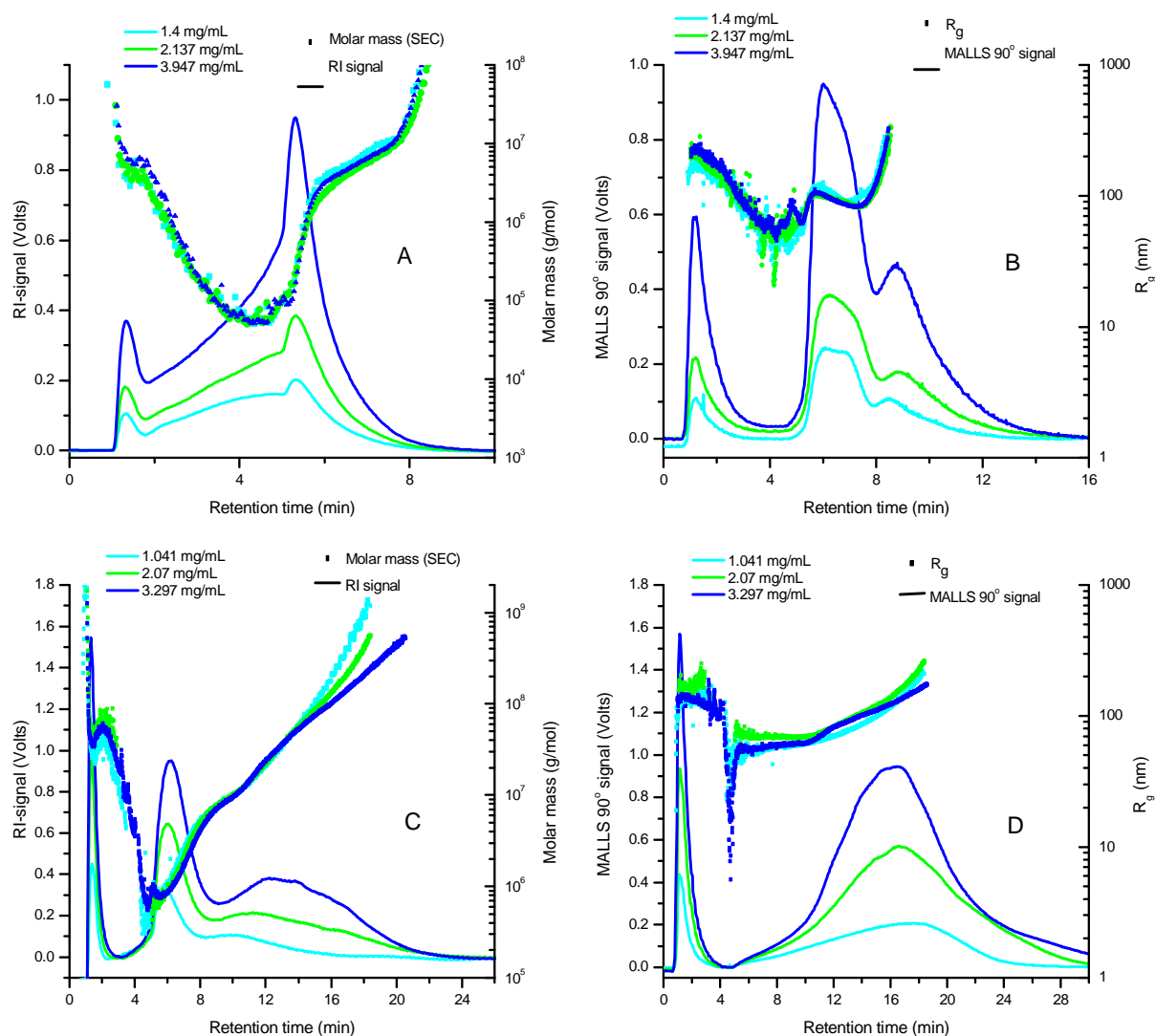

Fig. 4.11 Molar mass-(A, C) and R_g (B, D) plots for CD84 (A, B) and CD73 (C, D) without focusing for the 5.5 mL/min cross-flow (AF4). The RI- and MALLS 90° signals are overlaid respectively

Chapter 4: Polyrotaxanes

CD73 shows similar behaviour as with the measurement with focusing, except for appearance of the early eluting peak. The main peaks of both samples elute earlier due to the absence of the focus flow, which in essence reduces the run time and retention of polymer molecules inside the channel. CD73 still has a much longer run time compared to CD84 under the same conditions. RI-signals of the lower eluting species of CD73 and the main peak of CD84 coincide very well at about 6 minutes (Fig. 4.11 A and C), which also support the assumption made that lower molar mass species are present in CD73. The molar mass and R_g plots of both samples show a very interesting phenomenon for the early eluting peaks of both samples. Both molar mass and size decrease from high to low values upon elution time.   This elution pattern is characteristic of steric or hyper-layer modes in AF4 as was discussed in Chapter 2.2.2. Since the maximum molecular sizes observed in AF4 are in the region of 250 nm, steric mode is excluded from this assumption. Due to the absence of a focus-flow the molecules are immediately exposed to the cross-flow field and the axial parabolic flow, therefore without band broadening prevention. The molecules are swept away immediately down the channel and the high cross-flow will force the molecules to literally rebound of the accumulation wall, resulting in larger molecules ending up in faster flowing layers. This will result in a reverse in the elution order from big to small molecules.[19-23] After a few minutes the cross-flow decreases exponentially (Fig. 4.2) and the elution pattern returns to the normal mode. This is due to a decrease in the cross-flow force and a consequent reduction in the hyper-lift forces. For CD84 the latter part of the third MALLS peak (Fig. 4.11 B) could not be integrated and quantified, which is possibly due to molecules very high in molar mass as a result of entanglements of chains that are insoluble or gel-like species. For sample CD73, the molar mass and R_g readings for the high molar mass fraction are very well in agreement with the measurement where focusing was applied.

The reduced cross-flow of 2.5 mL/min with focusing showed comparable elution behaviour for both CD84 and CD73 compared to the 5.5 mL/min cross-flow (Fig. 4.12 A). One noticeable observation can be made at early elution times where the molar mass and radii first decreases before increasing to higher values. Despite focusing, it appears as if the hyper-layer mode dominates up to an elution time of 8 minutes before recurring to normal mode AF4. Due to the reduced cross-flow, the forces might therefore not be strong enough to push the bigger molecules against the accumulation wall, as a result they will reside in faster flow layers, and elute earlier than expected.

The MALLS signal of CD84 showed an appearance of a distinct second peak at higher elution times at approximately 17 minutes, which could be due to aggregation or entanglements. The same shoulder was also observed as a minor peak when the 5.5 mL/min cross-flow was applied for the highest concentration measurement without filtering (Fig. 4.9 B). A small part of this specific peak was quantifiable and the obtained radii appeared to be larger in comparison to the 5.5 mL/min measurement (Fig. 4.9 B), supporting the assumption made for the presence of ultra-high molar mass species. Another interesting observation is that lower molar masses are detected for the lower cross-flow, which is due to the reduced force applied resulting in less smaller molecules being lost through the membrane. It is clearly evident that higher molar masses are lost through the membrane as a result of the 5.5 mL/min cross-flow rate.

Chapter 4: Polyrotaxanes

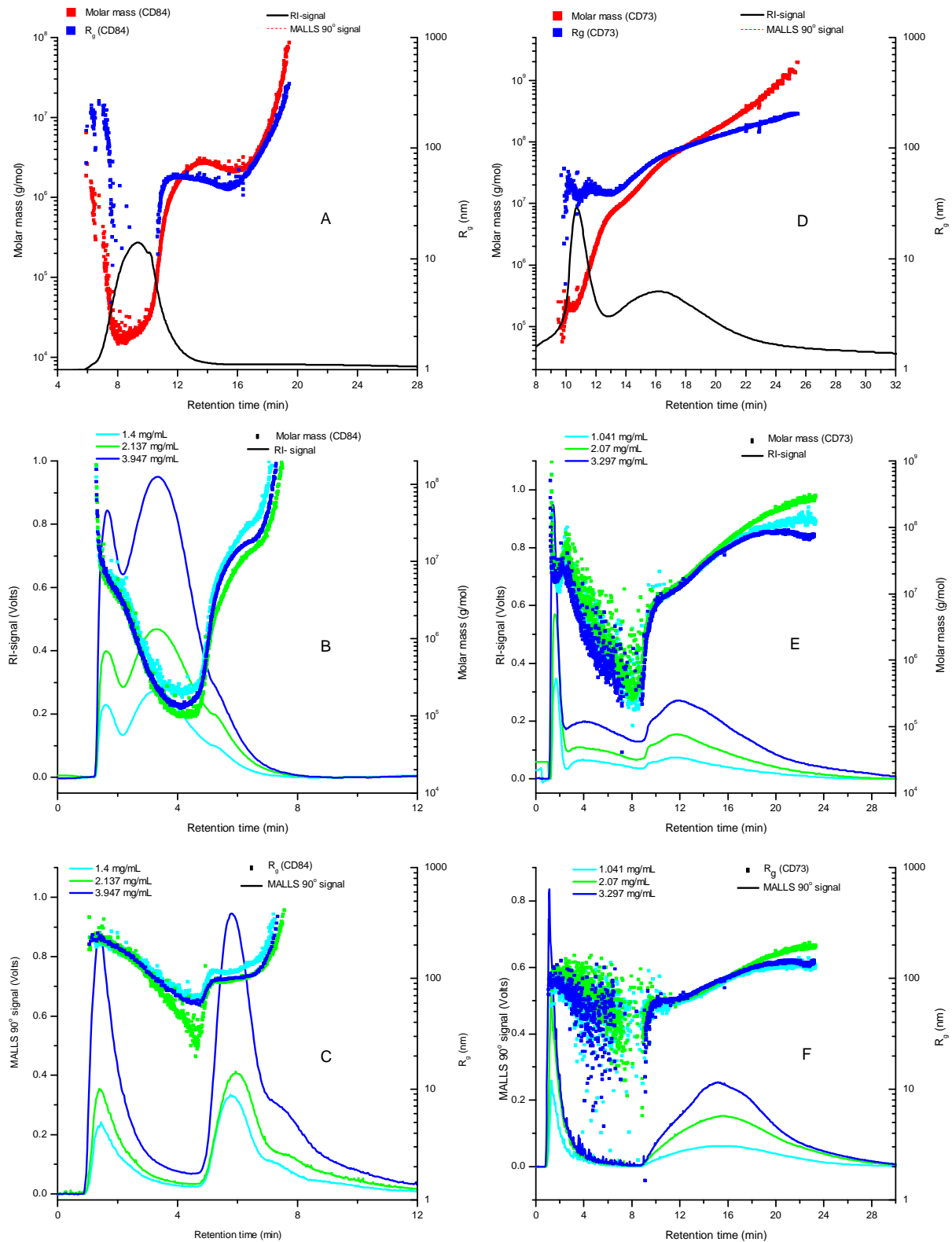**Fig. 4.12** Molar mass-, Rg plots, RI- and MALLS 90° signals f or CD84 and CD73 for the 2.5 mL/min cross-flow profile (AF4): A and D are with focusing using the least concentration for both samples while B, C, E and F are without focusing.

After the focus-flow was switched off a similar trend in the MALLS signals was observed for both samples compared to the higher cross-flow measurements. The early eluting peak was evident once

more, but higher in intensity compared to the 5.5 mL/min cross-flow measurements. The hyper-layer mode of AF4 was once more visible for the early eluting fraction in molar mass and radii, and transition back to normal mode AF4 took place after a short period (Fig 4.12 B, C, E and F). The molar masses and radii of CD84 and CD73 were in good agreement throughout the elution proving that a concentration increase did not cause any channel overloading.

The MMD of CD73 (Fig. 4.13) compares very well with the MMDs in Fig. 4.10 indicating that again two distinct species were observed for CD73 and that the lower molar mass species correspond very well with the single measurement of CD84. The 5.5 mL/min measurements gave better separation regarding the mode in AF4, i.e. if a higher starting cross-flow is used, the tendency of elution in normal-mode AF4 only is higher compared to when a lower starting cross-flow rate is used for these specific complex molecules. The focus flow is a valuable tool to use for the enhancement of separation. Focusing samples leads to a decrease in band broadening and a tendency towards normal mode separation throughout the elution range.

The deactivation of the focus flow can lead to multimodal peaks, which can only be resolved by using sufficient detectors such as MALLS coupled to the AF4 system. If an RI detector was the only detector, the early eluting species would have been difficult to identify with calibration standards. In addition the focusing and cross-flow work well in tandem for an optimum separation of any complex system in question.
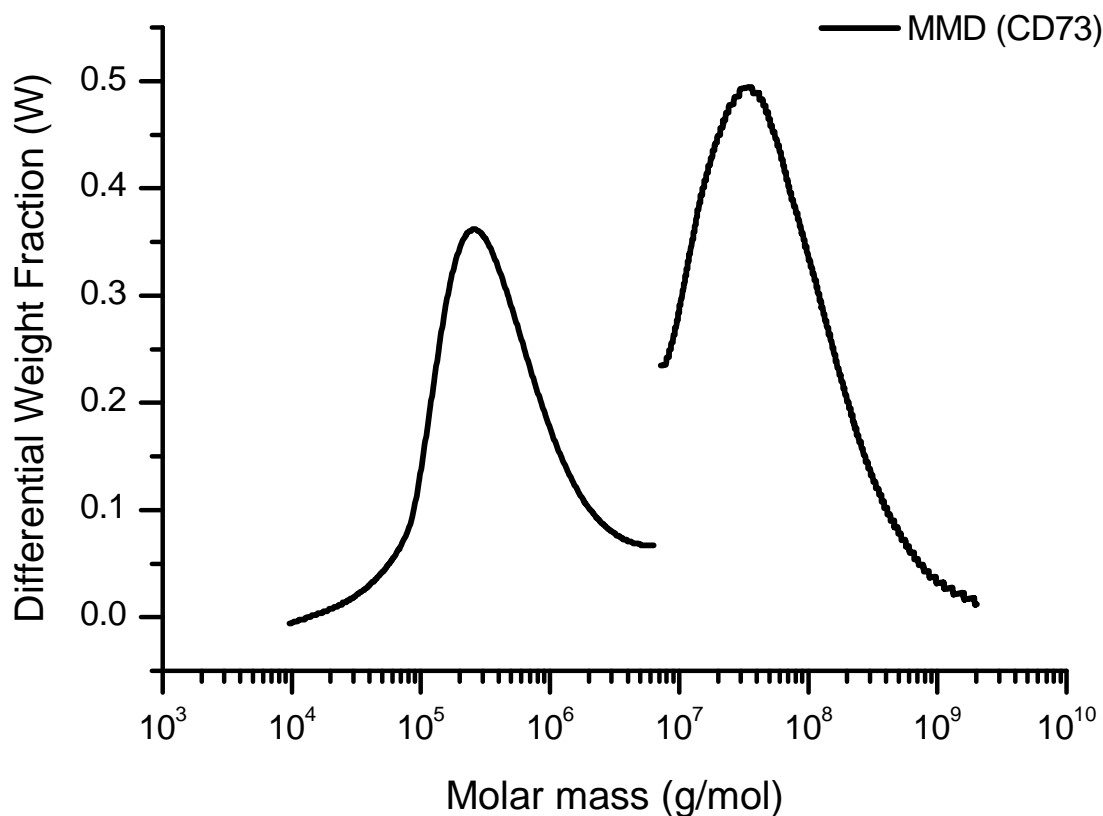

Fig. 4.13 MMD of CD73 with focus at a cross-flow rate of 2.5 mL/min (AF4)

4.4 Conclusions

Polyrotaxane polymers and their precursors were studied by SEC and AF4 coupled to MALLS and RI detection, respectively. It was possible to identify the individual species from the bimodal MALLS peaks observed for the polyrotaxane sample. It was proven that in SEC the abnormal elution (U-curve) could be minimised by increasing the particle size range of the used column set (mixed B and C to mixed A and B) as well as the molar mass range (10 million to 40 million g/mol).

Based on the observations from both column sets, it can be concluded that the second column set is a better choice when analysing polyrotaxane samples of such a complex nature. The non-SEC effects such as adsorption, entanglements with the column packing and shear degradation were minimised tremendously. It was possible to eliminate the late-elution phenomenon in order to properly address the later eluting lower molar mass species. In addition a higher recovery was obtained and more distinct peaks could be identified by the second column set. Higher concentrations were needed for a proper RI-signal for both samples since the dn/dc values for both samples are very low in THF as solvent. Toluene would be a better solvent for elimination of π-π interactions between the aromatic stopper groups and the styrene based stationary phase. However, the dn/dc values of both samples in toluene are even lower compared to THF. Therefore toluene was not used and other mobile phases could be investigation for better RI detector signal responses. The detected sizes obtained from both the precursor polymer and the final polyrotaxane were shown to be homogeneous in size for the SEC measurements. In AF4 this was not the case for the high molar mass species since larger molecular sizes were observed.

For SEC it must be concluded that irrespective of the chosen column set and experimental conditions rather untypical elution behaviour is obtained. In addition, due to filtration of the samples before injection or at the inlet frits of the columns, the samples are exposed to significant mechanical stress that may change the molecular structure of the samples. Therefore a further study on the optimal column conditions is highly recommended.

It is assumed that the reason for the SEC behaviour could be that shearing or trimming of chains take place in both column sets, and consequently the maximum size that can pass through the stationary phase are in the region of 40 nm for these complex polymers. The bimodality observed in the polyrotaxane sample (CD73), especially the low molar mass species could be ascribed to unreacted starting material (CD84) present in CD73. The molar mass and radii readings obtained for the low molar mass fraction showed excellent agreement when it was compared to CD84. This was evident in all the different experimental conditions used in AF4.

4.5 References

(1)   Zhao T.; Beckham H. W. *Macromolecules* **2003**; 36(26), 9859-9865.

(2)   Wyatt P. J. *Anal. Chim. Acta* **1993**; 272(1), 1-40.

(3)   Podzimek S. *Light Scattering, Size Exclusion Chromatography and Asymmetric Flow Field Flow Fractionation: Powerful Tools for the Characterization of Polymers, Proteins and Nanoparticles*. New York: John Wiley & Sons; **2011**.

(4)   Wintermantel M.; Antonietti M.; Schmidt M. *J. Appl. Polym. Sci.: Appl. Polym. Symp.* **1993**; 52, 91-103.

(5)   Laguna M. T. R.; Medrano R.; Plana M. P.; Tarazona M. P. *J. Chromatogr. A* **2001**; 919(1), 13-19.

(6)   Podzimek S.; Vlcek T.; Johann C. *J. Appl. Polym. Sci.* **2001**; 81(7), 1588-1594.

(7)   Vareckova D.; Podzimek S.; Lebduska J. *Anal. Chim. Acta* **2006**; 557(1-2), 31-36.

(8)   Kim C.; Morel M.-H.; Beuve J. S.; Guilbert S.; Collet A.; Bonfils F. *J. Chromatogr. A* **2008**; 1213(2), 181-188.

(9)   Otte T.; Pasch H.; Macko T.; Brüll R.; Stadler F. J.; Kaschta J.; Becker F.; Buback M. *J. Chromatogr. A* **2011**; 1218(27), 4257-4267.

(10)   Otte T.; Klein T.; Brüll R.; Macko T.; Pasch H. *J. Chromatogr. A* **2011**; 1218(27), 4240-4248.

(11)   Otte T.; Pasch H.; Brüll R.; Macko T. *Macromol. Chem. Phys.* **2011**; 212(4), 401-410.

(12)   Liu Y.; Radke W.; Pasch H. *Macromolecules* **2006**; 39(5), 2004-2006.

(13)   Hirabayashi J.; Ito N.; Noguchi K.; Kasai K. *Biochemistry* **1990**; 29(41), 9515-9521.

(14)   Trathnigg B. In: Meyers R. A., (ed). *Encyclopedia of Analytical Chemistry*. Chichester, United Kingdom: John Wiley & Sons; **2000**; p. 8008-8034.

(15)   Esser K. E.; Braun D.; Pasch H. *Angew. Makromol. Chem.* **1999**; 271(1), 61-67.

(16)   Pasch H. *Adv. Polym. Sci.* **2000**; 150, 1-66.

(17)   Pasch H.; Esser E.; Kloninger C.; Iatrou H.; Hadjichristidis N. *Macromol. Chem. Phys.* **2001**; 202(8), 1424-1429.

(18)   Topchieva I. N.; Tonelli A. E.; Panova I. G.; Matuchina E. V.; Kalashnikov F. A.; Gerasimov V. I.; Rusa C. C.; Rusa M.; Hunt M. A. *Langmuir* **2004**; 20, 9036-9043.

(19)   Janca J. Field-flow fractionation.In: Heftmann E., (ed). *J. Chromatogr. Libr.* Amsterdam: Elsevier; **1992** p. A449-A479.

(20)   Giddings J. C. *Science* **1993**; 260(5113), 1456-1465.

(21)   Melucci D.; Zattoni A.; Casolari S.; Reggiani M.; Sanz R.; Reschiglian P. *Journal of Liquid Chromatography & Related Technologies* **2002**; 25(13), 2211 - 2224.

(22)   Farmakis L.; Koliadima A.; Karaiskakis G.; Zattoni A.; Reschiglian P. *Food Hydrocolloids* **2008**; 22(6), 961-972.

(23)   Schimpf M. E.; Caldwell K.; Giddings J. C. *Field Flow Fractionation Handbook*. New York: John Wiley & Sons; **2000**.

Chapter 5: Overall conclusions and recommendations

Chapter 5: Overall Conclusions

In this study we focused on the application of AF4 coupled to MALLS and RI detection to various polymer systems, i.e. polystyrene reference materials as model polymers, polybutadiene rubbers and complex architecture polymers namely polyrotaxanes.

5.1 Conclusions for chapter 3

The AF4-MALLS-RI system was fully implemented, and the flexibility of the focus and cross-flow enabled a proper study based on polystyrene polymers. We showed that it was possible to adjust the cross-flow gradient such as to separate narrowly dispersed polystyrene standards from each other. The easily programmable flow system allows for a complete change in the flow profile, which is not possible in SEC which requires a complete change of the column set being very costly if new columns have to be purchased. It was shown that none of the column sets used could assure proper baseline separation. In AF4 the introduction of linear gradients within the exponential cross-flow profile was sufficient to achieve acceptable separation. The integrated values also showed that AF4 gave molar masses and radii closer to the values given by the producer compared to SEC. The results showed that both SEC and AF4 separation systems gave similar molar masses for a mixture of polystyrene standards. These samples could be analysed accurately.

Polybutadiene samples, which had different degrees of branching and gel content were then subsequently analysed by applying an optimized cross-flow. Various dissolution studies were done on a number of polybutadiene samples, and it was found that the dissolution time and temperature have an effect on the obtained recovery in SEC. Longer dissolution times were used for all the samples to achieve recoveries in the region of 100%. Abnormal elution behaviour was observed in SEC when different dissolution times, temperatures, and filtering were applied. This phenomenon is usually observed in high molar mass branched polymers and was not expected for this specific sample since it was only slightly branched and no apparent gel was present. The abnormal elution behaviour was more pronounced in the R_g vs. time plot compared to the molar mass plot since R_g is more sensitive for differences in local dispersities. The observed elution behaviour differences were probably due to insufficient dissolution and the presence of very small amounts of gel species which were retarded in the pores of the stationary phase. Gel species were observed in AF4 measurements with and without filtering at the high molar mass end and no abnormal elution behaviour was observed. The observations from SEC and AF4 confirmed the presence higher molar mass species due to distinct gel peaks observed in the respective MALLS signals

Another sample which was known to have long chain branching present was analysed by SEC and AF4. In SEC the expected upswing was observed for both molar mass and radii plots and the calculated slope from the R_g-M relationship (conformation plot) confirmed that long chain branching was present. The slope was not accurate, however, due to the upswing phenomenon observed in the conformation plot. AF4 measurements were subsequently performed and no upswing or separation irregularities were observed which lead to accurate slope determinations.

Chapter 5: Overall Conclusions

Finally a sample which appeared to be monomodal in SEC measurements was compared to AF4 measurements and it was found that bimodal MALLS traces were observed indicating that very small quantities of very large structures were present in the sample, possibly as a result of insoluble cross-linked gel species. The filtered sample could be correlated to molar mass and R_g values and larger values were observed compared to the R_g and molar mass readings of the earlier eluting species. Based on these observations it could be concluded that in AF4 much larger polymer species can be detected compared to SEC analysis despite the low response from the RI detector. This makes it possible to quantify gel species relative to the soluble fraction which is very important especially in the tire industry.

Chapter 3 showed that it is possible to get similar results from both SEC and AF4 for model polymers. It was shown that AF4 is superior to SEC in many facets especially for ultra high molar mass species. The different applicable flows and the option to measure samples without filtering make AF4 an ideal tool for complex polymeric systems.

Future recommendations include the collection of the polymer fraction which shows abnormal elution in SEC and the re-injection of the collected fractions in SEC and AF4. This will indicate whether high molar mass species are present in the late eluting fraction, which might confirm that high molar mass branched species are retarded in the pores of the SEC column eluting later with regular eluting species. Another study could also be conducted to investigate the dissolution procedure to minimise abnormal elution behaviour in SEC. Furthermore the late eluting gel fraction in AF4 for PB 5 could be collected and re-injected in AF4 for accurate size and molar mass determinations.

5.2 Conclusions for chapter 4

In this study we conducted experiments on complex polymer systems investigating various aspects and their effects on elution behaviour, molar masses and radii. Initial results for specific polyrotaxane samples showed promising results in terms of the vast differences observed between SEC and AF4. The AF4 technique showed extreme superiority over SEC in terms of the molar mass and radii calculations. While SEC showed a strong reincrease of molar masses for later eluting species, AF4 showed an increase to higher values over the entire elution range. In addition much higher molar masses and radii were observed for AF4 compared to SEC.

A follow up study was done by comparing the precursor PMMA-grafted CD to the complete polyrotaxane. In this case some problems were encountered regarding solubility of the polyrotaxane. Despite the solubility issues, a proper study could still be conducted varying column sets (SEC), cross and focus flows (AF4), as well as the concentration. In SEC the same observation was made as the initial study, i.e. a re-increase in molar mass at later elution times. However, this was only true for column set one, where the stationary phase had particle sizes of 10 and 5 µm, respectively. The second column set (20 and 10 µm particles) did not show the abnormal elution behaviour indicating that non-SEC effects were present for the first column set.

Chapter 5: Overall Conclusions

For the AF4 measurements different starting cross-flows were used and the results from the polyrotaxane (CD73) and its precursor material (CD84) were compared with and without applying a focus flow. The higher initial cross-flow proved to be a better starting cross-flow compared to the lower cross-flow for both samples. The high initial cross-flow of 5.5 mL/min proved to be strong to force the bigger and higher molar mass molecules close the accumulation wall. The lower cross-flow (2.5 mL/min) showed overlapping of steric-hyperlayer and normal modes of separation. The overlapping of AF4 separation modes was also noticeable when both cross-flows were applied without any focusing. Without focusing the molecules do not have enough time to migrate into different flow velocity zones, and are additionally directly exposed to the strong cross-flow forces. This potentially leads to overlapping modes of AF4 separation. The molar mass and radii plots for both samples and both cross-flows without focusing showed an initial decrease for the first few minutes (steric-hyperlayer mode), after which the values increased again (normal mode of separation). Moreover the maximum values observed for the early and later eluting species in AF4 showed good agreement, proving that no aggregation took place, but merely an inverse in the mode of the separation mechanism.

Based on these results, it was showed that in AF4 much larger radii and molar masses were detected compared to SEC results, more importantly the focus and cross-flow pumps allowed for added versatility in terms of fine tuning the separation.

Future recommendation for the polyrotaxanes would be to fractionate the late eluting fraction of SEC and re-inject it for SEC and AF4 analysis. Additionally the fractions could be further characterized by Fourier Transform Infrared Spectroscopy for the identification of the functional groups present in the collected fractions. In the AF4 measurements the early eluting species without focusing could also be collected and re-injected in AF4, by applying a focus flow.

Acknowledgements

First of all I would like to thank the Lord Almighty for His guidance and making this journey a successful one.

A would like to thank the department of Chemistry and Polymer Science, post graduate bursary office, Mondi business paper, Freeworld Coatings, NRF and PPS insurance for financial assistance throughout my postgraduate studies.

I am truly grateful to Prof. Harald Pasch for allowing me to be a part of his research group for the past two and half years. Thank you for all your guidance and support throughout my studies thus far. It surely would not have been an easy one without your invaluable scientific input. I know your patience was tested a lot at times, but your availability made a lot of things possible without any difficulties. All the staff members and students of Polymer Science are also thanked for their assistance over the past few years.

Thank you to all my family members and friends whose words of wisdom allowed me to push through the difficult times. A special word of thanks goes out to my mom Rosaline, brothers Elroy, Howard, Melvin and their families, sisters Vainola and Laetitia. Your continuous support is invaluable to me and is appreciated it a lot. To my late dad Esrick and brother Theodore, you are genuinely missed, and it would have been great to have you around for this special moment. This thesis is dedicated to all of you.

I would also like to express my gratitude towards Tino Otte who introduced me to the secrets of FFF. Thanks for all the discussions for the past two years, it is much appreciated. Also Petra Arnoutse who made my stay in Amsterdam for the SCM-5 conference a memorable one.

Special thanks have to go out to Nadine for supporting me during the stressful times of deadlines, exams, presentations, conferences to name a few. The past few years would have been difficult without all your support.

Thank you all